SEISMIC STRATIGRAPHY AND BURIAL HISTORY FOR SOURCE AND RESERVOIR PREDICTION IN THE LÜDERITZ BASIN, LICENSE BLOCKS 2412B AND 2413B, OFFSHORE NAMIBIA

Reginalda Joseph

201169312

Supervisor: Dr. Ansgar Wanke (UNAM Geology Department)

A THESIS SUBMITTED IN PARTIAL FULFILMENT

OF THE REQUIREMENTS FOR THE DEGREE OF MASTER OF SCIENCE

(PETROLEUM GEOLOGY)

OF

THE UNIVERSITY OF NAMIBIA

WINDHOEK

2020

ABSTRACT

*The Lüderitz Basin is one of the four Namibia's offshore basins on the western African passive margin that evolved during continental break-up and subsequent opening of the South Atlantic during the late Jurassic and Cretaceous. It is considered as a hydrocarbon frontier that is largely under-explored with only one well (*2513/8-1*) drilled since the wake of hydrocarbon exploration along the Namibian offshore in the 1990s. Selected lines of the GPN13 2D seismic dataset on blocks 2412B/2413B and well 2513/8-1 were used to predict lithofacies in the basin based on seismic stratigraphic interpretation. A Wheeler diagram was constructed to obtain better insight into the time relationships of the depositional systems, and their relationships to surfaces of non-deposition, condensation and erosion. In addition, two model well locations were selected in the basin, one on the shelf and the other at the base of slope. The Cretaceous and Tertiary succession was divided into 19 Seismic Intervals (SI) based on the recognition of 11 seismic stratigraphic surface. As no direct well tie calibration could be carried out the assigning of stratigraphic ages required comparison of the GPN13 lines with interpretations from neigbouring areas contained in previously studies. Lithofacies were predicted based on seismic facies, system tracts, and analogue interpretations presented in publications on studies of neighboring areas. The lithology model proposes the presence of several source, reservoir and seal rock units in both, the syn-rift and post-rift succesions of the study area. The modelled thermal history suggests that potential Lower Cretaceous source rocks may have generated petroleum only at locations of thick overburden, such as the base of slope location.*

Contents

LIST OF TABLES

LIST OF FIGURES

LIST OF ABBREVIATIONS AND/ OR ACRONYMS

AFTA- Apatite Fission Track Data

BSR- Bottom Simulating Reflection

CFBs- Continental Flood Basalts

HST- Highstand System Tract

HC- Hydrocarbon

LST- Lowstand System Tract

MD- Measured Depth

MFS- Maximum Flooding Surface

PSE- Petroleum System Element

PSTM- Prestack Time Migration

RSL- Relative Sea Level

SDRs- Seaward Dipping Reflectors

SI- Seismic Intervals

TS- Transgressive Surface

TOC- Total Organic Content

TST- Transgressive System Tract

UNAM- University of Namibia

U/C- Unconformity

ACKNOWLEDGEMENTS

First and foremost, I would like to thank my Heavenly Father for blessing me with the energy, motivation and patience throughout my entire course work and for making this research possible. Secondly, I am particularly grateful for the interaction with my supervisor Dr. Ansgar Wanke, thank you for all your effort to make sure I fully understand what I was working on and for guidance. I also like to extend my appreciation to Yusneurys Perez Martinez and Raydel Toirac Proenza who cheerfully welcomed me to their esteemed office (Pioneer Oil & Gas Consulting) inorder to carry out my data interpretation and for having paused their own research to answer my inquiries. This research project received generous financial support from Petrofund, to whom I wish to express my gratitude. Furthermore, I would like thank Sungu Sungu and Pioneer Oil & Gas Consulting for providing access to the research data.

Special thanks are due to my friend Frieda Kahewa-Ketu Thomas who never left me alone even in the hardest situations, I could not wish for a better friend and classmate. I would also like to acknowledge the patience and support my love Fernando Immanuel and my mother Martha Shiningayamwe had given me throughout my often overtime-working hours, their generosity cannot be appreciated by words. Lastly, I would like to send out a shout out to Tate Joe for the late hours he had been up just to make sure Kahewa and I get home safely after our long night research work at school.

DECLARATIONS

I, Reginalda Joseph, declare hereby that this study is a true reflection of my own research, and that this work, or part thereof has not been submitted for a degree in any other institution of higher education.

No part of this thesis/dissertation may be reproduced, stored in any retrieval system, or transmitted in any form, or by means (e.g. electronic, mechanical, photocopying, recording or otherwise) without the prior permission of the author, or The University of Namibia in that behalf.

I, Reginalda Joseph, grant The University of Namibia the right to reproduce this thesis in whole or in part, in any manner or format, which The University of Namibia may deem fit, for any person or institution requiring it for study and research; providing that The University of Namibia shall waive this right if the whole thesis has been or is being published in a manner satisfactory to the University.

Irrespective of the above, access to the thesis and parts thereof must be restricted according to the accompanying Confidentiality Agreement with Pioneer Oil & Gas Consultiung dated 20 March 2019.

……. [signature] Date 21/08/2020……..

Reginalda Joseph

CHAPTER 1: INTRODUCTION

1.1 Structure and background

This report documents a master's thesis work that was carried out under an agreement between the Geology Department of the and the data provider. It presents results of the study done on the of the Lüderitz Basin, license blocks 2412B and 2413B and well reports for well 2513/8-1. The overall goal of this research is to predict petroleum systems elements such as source, reservoir, and seal with a seismic stratigraphic approach in the northern Lüderitz Basin.

The Lüderitz Basin (Figure 1) is one of the four Namibia's offshore basins of the western African passive margin. The margin evolved during continental break-up and subsequent opening of the South Atlantic during the Jurassic and Cretaceous (Bray et al., 1998). The other basins are the Namibe, Walvis and Orange basins. Most authors accept that rifting happened in a transient volcanic environment, leaving encrypting fingerprints on the sedimentary successions (Aizawa et al., 2000; Bray et al., 1998; Conti, 2013; Gladczenko et al., 1998).

The Lüderitz Basin has not been extensively studied with only one well drilled since the wake of hydrocarbon exploration along the Namibian offshore by Norsk Hydro in 1998. The Lüderitz Basin is like the other Namibian offshore basins considered as a hydrocarbon frontier that is largely under-explored. A fair coverage of 2D seismic allows for a seismic stratigraphic interpretation. As well control in the Lüderitz Basin is limited; this study aims to predict petroleum systems elements such as source, reservoir, and seal with a seismic stratigraphic approach.

According to Martinez (2013) seismic stratigraphy is the study of stratigraphy and depositional facies as interpreted from seismic data. A seismic stratigraphic study includes the recognition of seismic reflection terminations such as onlap, downlap, toplap, offlap, and erosional truncations. Recognition of seismic stratigraphic units and their seismic facies, such as reflection configuration, frequency and amplitudes, allow for a lithofacies prediction and herewith a prediction of intervals that may contain source, seal, and reservoir lithologies in the Lüderitz Basin.

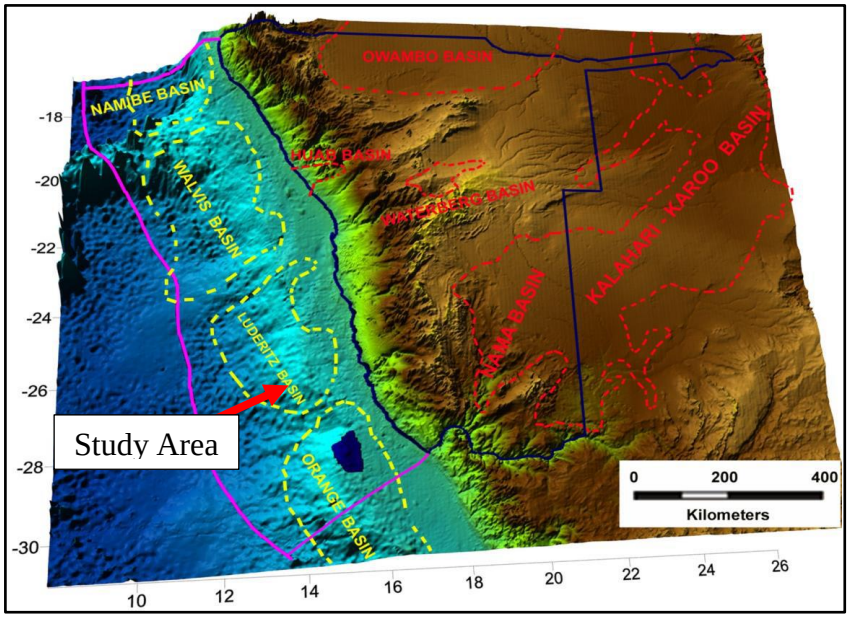

Figure 1: Regional geographic map of Namibia with the main hydrocarbon exploration basins (dashed lines). The purple line indicates Namibia's marine exclusive economic zone. Image modified from Nepembe (2017).

1.2 Exploration history

Exploration for hydrocarbons along the Namibian shelf margin began in the late 1960's and the first successful discovery was the Kudu gas field that was discovered in 1974. In 1987-1988 Swakor, the predecessor company of the present National Oil Company NAMCOR, drilled further two wells in the Kudu field. The Kudu 2 well was not tested but Kudu 3 proved the existence of a major gas field. The proven hydrocarbons were an asset in Namibia's first licensing round.

To date, 48 exploration and one production licenses have been issued to Namibian and international oil and gas companies. A total of 24 wells (exploration and Kudu appraisal) have been drilled on the Namibian passive margin (Figure 2). One well has been drilled in the Lüderitz Basin by Norsk Hydro (2513/08-1) in 1998. Four wells have been drilled during the 2012/2013 exploration campaign; namely the Murombe, Wingat, Moosehead and Kabeljou. The Murombe and Wingat wells were drilled within the Walvis Basin, of which the Wingat well intersected thin sandy lenses containing light oil of 38˚ to 42 ˚ API within the Aptian source rock. The other two are the Moosehead and Kabeljou wells were drilled within the Orange Basin with no luck of a commercial breakthrough. Two recent wells have been drilled in 2018 in the Walvis Basin: Cormorant-1 and Prospect S wells. The Cormorant-1 well came up dry and Prospect S well penetrated the anticipated turbidite reservoir sands, in line with the pre-drill prognosis, however the reservoirs were water-bearing. No later wells have been drilled to date at the Namibian margin.

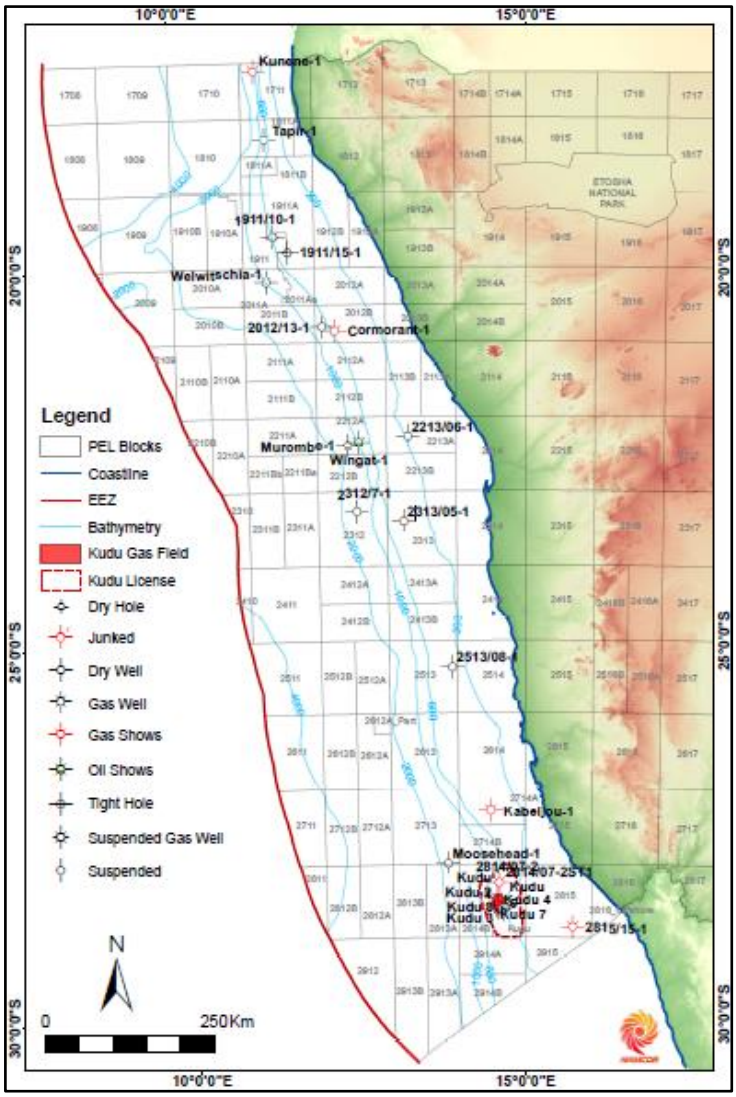

Figure 2: Exploration wells on the Namibian passive margin including hydrocarbon discoveries as well as gas/oil shows, Namcor (2019).

1.3 Problem statement

There is limited information on the lithofacies in the Lüderitz Basin due to limited well control. Furthermore, there are no wells on the slope and deep marine settings; therefore there is no proof of lithofacies such as source, reservoir and seal lithologies existence in those parts of the basin. Hence a petroleum play cannot be directly defined and a predictive lithofacies model is required.

1.4 Objectives

- The study aims to predict lithofacies in the basin based on seismic stratigraphic interpretation
- Construct a burial history at selected model well locations
- Conclude on maturation and possible timing of hydrocarbon (HC) expulsion

CHAPTER 2: LITERATURE REVIEW

2.1 Regional Geological Evolution

The volcanic margin off Namibia experienced massive, transient magmatic activity during final continental breakup and initial seafloor spreading during the Early Cretaceous breakup of South America from Africa (Gladczenko et al., 1999) (Figure 3). The margin has a wide, stable shelf that extends up to 230 km offshore and lies as deep as 500 m below sea level (Kirkpatrick et al., 2019). Hinz (1981) and Austin & Uchupi (1982) first pointed out that the southwest African margin is of volcanic character shown by prominent seaward dipping reflectors (SDRs) that characterize the outer margin off Namibia south of the Walvis Ridge (Gladczenko et al., 1999) and are interpreted to be the result of a huge subaerial basaltic extrusive event associated with break-up. These SDRs continue south along the African margin, and are also present on the conjugate Brazil-Argentine margin (Hinz et al., 1999).

It is during this break-up, that a linear array of four major basins developed parallel to the continental margin. The four main Namibian offshore basins are: the Orange Basin has been the depocentre for sediments of the Orange River since at least Early Cretaceous times, the Lüderitz Basin, which is an elongated basin fronting the Lüderitz Arch, a westward plunging basement nose, the Walvis Basin that is situated to the south of Walvis Ridge which is a major volcanic feature of Cretaceous age that erupted along an east-west trending transverse fracture, and the Namibe Basin which is situated further north and is a narrow basin flanking a steeply faulted slope and narrow shelf area (Maslanyj et al., 1997) (Figure 3).

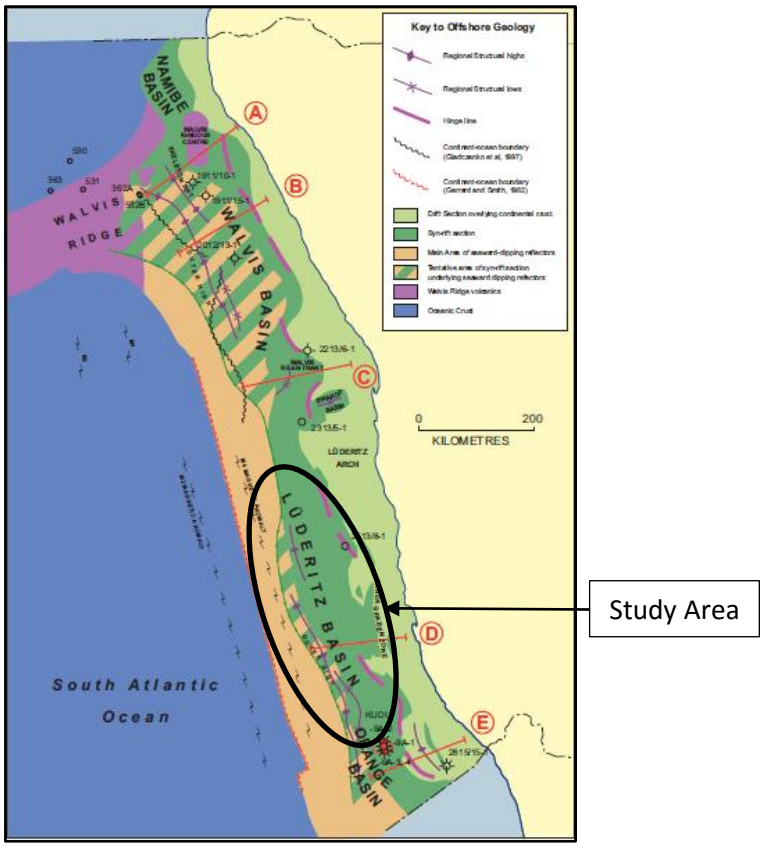

Figure 3: Locality of Namibia's offshore sedimentary basins (Bray et al., 1998).

It is further stated in Gladczenko et al. (1999) that volcanic margin formation is commonly related to continental breakup in the presence of a mantle plume, and in the case of the Namibian volcanic margin, the emplacement of the Paraná-Etendeka continental flood basalts (CFBs) (Figure 4 & 6), between 133 and 130 Ma is the initial manifestation of the Tristan mantle plume in the South Atlantic (Gladczenko et al., 1997). The Paraná-Etendeka continental flood basalts invaded the Southern Gondwana just prior to or concomitant with rifting. The oldest M5 magnetic anomaly of South America indicates sea floor opening ages of around 135Ma. This is in turn contradicted by a 3-4 Ma difference of the Namibian conjugate (Gladczenko et al., 1999). This

development poses a question as to whether the extensive continental flood basalts of the Etendeka province erupted coevally or prior to rifting on the Namibian conjugate. The Walvis ridge and Rio de Grande rise on the Namibian and South American margins respectively represent trails of this plume (Gladczenko et al., 1999; Müller & Nürnberg, 1990; Rayment & Dingle, 1992/93).

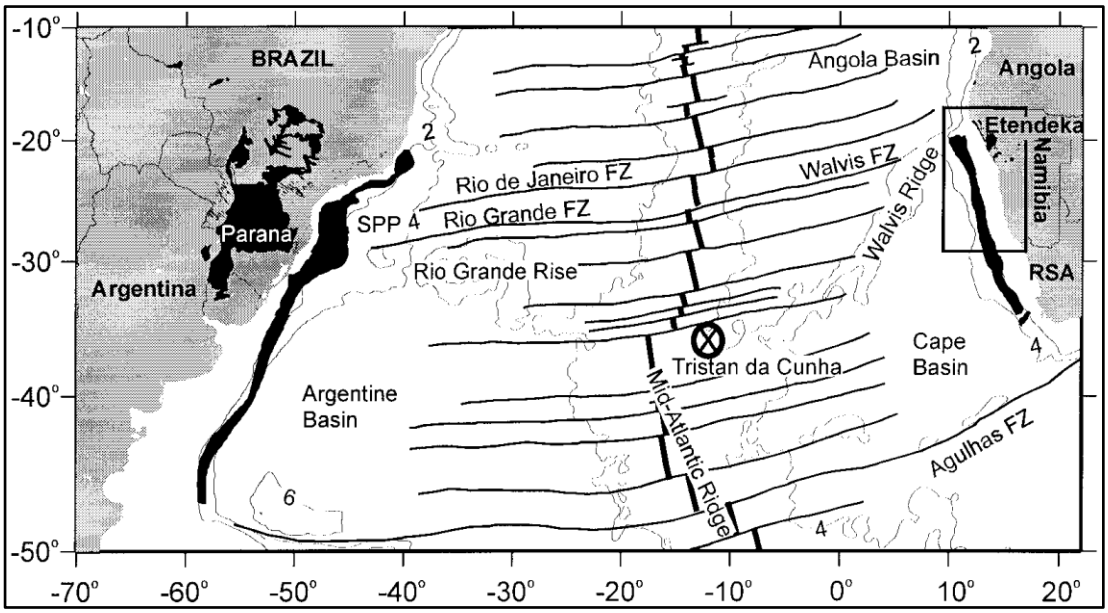

Figure 4: Simplified bathymetry (km) and plate tectonic features in the South Atlantic Ocean. Continental flood basalts and seaward dipping wedges outlined in black (Gladczenko et al., 1999).

According to Gladczenko et al. (1999), late Precambrian tectonism, commonly termed the Pan African and Brasiliano orogenic events affected vast parts of the African and South American continents and the Upper Proterozoic-Lower Paleozoic Damara, Kaoko and Gariep belts of Namibia and South Africa (Figure 5 & 6) are regarded as integral parts of these orogens. Following the dominantly compressional setting that led to the

late Paleozoic configuration of Gondwana, the region became dominated by complex rift systems. The history of extension prior to the Early Cretaceous opening of the Atlantic Ocean is not fully resolved, however, Light et al. (1993) suggested a Late Carboniferous to Early Permian proto-Atlantic rift with a shallow sea along its axis. In addition Grill (1996) and Stollhofen et al. (1998) interpreted the N-S extensional faults to be related to a major detachment along which the South Atlantic eventually opened and controlling basin development from the Early Permian thereof.

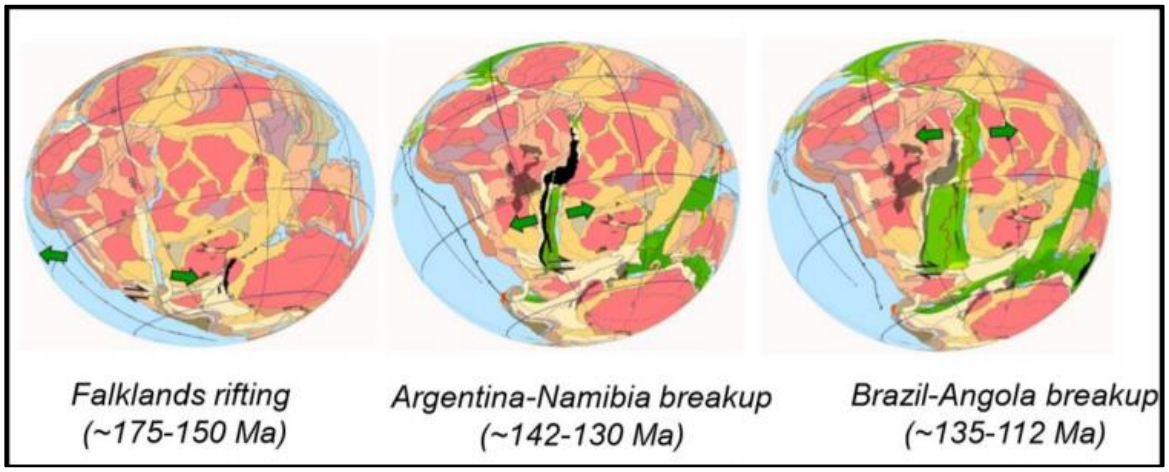

Figure 5: Tectonic evolution of Gondwana during the Mesozoic rifting period; copied from Conti (2014).

Variation in sedimentary depocenter location on passive margins is an important feature of the Namibian passive margin and its conjugate, the Pelotas Basin in Brazil and Uruguay (Saunders et al., 2013). North of the Walvis ridge the basin is hypothesized to have developed after a jump in rifting along the Walvis and Rio de Janeiro fracture zones resulting in restricted marine conditions during the Aptian to Albian times (Figure 5). Volcanism is reportedly absent in the Namibe basin but SDRs are still mapped north

of the Rio de Grande rise all the way to the Rio de Janeiro fracture zone which probably indicates cessation of magmatism after the Walvis ridge formation (Gladczenko et al., 1999). It is for this reason, that the northern part of the Namibian margin has been classified as a non-volcanic margin which is contradictory because of its close proximity to Etendeka flood basalts, magmatic activity on the conjugate Saó Paulo as well as the proximal Walvis ridge. The core of this argument is therefore that the northern Namibian margin postdates breakup as evidenced by drilling results from DSDP sites 530 and 362 that were interpreted by Sibuet et al. (1984). Therefore the late Aptian-Early Albian time interval is the likely period of formation for the Namibe basin (figure 6). This also further proves the claim by several authors such as Cartwright & Booth (1997), Clemson et al. (1997); de Vera et al. (2010); Gladczenko et al. (1999); Jungslager (1999); and Kuhlmann et al. (2011) that South Atlantic rifting started in the south and propagated towards the north in an unzipping fashion (Figure 4 above).

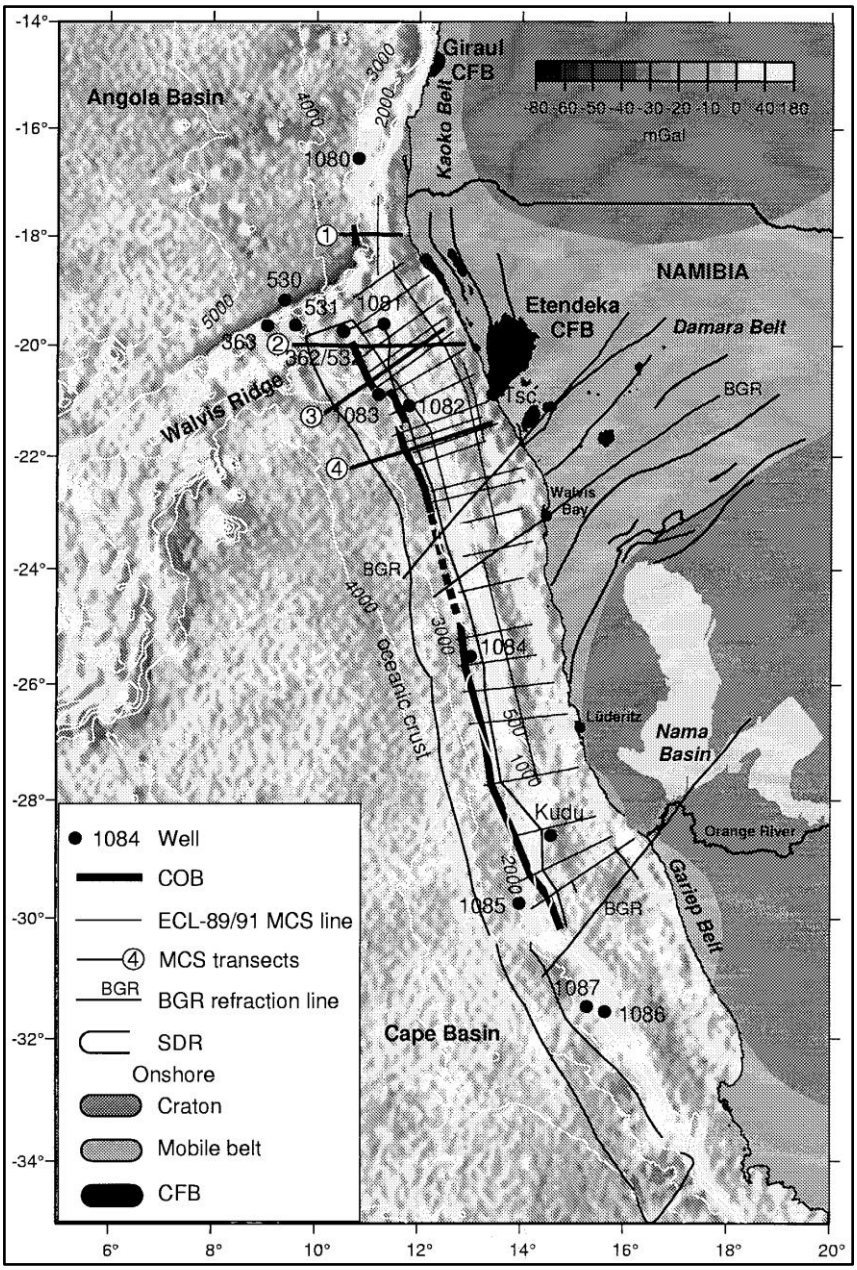

Figure 6: Illustration of the tectonostratigraphic evolution of the Namibian margin with Pan-African orogenic belts indicated; the Upper Proterozoic-Lower Paleozoic Damara, Kaoko and Gariep belts of Namibia and South Africa (Gladczenko et al, 1999).

The Namibia Offshore Passive Margin is dissected into distinct tectono-magmatic zones (Figure 7 below) with the help of effusive magmatism combined tectonic forces that are associated with the entire >1600km volcanic-rifted margin of Namibia. The first tectono-magmatic zone is the oceanic crust which when imaged seismically is denoted by an apparent lack of continuous reflectors. With a combination of gravity modelling and seismic imaging Gladczenko et al. (1999) arrived at an average thickness of about 6km for the oceanic crust. The top of the oceanic crust is partially rubbly and undulating, suggesting sub-aerial to shallow marine environments of deposition. The surface then transits into a more regular smooth and continuous top that occasionally downlaps onto a landward dipping shear/fault that is deciphered as the marginal hinge line. The more regular surface tops high amplitude acute reflectors that dip seaward hence termed Sea-Dipping Reflectors (SDRs).

SDRs as mentioned earlier, are basaltic lava flows that are possibly interbedded with sediments and stretch 75-175 km wide with a thickness of 4-5km (Gladczenko et al., 1999; Torvsik, et al., 2009), their smooth top surface therefore ensembles sub-aerial volcanism. The SDRs thin progressively landwards until termination near the shelf break. Gladczenko, et al. (1999) as well as McDermott et al (2015) both agree that these (SDRs) are the same age as rifting and could therefore be an outer extension of the Etendeka-Paraná igneous province (132Ma). The SDRs package have been penetrated by recent drilled wells (Moosehead, Murombe and Kabeljou) and are characterized by basaltic flows intercalated with aeolian sands, lacustrine shales and fluvial sediments which indicates volcanism in sub-aerial environment (McDermott et al., 2015).

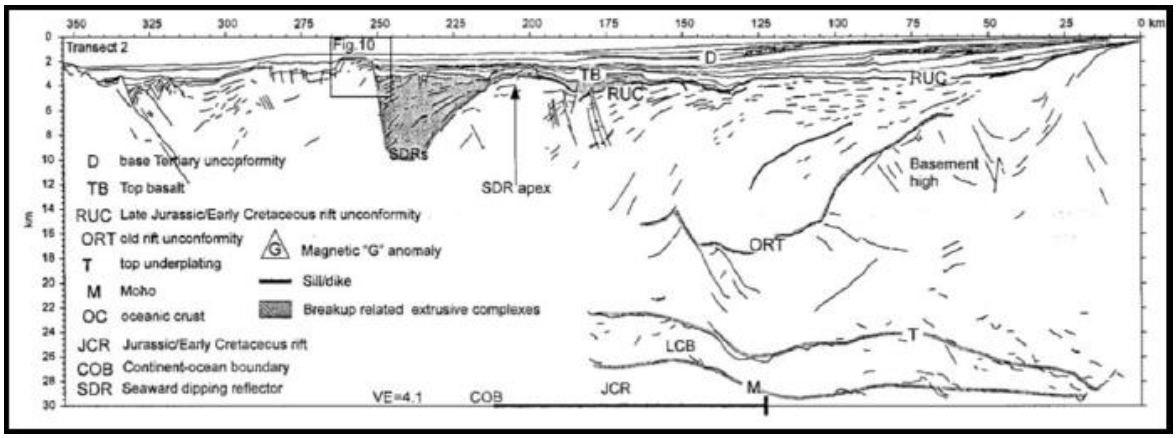

Figure 7: Crustal structure of the Namibian shelf margin based on seismic transect from the Luderitz basin (Gladczenko et al., 1999).

2.2 Tectonostratigraphy offshore Namibia passive margin

Several authors such as de Vera et al. (2010), Jungslager (1999), and Light et al. (1992/93) have dissected the strata of of the Namibian volcanic-rifted margin in five tectono-stratigraphic megasequences corresponding to five phases of rift development (Figure 8 & 9). These are namely:

- Late Cretaceous to Tertiary Thermal Sag (Horizon P to Sea Floor)
- Late Hauterivian-Aptian Transitional (Horizon P to Q)
- Late Jurassic to Early Cretaceous Synrift II (Horizon R to Q)
- Early Cretaceous Synrift I (Horizon T to R)
- Permo-Carboniferous to Jurassic Pre-rift (Horizon W to T)

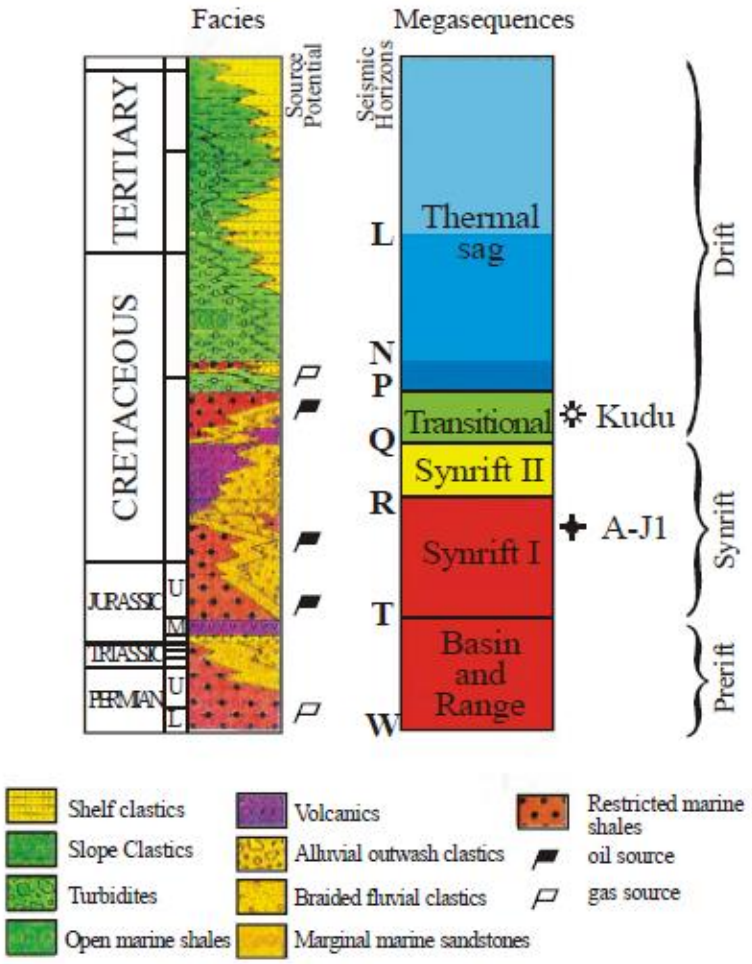

Figure 8: Stratigraphy and seismic horizons of the south-west African offshore, after Light et al. (1993).

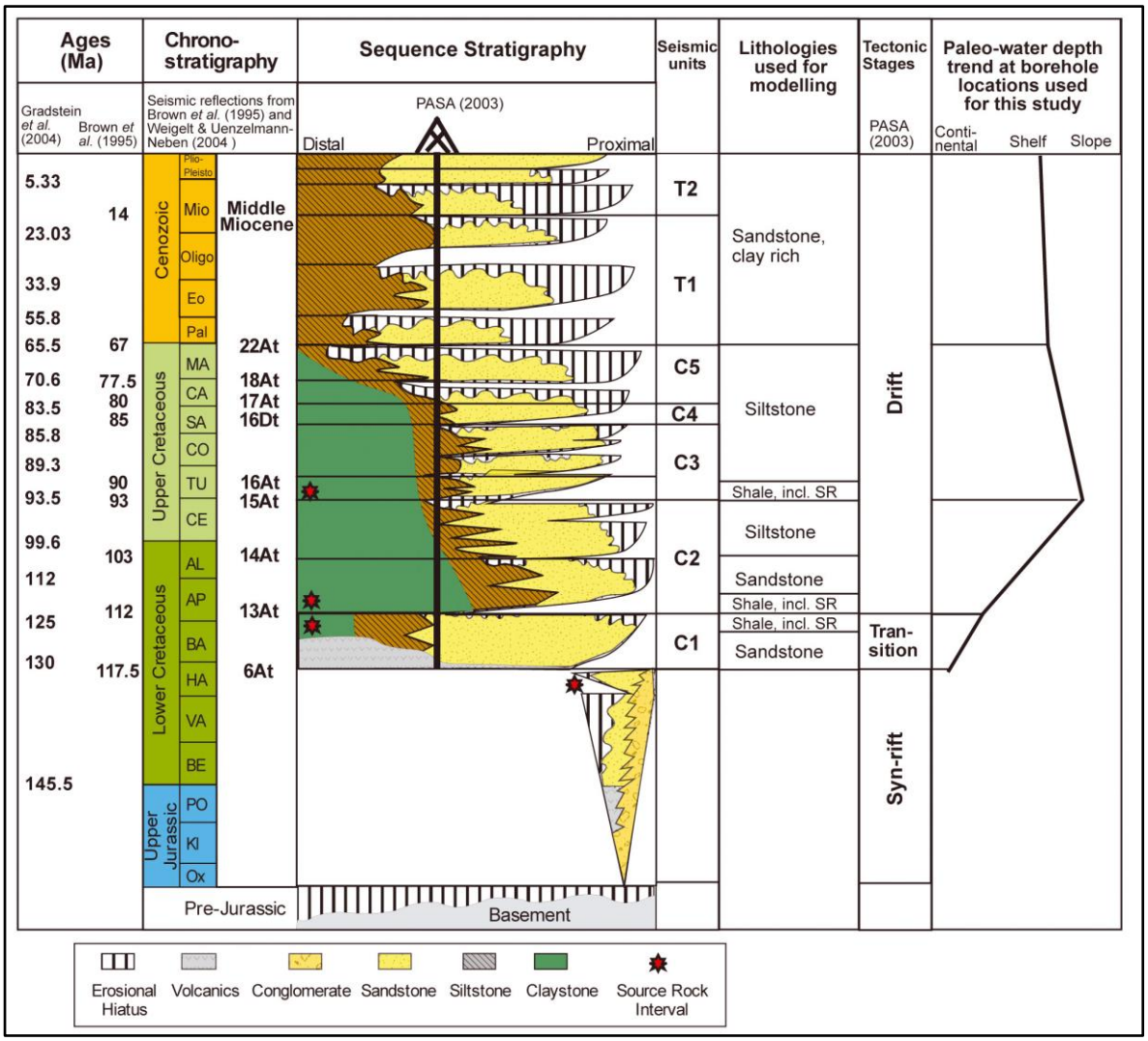

Figure 9: Regional seismic horizons and their tectonostratigraphic significance illustrating the major stratigraphic units and unconformities in the Orange Basin (Kuhlmann et al., 2011).

Permo-Carboniferous to Jurassic Pre-rift (Horizon W to T)

The Pre-rift megasequence also known as the Basin-and-Range megasequence consists essentially of the Karoo formations as defined within the main Karoo Basin and southern Namibia (Kent, 1980). Possible Karoo Supergroup rocks are preserved in small half-

grabens and are truncated by an angular unconformity, which likely represents significant erosion of Karoo Supergroup material over a prolonged period (Aizawa et al., 2000; Clemson et al., 1997). According to Light et al. (1992), interpretation of the seismic facies of the pre-rift sequence becomes difficult with increasing depth due to the deterioration in seismic signature, with almost total character loss in places, particularly beneath overlying highly reflective intervals. However, seismic reflectors along a N-S trending belt were interpreted to display a complex pattern of high amplitude, discontinuous, irregular and hummocky events, which probably represent arid continental deposits with aeolian dunes, fluvial sands, lower energy braid plain silts and shales, and extensive tracts of subaerially extruded lavas (Light et al., 1992). While in the western part of the Orange Basin, seismic reflection character suggests a rather more uniform sequence, where reflectors are generally more continuous, indicating a shallow water-lain sand and shale sequence, possibly of shallow marine origin.

Early Cretaceous Synrift I (Horizon T to R) and Late Jurassic to Early Cretaceous Synrift II (Horizon R to Q)

The first synrift phase (Synrift I) is confined to the southern half of the Namibian offshore area, whereas the second synrift phase (Synrift II) is present, and thickens rapidly northwards, within the Walvis Basin towards the Walvis Ridge (Maslanyj et al., 1991). The Syn-rift Megasequence consists of Late Jurassic to Hauterivian (160-127 Ma) basin ward-dipping high amplitude, low frequency continuous to discontinuous seismic reflectors with fanning geometries that increase in dip with depth and thicken

towards the basin (a typical growth strata geometry) and underlie the present day slope of the margin (De Vera et al., 2010) (Figure 11).

According to Maslanyj et al. (1991), the Synrift I interval represents a wedge-shaped, generally westwards thickening sequence, which pinches out at the Medial Hinge Line in the east, usually due to erosion (Figure 10). Synrift II developed in the northern part of offshore Namibia and was associated with widespread volcanism (130-120 Ma) (Dingle et al., 1992/93). The lava distribution of the Etendeka flood basalt province is considered to be result of the northward propagation of the rifting during the initial stages of the opening of the South Atlantic Ocean.

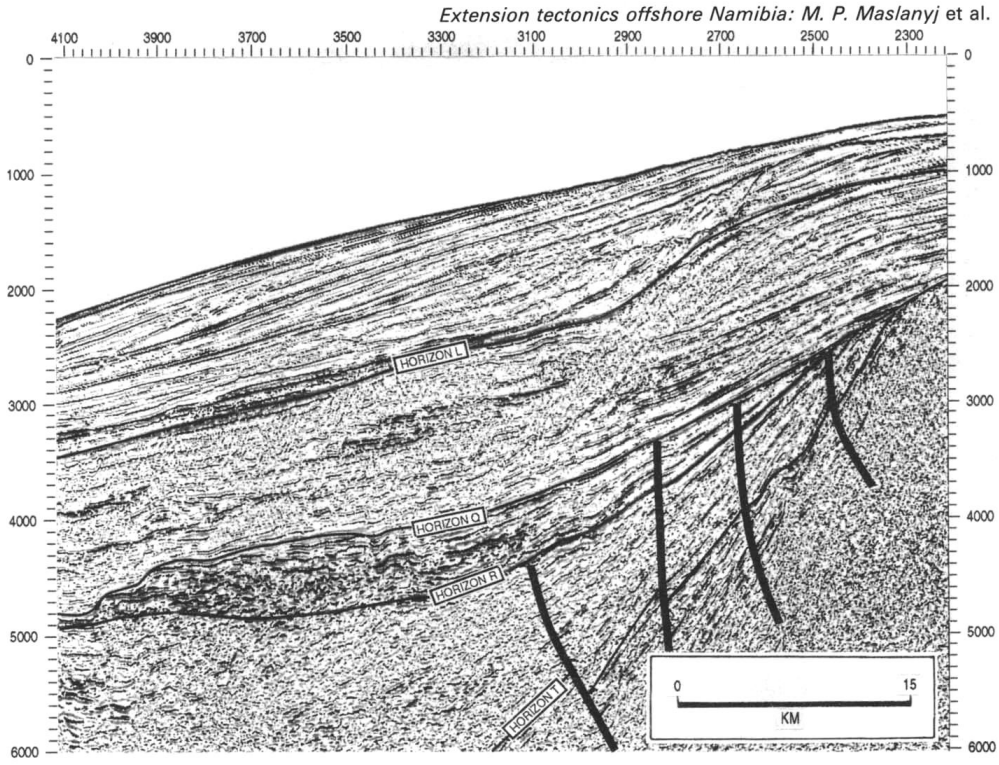

Figure 10: Seismic display of the Medial Hinge Line (right) and the Central Half Graben (Maslanyj et al., 1991).

High amplitude units at the base of the syn-rift section within the AJ graben of the Orange graben were interpreted by Jungslaeger (1999) as Late-Jurassic lacustrine source rocks (AJ-1 well drilled in 1988 penetrated a lacustrine Hautervian system). However, Aizawa et al. (2000) contradict that this amplitude essence at the base of the syn-rift could indeed be basaltic flows and quartz latites belonging to the Etendeka group of volcanics. Continental flood basalts have been indicated near the Namibian margin where they manifest themselves as tholeiitic basalts capping underlying Permo-Carboniferous sediments.

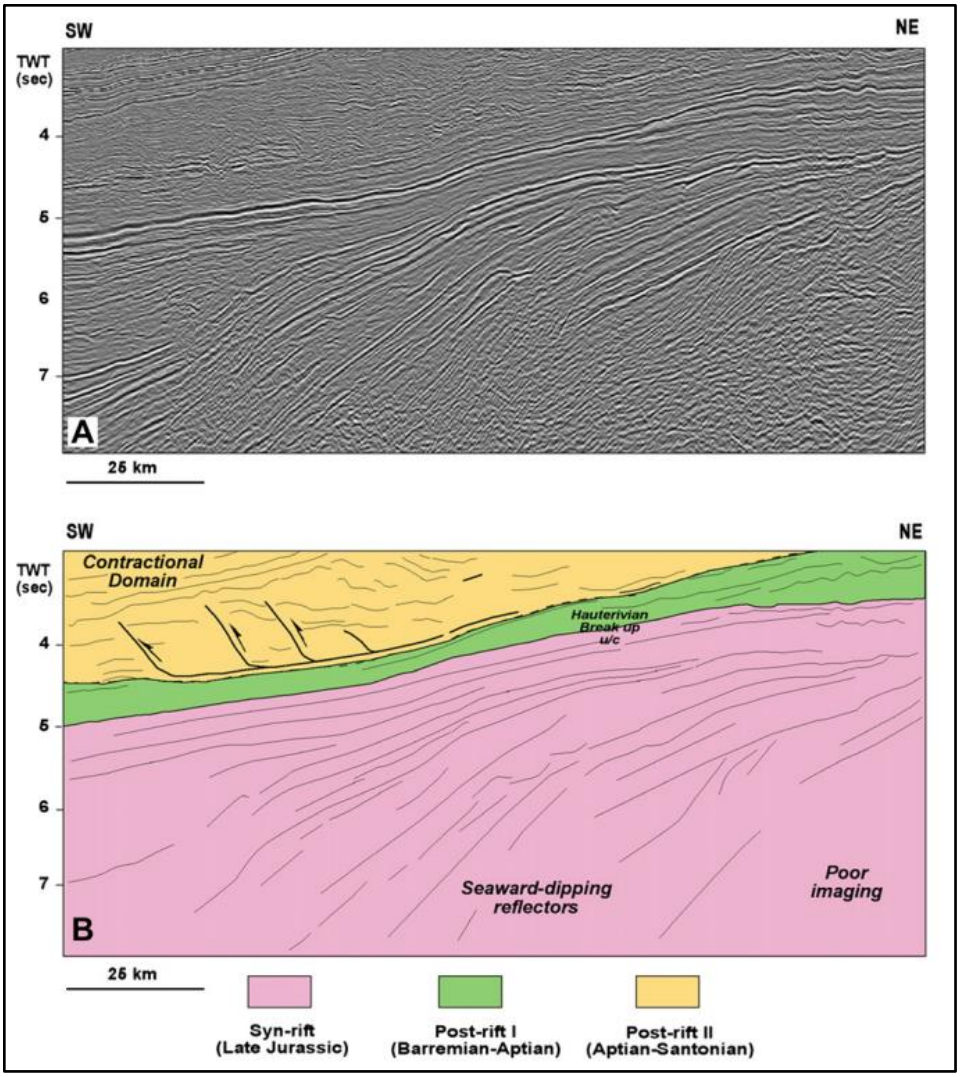

Figure 11: 2D seismic line showing the synrift seaward-dipping reflectors (De Vera et al., 2010).

Late Hauterivian to Aptian Transitional section (Horizon P to Q)

According to Light et al. (1993) the Transitional Megasequence marks the initial effects of thermal sag following the end of rifting, and is the first to contain signs of a developing shelf break. It is bounded below by Horizon Q (Hauterivian-Barremian), and

above by Horizon P (Mid-Aptian). This sequence comprises of a deepening-upward sequence of lower fluvial clastic fans overlain by a finer regime of silt and shales. A large marine-transitional source rock was deposited during the transgressive events of the Barremian-Aptian times with flooding culminating during the mid-Aptian (Kuhlmann et al., 2011; Light et al., 1993; Paton et al., 2007).

It is further stated in Light et al. (1993) that most of the Q to P succession has been intersected in the Kudu wells west of the Medial Hinge Line, where it ranges from continental beds (basalts, and aeolian to fluvial sands) in the lower part, through shallow marine sandstones containing abundant carbonate cements, to shelly sandstones that locally grade into lagoonal shales, and deeper marine siltstones and sapropelic shales at the top (Figure 12).

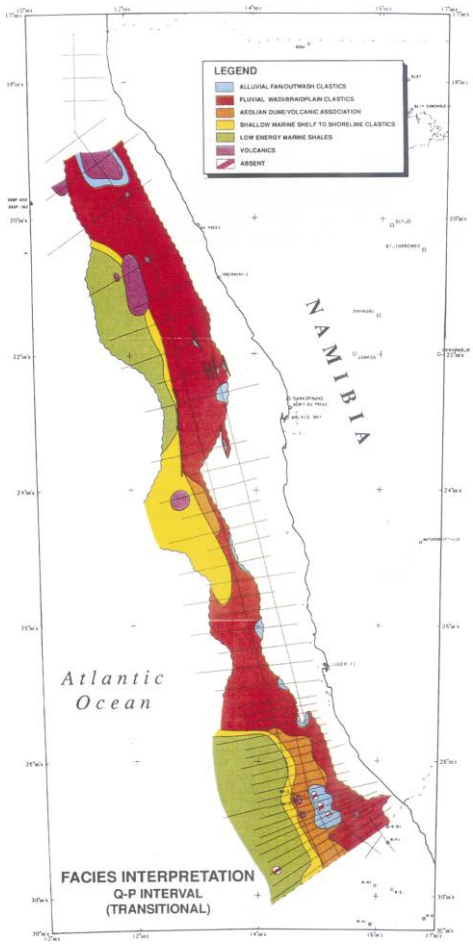

Figure 12: An interpreted facies distribution map of the basal part of the Q-P transitional interval, representing the latest phase of rifting prior to the onset of thermal sag (Light et al., 1993).

Mid-Late Cretaceous to Tertiary Thermal Sag section (Horizon P to Sea Floor)

This megasequence developed from the late Lower Cretaceous (Albian) during continued sagging and tilting of the continental margin offshore Namibia (Light et al., 1992) (Figure 9). Light et al. (1993) characterize this sequence as a progradational succession that downlaps onto Horizon P. While in the region of the Hinge Line,

Horizon N is frequently truncated and displaced by a major late Cretaceous/Tertiary-age listric slump detachment system that extends down close to the level of Horizon P (Figure 13). West of Lüderitz and off the Orange River Delta, zones of large-scale high angle listric gravity-induced faulting have caused rotation of down faulted blocks of sediment, imparting high angle reverse (landwards) dips. To the west of the megasequence, slumping often terminates in a mounded toe region or in a succession of mass flow gravity slides, slumps and stacked thrusts.

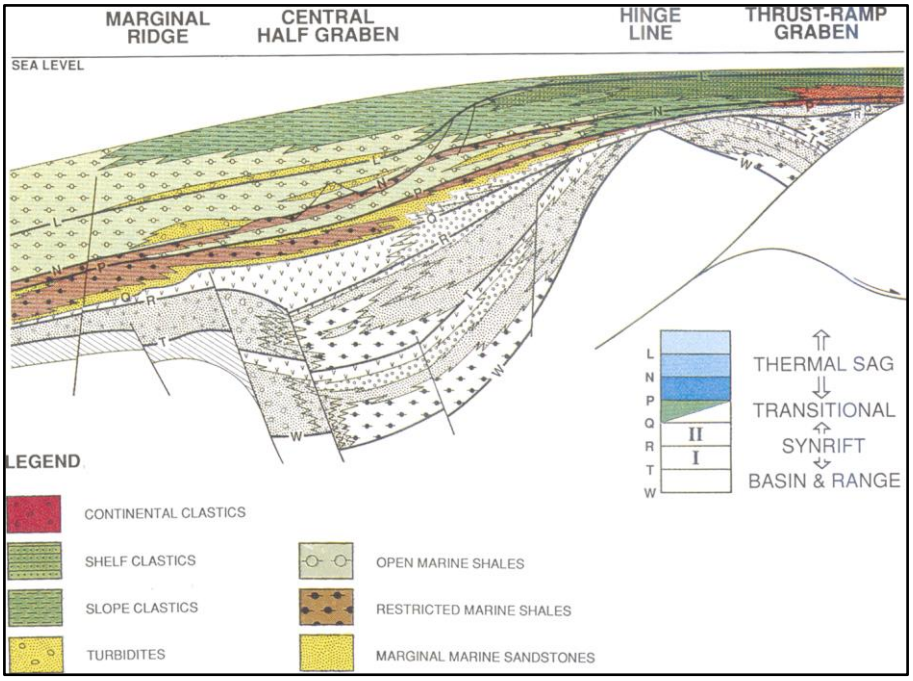

Figure 13: Thermal sag sequences (Light et al., 1993).

North of the Walvis Ridge, Tertiary sections are thick in contrast to the thin syn-rift sequences, whereas south of the Walvis Ridge the Basin & Range and syn-rift successions are extremely thick, and the Tertiary is mostly relatively thin. Their

dominant seismic character is transparent, with some high amplitude, continuous reflectors, and occasional zones of discontinuous, slightly wavy reflectors. The general description made by Light et al (1992) is that the Tertiary sequence represents rather low energy conditions, with deposition of clay and sands, and occasional thin beds of shelly limestones and extensive erosional episodes by offshore, coast-parallel, marine currents.

Namibian Margin Sequence Subdivsion

The passive margin of Namibia consists of a 3-5 km thick wedge of mainly clastic post-rift sediments that overlie a rifted Proterozoic continental basement (Light et al., 1993) and it's overlain in turn by syn-rift siliciclastics and volcanics of late Jurassic to Early Cretaceous age (Clemson et al., 1999). Light et al. (1993) and Bagguley & Prosser (1999) identified five megasequences offshore Namibia on the basis of reflection terminations and geometries, each of these is related to a major phase of basin evolution (as defined by Hubbard et al., 1985) which involve the early stages of rifting and the subsequent opening of the South Atlantic.

Light et al (1993) define the megasequences as tectono-stratigraphic sequences as shown in the scheme of table 1. Bagguley & Prosser (1990) identified almost identical sequences which they numbered from MS 10 to MS 50 (Figure 14). MS 10 to MS 30 relate to early stages of rifting (MS 10) and the opening of the South Atlantic (M S20 and MS 30). These megasequences are overlain by MS 40 (the transitional megasequence) which is in turn overlain by the main post-rift succession (defined as MS 50). The MS 50 succession consists of a prograding clastic wedge which, on the basis of seismic reflection geometries, can be subdivided into MS50a and MS50b (Figure 14)

and is dated as Turonian-Maastrichtian and Tertiary respectively, based on biostratigraphy from the Kudu wells (McMillan, 1990, 1994).

Table 1: Tectono-stratigraphic sequence divisions (Light et al., 1993) and Bagguley& Prosser, 1990).

Sequence Stratigraphy	**Seismic Horizons (Light et al., 1993)**	**Seismic Horizons (Bagguley & Prosser., 1990)**
Thermal Sag	(Horizon P-sea floor)	MS50b
Transitional	(Horizon Q-P)	MS50a
Syn-rift II	(Horizon R-Q)	MS40
Syn-rift I	(Horizon T-R)	MS20 & MS30
Basin & Range	(Horizon W-T)	MS 10

Seismic stratigraphic analysis of the post-rift megasequences of the Namibian margin enabled depositional features to be interpreted in terms of the likely controls of their formation. The scale of the information derived from seismic stratigraphic depositional system analysis is fundamental in understanding processes of sedimentation on passive margins; processes which may not be so readily apparent at well-log scale studies.

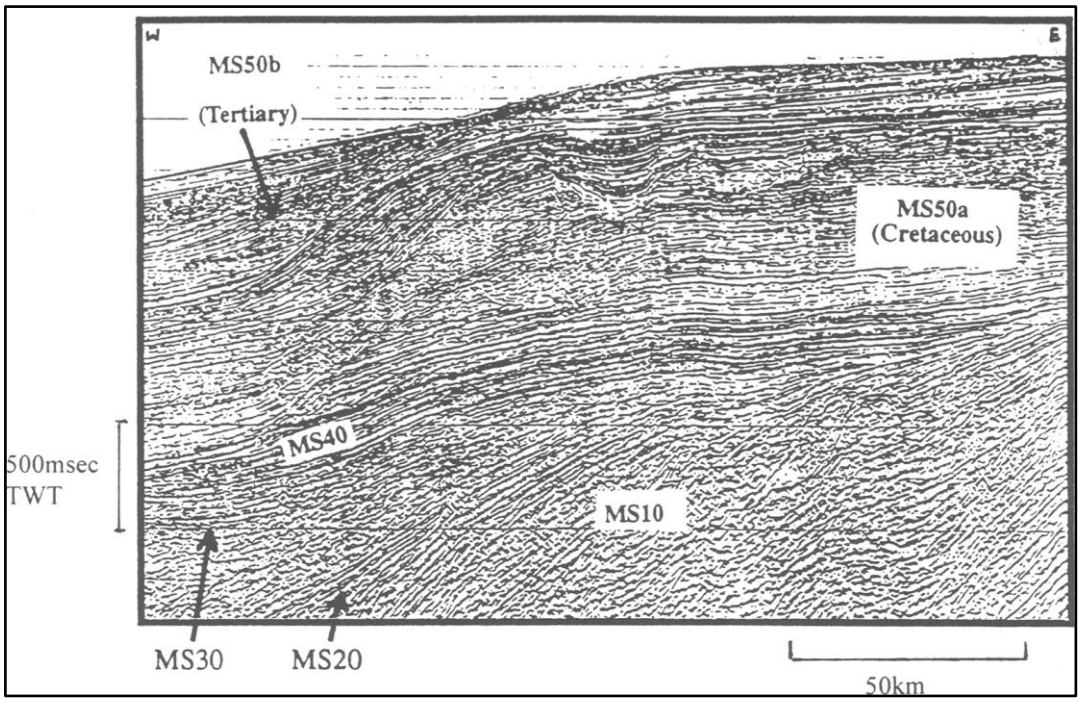

Figure 14: Seismic profile showing megasequence development along the Namibian margin from early rift phases (MS10-MS30) to the development of the clastic post-rift wedge (MS50) (Bagguley & Prosser, 1999).

Bagguley and Prosser (1999) used seismic stratigraphy to interpret seismic channel forms and shallow mounded features in the post rift succession. They interpreted the seismic channel forms on the inner shelf as incised valleys that were created during a fall in relative sea level. The valleys are filled with horizontal seismic facies suggesting that they filled during progressive periods of rising relative sea level, implying late lowstand or transgressive sediments. The channel forms are occurring in the Orange, Lüderitz and Walvis Basins, where they are observed to have developed contemporaneously with laterally extensive unconformities at the Cretaceous-Tertiary boundary and at several different stratigraphic levels within the MS 50a (Turonian-Maastrichtian) unit.

Prominent seismic channel forms also occur in the outer shelf and upper slope. They are interpreted as upper slope smaller scale channels features and larger scale submarine canyons (Bagguley & Prosser, 1999) (Figure 15). The submarine canyons are described as erosional as distinct truncations are found at their lower boundaries and are recognized at Turonian and Tertiary levels. The majority of the canyons identified are infilled by two distinct seismic facies (Bagguley & Prosser, 1999); the lowermost of these facies is characterized internally by chaotic reflections and externally by a mounded form. This basal fill is overlain by the more continuous, parallel, and moderate to high amplitude reflections of the upper fill which drape the walls of the canyons; a geometry consistent with submarine origins (Bagguley & Prosser, 1999). Therefore, in contrast to the parallel reflections which infill the previously described incised valleys of the inner shelf, the draping upper canyon fills must have been submerged at the time of deposition, thus implying a dominantly submarine origin.

Bagguley & Prosser (1999) distinguish between attached and detached submarine canyons depending on whether they can be shown to link back into fluvial systems on the shelf; attached canyons will be more likely to be able to support the development of deepwater, sand-rich submarine fans.

A series of shallow mounded features was also identified on the shelf, which were interpreted as palaeo dune fields, or carbonate build-ups, or longshore clastic mounds. Bagguley & Prosser (1999) offer a transgressive and alternative lowstand setting model for shelfal mound deposition.

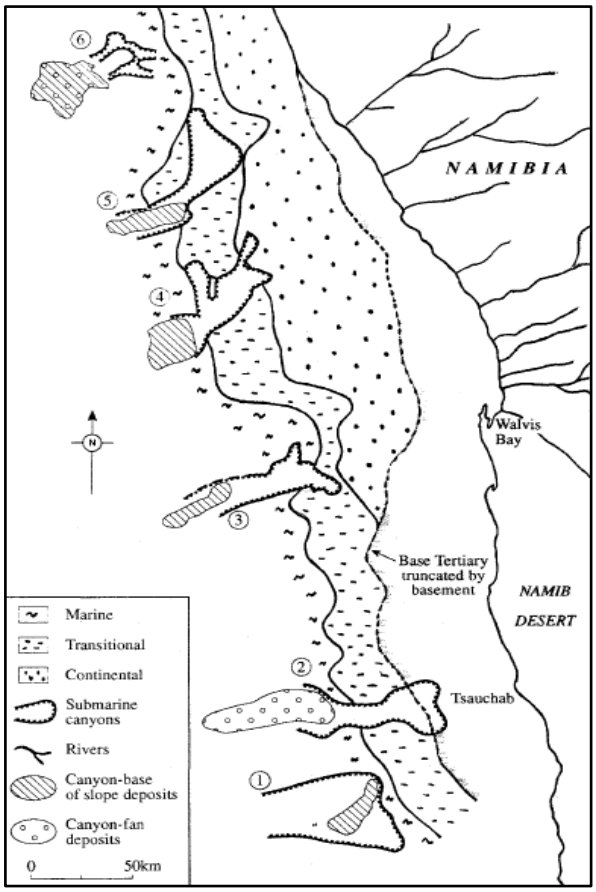

Figure 15: Spatial distribution of submarine canyon systems (numbered 1-6) developed at the Cretaceous-Tertiary boundary (Bagguley & Prosser, 1999).

2.4 Geology of the Lüderitz Basin

The Lüderitz Basin is an elongated basin fronting the Lüderitz Arch, a westward plunging basement nose (Maslanyj et al., 1991), it is located south of the Walvis Basin and north of the Orange Basin. Like the other offshore basins on the Namibian passive margin the Lüderitz Basin formed during the opening of the Atlantic Ocean in the late Jurassic to the early Cretaceous. Both four offshore basins have the same morphology with a common mechanism of formation (Hodgson et al., 2013). Due to variations in sedimentation rate and thicknesses, geographic as well as geomorphologic disparities

caused by the several stress regimes, sediments input into the basin varies significantly, finding that sediments in the Lüderitz Basin are mainly thick shallow marine to deltaic sandstones deposited in the upper and lower Cretaceous, overlying continental clastics and volcanics.

The Lüderitz Basin displays a thin late Cretaceous section but the Tertiary developed rapidly accumulating a thick clastic section laterally offset from the present mouth of the sediment source (Hodgson et al., 2013), propbably mainlay the Orange River. Furthermore Hodgson et al., (2013) discovered a solid gas hydrates accumulate layer near the surface recognized by the Bottom Simulating Reflection (BSR) near the top of the Tertiary sequence.

Figure 16 displays an idealized cross section of the Lüderitz Basin, the ‘M4” anomaly in the cross section is a magnetic anomaly representing volcanism of the SDRs with significant underplating, while the ‘G’ (gravity) anomaly represents a basement high.

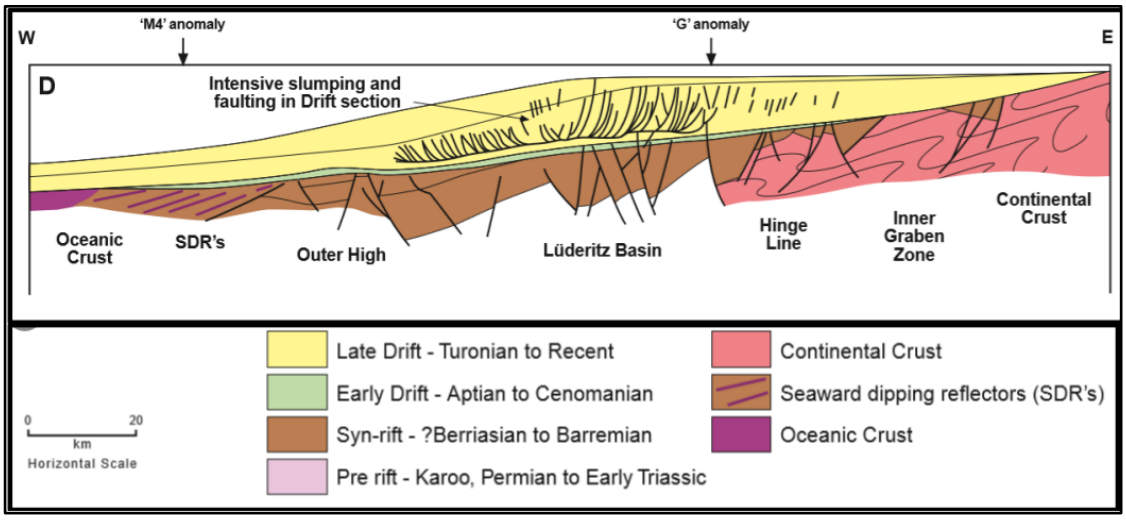

Figure 16: Idealized cross section of the Lüderitz Basin (Bray et al., 1998).

2.5 The Lüderitz Basin in comparison to neighboring basins

With a common mechanism of formation, unsurprisingly all of the four Namibia Offshore basins have similar basement morphologies (Figure 17). Aizawa et al. (2000) identified from the regional stratigraphy that the concentration of much of the offshore sediment volumes are in the Orange and Walvis basin, and thinner sequences are preserved in the central margin. This shows that sediment input from the Southern African Plateau has varied significantly into each basin through time and varied greatly both within and between basins. Such variation in sedimentary depocenter location is an important feature of the Namibian passive margin and its conjugate, the Pelotas Basin in Brazil and Uruguay (Saunders et al., 2013). During most of the post rift development the Walvis and Orange basin were the main depocenters. In contrast much of the post rift section in the Lüderitz basin is poorly developed with deposition directly onto the basement high of the Lüderitz Arc (Stewart, 2000). Herewith the Lüderitz Basin displays a thinner Late Cretaceous section compared to the Orange Basin and yet displays a thicker Tertiary section (Figure 19). The Tertiary section in the Lüderitz Basin developed very rapidly, accumulating a thick clastic section. The rapid Tertiary aggradation triggered conspicuous gravitational collapse tectonics (figure 17).

This development correlates with a shift in maximum sediment influx northwards towards the Lüderitz and Walvis basins during the Tertiary period compared to the Orange Basin (see figure 18). In the Orange Basin growth-faulting during drift phase sedimentation is widespread, but is almost absent in the other two basins (figure 19). In addition, numerous submarine canyons incised into the Late Cretaceous and Early Cenozoic times are present within the Lüderitz as well as Walvis basins but are

essentially absent within the Namibian portion of the Orange Basin (Clemson et al., 1997).

The basement structure of the Lüderitz basin shows less stretching and herewith less syn-rift subsidence compared with the Walvis and Orange basins. Dingle et al. (1992/93) explain this difference with the buoyancy of prominent granitic cratonic basement underlying the Lüderitz Basin.

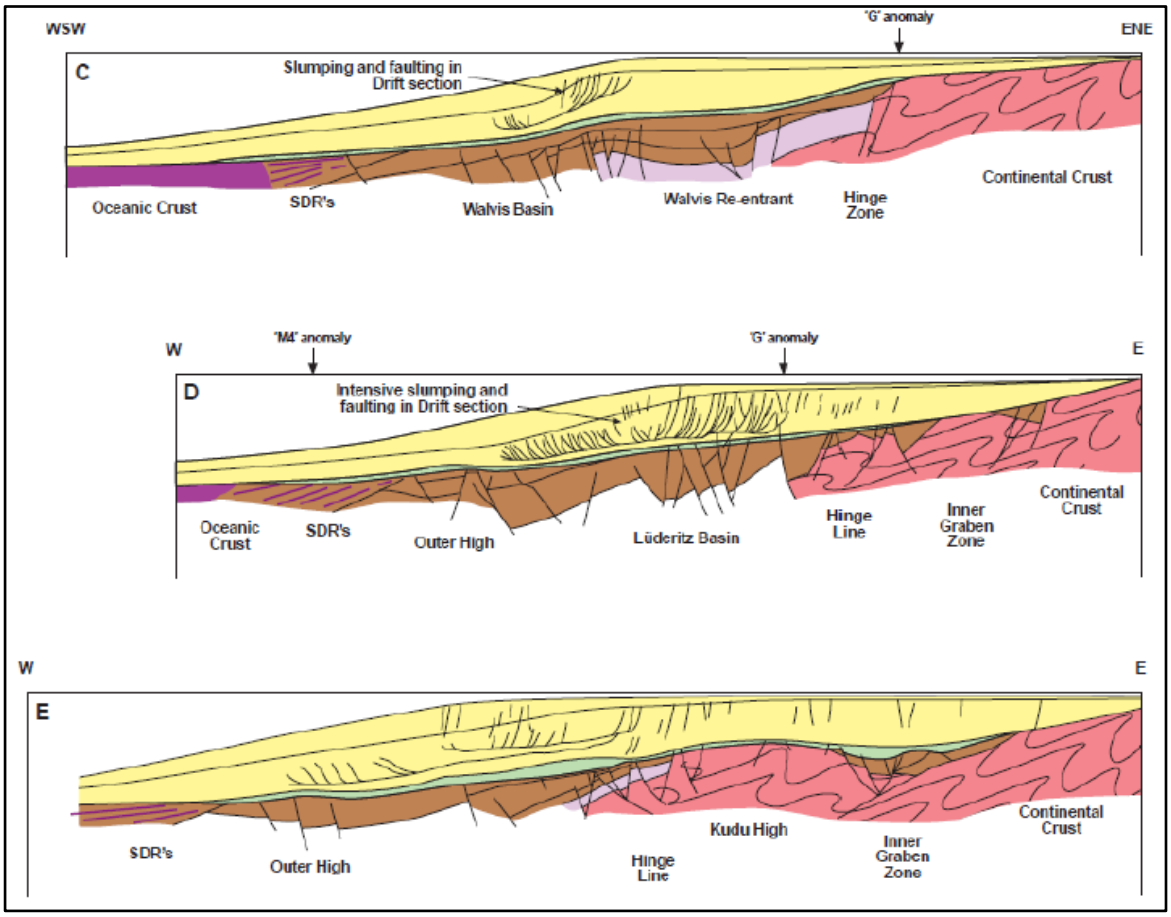

Figure 17: The structural framework for the southern basins. The top diagram represents the Walvis basin, beneath the Lüderitz basin and the bottom is the Orange basin. The Lüderitz basin's drift section is subjected to more intense gravitational collapsed structures compared to the other two basins (Bray et al., 1998).

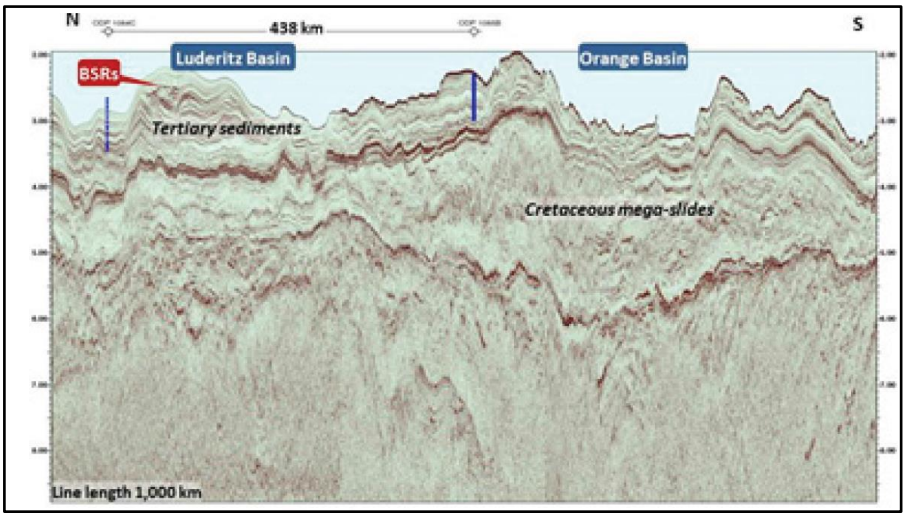

Figure 18: Sediment variation within the Orange and Lüderitz basin (Intawong & Hodgson, 2015).

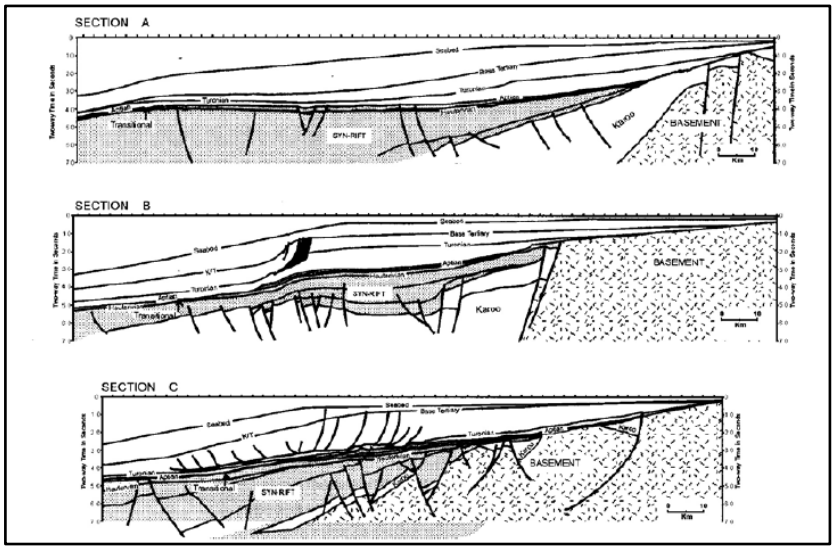

Figure 19: Geomorphic evolution of the Namibian offshore across three basins: Walvis Basin (section a), Lüderitz Basin (section b) and Orange Basin (section c) (Aizawa et al., 2000).

2.6 Hydrocarbon potential

According to Bray et al. (1998), there are at least two oil-prone source rock intervals found in the early to mid-Cretaceous drift section of the Namibian Passive Margin (Figure 20). One of these source rocks was deposited during the early Aptian (marine shale) when restricted marine conditions prevailed in the South Atlantic (Jungslager, 1999; Kuhlmann et al., 2011), before the Falkland Plateau had cleared the southern tip of Africa allowing full global ocean circulation. While the second source rock interval accumulated during the Cenomanian to Turonian (also marine shale), coinciding with the mid Cretaceous Oceanic anoxic event (Jungslager, 1999). The Synrift section (with potential lacustrine intervals) may also provide source rock potential and has been speculated for the Lüderitz Basin, its existence has been proven by the AJ-1 oil discovery well in the Orange Basin in South Africa (Bray et al., 1998,).

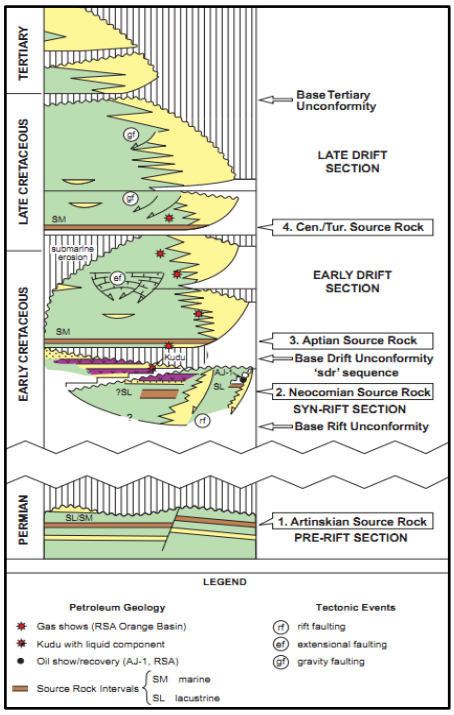

Figure 20: Generalized Stratigraphy of Source Rocks of the Namibian Offshore Passive Margin (Bray et al., 1998).

The Lower Aptian containing a marine oil and gas prone source rock is approximately 140 m to 300 m thick in the Kudu wells, 200 m in Moosehead-1 well and overlying several thinner source intervals in the Barremian (Bray et al., 1998). The pyrolysis parameters indicate Type II kerogens characteristic of a source with both oil and gas potential. A good quality Aptian source rock is also developed in the South African Orange Basin found southeast of the Kudu well. The Cenomanian-Turonian interval appears to be absent in the Kudu wells however an oil prone source rock of similar age is occurring in the Walvis Basin (Bray et al., 1998) and a gas prone source rock in wells

A-H1, K-A2, K-A3, K-H1, K-F1, A-L1, K-D1, A-U1, A-C1 and A-C3 of the southern Orange Basin drilled on the continental shelf.

According to Bray et al. (1998), source rock potential may also be found in the syn-rift section of the margin, and it's predicted that lacustrine environments were developed during early rifting making it possible to preserve organic rich, oil-prone claystones that are making up this source rock (Jungslager, 1999). Furthermore, there is a possibility of oil source potential in the pre-rift Karoo section, this is supported by regional presence of rich oil prone marine source rocks developed widely in the southern Africa as the Permian Whitehill Formation and its equivalent the Irati oil shales of South America. A live oil seep found onshore Namibia has been geochemically linked to the Permian Whitehill Formation (Summons et al., 2008). Figure 21 below shows source rock distribution potential along the Namibia offshore Passive Margin.

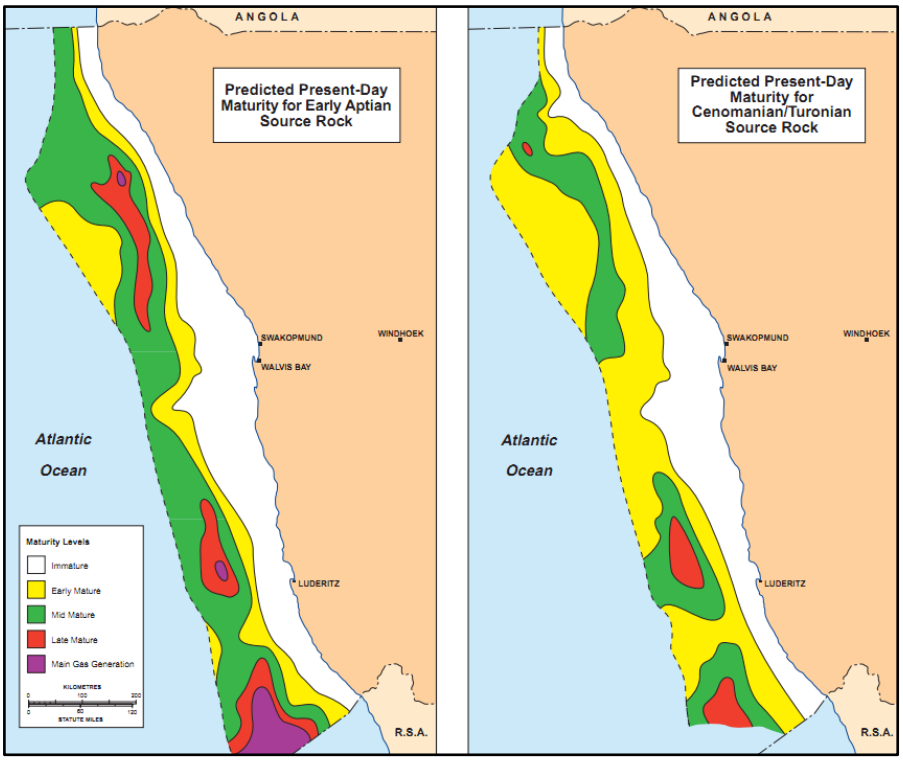

Figure 21: Source Rock distribution along the Namibia offshore Passive Margin (Bray et al, 1998).

It is stated in the NAMCOR E &P Booklet (2016) that Early Cretaceous transitional reservoirs have been proven by the Kudu field comprising of aeolian sandstones intercalated with volcaniclastics, marine sandstones and shaly limestones. These reservoirs have an average net thickness of 50 m and a porosity of up to 20%. Other potential deep water reservoirs also exist in the form of basin floor fans overlying the mid-Aptian and top Santonian unconformities in the deeper section north of Kudu, along with marginal marine/fluvial sand deposits within the syn-rift section (Spectrum Newsletter, 2012).

The Lüderitz Basin also contains potential reservoirs within the Lower Cretaceous, Upper Cretaceous and likely in the Palaeogene, the thick shallow marine shelfal sand proven in well 2513/8-1 at a gross interval of 1363-1408m with an average porosity of 17% (NAMCOR E&P Booklet, 2016).

A regional top seal for the Orange Basin is proven at the Aptian-Albian shale level by the big pressure differential between over-pressured Aptian-Albian carbonates and the younger normally pressured sandstones (NAMCOR E&P Booklet, 2016). Mesozoic intra-formational shale occurring at various intervals has been identified as prospective cap rock in the Walvis basin, while in the Orange basin, the Barremian and Aptian source rock also serves a seal rock (NAMCOR E&P Booklet, 2016).

CHAPTER 3: MATERIALS AND METHODS

Seismic data, well reports, and industry technical communications (brochures, farm out flyers, presentations) created the data base upon which seismic stratigraphic interpretation and 1D burial history studies were carried out.

3.1 Data

3.1.1 Seismic data

Selected lines of the GPN13 2D seismic dataset on blocks 2412B/2413B were used for this study. The GPN13 seismic lines were acquisitioned by the MV Osprey Explorer Survey vessel in 2013 covering a seismic survey length of 2012.875 km (Figure 22) in the Lüderitz basin, offshore Namibia. Shots were generated from a source volume of 107.95 m^3, while the survey shot point intervals measured 25.0 m reaching a recording length of 9000 ms. The deliverables from processing included velocity correction, PSTM angle stacking and PSTM.

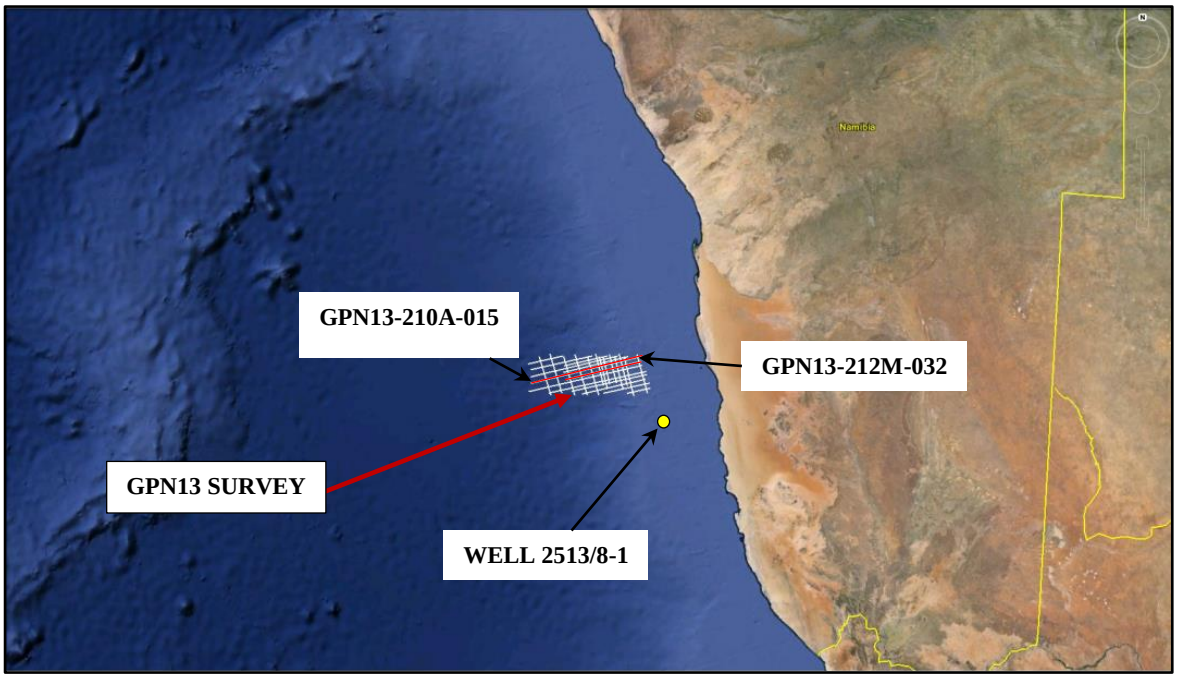

Figure 22: GPN13 Survey location map in the northern portion of the Lüderitz Basin, offshore Namibia. Highlighted in red are the two GPN 13 survey dip lines and location of well 2513/8-1 used for this study. Map modified from Geopartners (2014).

Two adjacent dip-lines (GPN13-212M-032 and GPN13-210A-15) were examined. Final interpretation was carried out on line GPN13-212M-032 (Appendix 2), while parallel line GPN13-210A-15 served for verification and comparison. Interpretation was carried on a workstation equipped with OpendTect V6.4.4/win64 seismic modelling software. This software is one of the accepted seismic interpretation tools in petroleum exploration.

3.1.2 Well data

The only exploration well in the Lüderitz Basin is well 2513/8-1 for which the final well report as well as the biostratigraphy report was accessible. The final well report contains information on drilling parameters, lithologies and a brief geological evaluation. The

biostratigraphy report includes information on biostratigraphy below the top Camapanian down to the Barremian well section. Within this interval a sequence stratigraphic interpretation and an estimate of paleo water depth is included.

Well 2513/8-1 is located almost 100 km SSE of the shelfal section of line GPN13-212M-032 (Figure 22). No seismic tie line into the study area was available and therefore the information of well 2513/8-1 can only tentatively be extrapolated into the study area.

Well 2513/8-1 was drilled in 1998 by Norsk Hydro AS, a Norwegian company, in the Lüderitz Basin (Figure 22). The well was drilled on the shallow shelf at a water depth of 243 m and reached a total depth of 2550 m MD, just below the Barremian interval; the uppermost section of the syn-rift. The well was drilled to test a pinchout structure; named the 2513-A-Lobe within the area of an interval with clear foreset pattern on seismic. Upon its completion, the well was declared dry, plugged and abandoned. According to the logging report, the well intersected lithologies that comprise of immature conglomerates, sandstones, siltstones, claystones and carbonates such as marl and limestones. The predicted reservoir was in essence immature conglomerates and sandstones. The well did not penetrate through any obvious organic rich shales (Gahlla, 1998).

3.2 Methods

3.2.1 Horizon Interpretation

Strong seismic reflectors were picked as they serve as marker horizons, often of stratigraphic significance. Seismic horizons were mapped manually and using semi-

automated tracking. Mapping of seismic marker horizons included the presumed main source rock intervals, tratigraphic surfaces such as unconformities, downlap surfaces, and onlap surfaces. Seismic facies mapping was carried out within stratigraphic packages that are bounded by the previously identified stratigraphic horizons.

3.2.2 Identification of Seismic Stratigraphic Surfaces

3.2.2.1 Seismic Stratigraphic Surfaces in Sequence Stratigraphy

Sequence stratigraphy is a stratigraphic discipline in which stratigraphic surfaces that represent changes in depositional trend are used for correlation and for defining specific types of sequence stratigraphic units (Embry et al., 2007). Depositional sequences are defined as relatively conformable successions of genetically related strata bounded at the top and at the bottom by unconformities and their correlative conformities (Mitchum et al., 1977). Sequence stratigraphy helps recognize packages of strata each of which was deposited during a cycle of relative sea-level change and/or changing sediment supply. These packages of strata are bounded by chronostratigraphic surfaces, these surfaces include unconformities formed during relative sea-level fall and flooding surfaces formed during relative sea-level rise.

Unconformities bounded sequences are composed of “parasequences” and “parasequences sets”, which are stratigraphic units characterized by overall upward-shoaling of depositional facies and bounded by marine flooding surfaces and their correlative surfaces (Vail, 1987; Van Wagoner et al., 1988, 1990). These depositional elements are themselves assembled into “system tracts” (Brown et al., 1997) according to position within a sequence and the manner in which parasequences or parasequences

sets are arranged or stacked. Upward-shaoling successions bounded by flooding surfaces (parasequences) are best developed in near shore and shallow-marine settings in both siliciclastic and carbonate environments (Allen & Allen, 2013).

A Transgressive Surface (TS) develops at the point at which the rate of creation of accommodation due to relative sea-level rise exceeds the rate of sediment supply to fill the space. A Transgressive Surface (TS) marks the start of retrogradational patterns within the sedimentary succession as accommodation outpaces sediment supply (Nichols, 2009). When the rate of sea-level rise slows down the depositional system reaches the point where the accommodation is balanced by sediment supply, and when this happens, transgression ceases and the shoreline initially remains static and then starts to move seawards. This point of furthest landward extent of the shoreline is called the Maximum Flooding Surface (MFS) (Nichols, 2009).

The Transgressive Surface (TS) and Maximum Flooding Surface (MFS) occur within the depositional sequence and allow it to be subdivided into three systems tracts – Lowstand (LST), Transgressive (TST) and Highstand (HST), that develop during a sinusoidal, base-level rise/fall cycle. The lower units are called Lowstand Systems Tract (LST) and consists of a basal unit of turbidites overlain by a progradational wedge which on-laps the upper slope portion of the sequence bounding unconformity. The LST is bound by the sequence boundary below and the transgressive surface above (Figure 24). The transgressive surface marks the change from progradational sedimentation below to retrogradational sedimentation above. The LST is interpreted to have developed during most of the base-level fall and the early part of sea level rise.

The middle unit is called the Transgressive Systems Tract (TST) and it consists of retrogradational sediments that overstep the LST and on-lap the shelfal portion of the subaerial unconformity. The TST is bounded by the transgressive surface below and the Maximum Flooding Surface (MFS) above (Figure 23). The MFS is defined as the surface of sequence stratigraphy that marks the change from retrogradational sedimentation below to progradational sedimentation above. The Transgressive Systems Tract is interpreted to have developed during high rates of base level rise. The upper systems tract is termed the Highstand Systems Tract (HST) and it consists of progradational sediments which were capped by a subaerial unconformity (sequence boundary on the basin flanks and by the correlative surfaces farther basinward (Figure 23 & Table 2). The HST is interpreted to have developed during the waning stage of baselevel rise and the early portion of base-level fall.

3.2.2.2 Reflection Termination Mapping

The seismic surfaces which form the upper and lower boundaries of depositional sequences are characterized by different reflection termination patterns (figure 23). Therefore reflector terminations (Figure 23) with features such as toplap, downlap, erosional truncation and onlaps are pivotal for seismic surface recognition. Mitchum et al. (1977) characterized the upper boundary being by toplap and/or an erosional truncation termination pattern whereas the lower boundaries are defined by downlaps and onlaps (Figure 23). These patterns derive from variation in relative sea level in conjunction with sediments supply, and herewith with changes in the amount of accommodation space available.

Toplap reflection terminations were identified by mapping the upper boundaries of depositional packages in the seismic, where termination of strata against overlaying surfaces was recognized. While onlaps surfaces were identified by mapping where horizontal strata progressively terminated against inclined surfaces and/or where inclined strata terminated up dip against surfaces that are of greater inclination. The downlaps where identified by mapping down dip terminations of inclined strata against horizontal or inclined surfaces. Erosional truncations were identified by mapping strong angularity with overlying younger strata and is indicative of an erosional unconformity. Onlaps, downlaps and toplaps indicate non-depositional hiatuses, whereas truncations indicate an erosional hiatuses or it may be the result of structural disruption (Vail et al., 1977a).

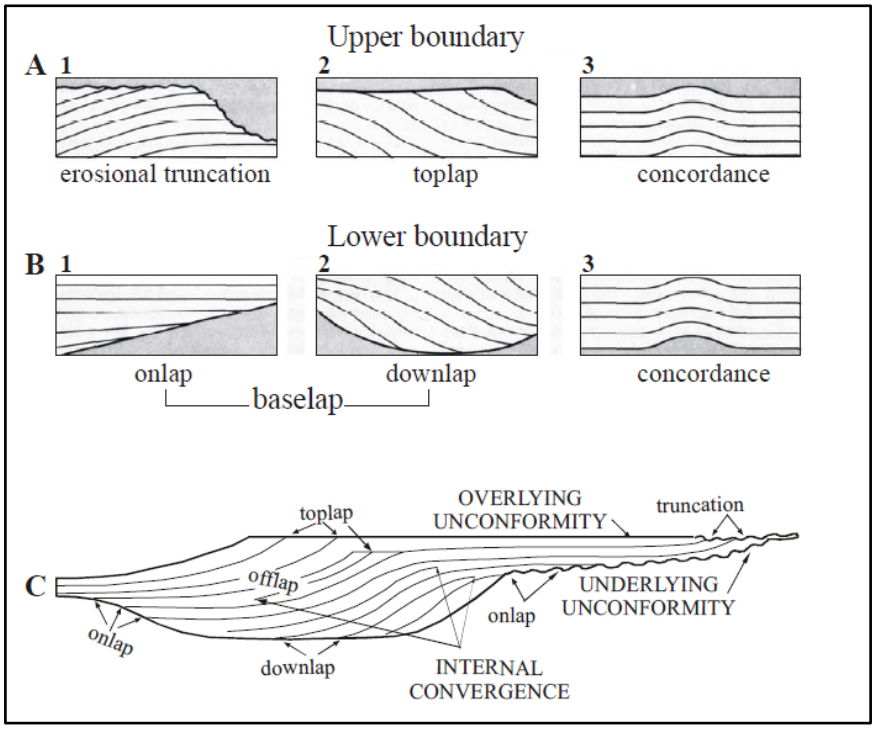

Figure 23: Reflection termination patterns indicating upper and lower boundaries of depositional sequences (Mitchum et al., 1977).

3.2.2.3 Identification of System Tracts

LSTs were identified on the seismic section by recognizing external forms of deposits such as mounds, fans, wedges, and by reflection configurations such as chaotic, hummocky and prograding clinoforms beyond the shelf edge (Figure 24 & Table 2). The TSTs were identified by mapping progressive units of retrostepping seismic onlaps bounded by a marine flooding surfaces on top, also a weak downlap pattern might be developed but is often below seismic resolution (Figure 24 & Table 2). Towards its top, the MFS, the TST is typically condensed. In seismic the downlap pattern was difficult to identity but could occasionally be recognized as subtle continuously downlapping events, with distinguishing reflection patterns and characters, above and below them.

HSTs were identified by mapping sigmoidal clinoforms that are downlapping onto a mostly weak, continuous reflection (MSF). The clinoforms may include aggrading and mostly younger prograding patterns.

Table 2: Depositional Features and Seismic Diagnosis (Reflection patterns, External Form) of various System Tracts. Modified from Nanda (2016).

System Tract	Depositional Features	Reflection Patterns, External Form
HST: Sea level above shelf edge and high sediment supply	Wedge of progradational stacks with aggradations	Sigmoidal clinoforms downlapping to a weak, continuous reflection (MFS)
TST: Transgressing sea level and little or no sediment supply	Thin retrograde onlaps, topped by a veneer of pelagic shale, the condensed section (MFS)	Weak/no downlap pattern, usually below seismic resolution
LST: Sea level below shelf edge and high sediment supply	Prograding sediments; typical wedge complex with deltas overlying slope/basin floor fans, fan deltas, submarine channel cut and fill features, etc.	Shingled/oblique progradational clinoforms, External forms of fans/ mounds with chaotic, hummocky reflections

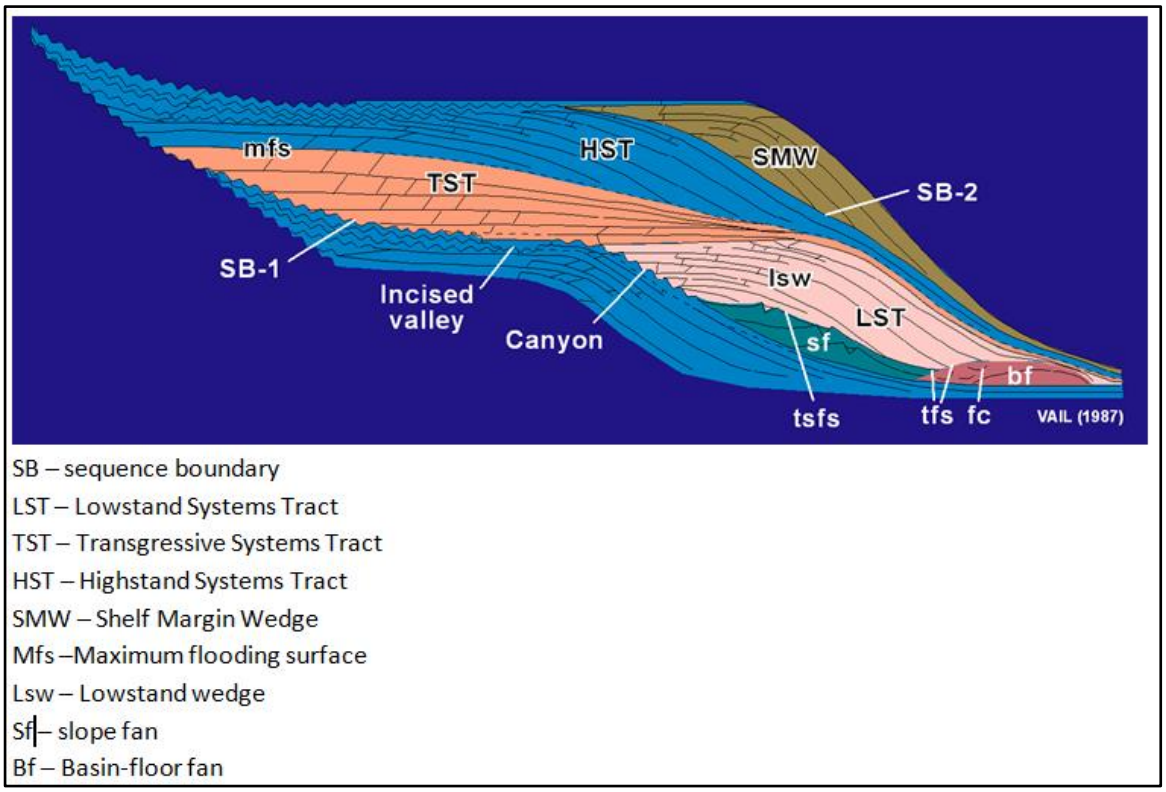

Figure 24: Illustration of the Depositional Sequence subdivisions (System Tracts); LST, HST and TST (Vail, 1987). The illustration contains further subdivisions, such as the basin floor and slope fan, which are included in this study in the LST, while the SMW is included herein in the HST.

3.2.3 Wheeler diagram construction

According to Qayyum et al. (2017), Wheeler diagrams are excellent tools to represent time stratigraphy. A Wheeler conversion assists in recognizing time relationships of the depositional systems, and their relationships to surfaces of non-deposition, condensation and erosion. These diagrams are produced by considering interpreted surfaces as snapshots of geologic times linked with transit cycles of the base level.

For this study a stratigraphic summary chart was created by hand on which the geologic time was plotted as the vertical scale and distance across the area of interest as the

horizontal scale and on which a variety of stratigraphic information was brought together. Therein the seismic reflections represent time lines and were numbered in order of deposition (starting from the oldest (numbered 1) to the youngest (top reflector). An equal time increment was given to each horizon, because there exists limited knowledge about the absolute age of most horizons.

The stratigraphic analysis of the selected 2D seismic section followed the principles of sequence stratigraphy to ultimately recognize changes in base level and identify sequences and their system tracts. For these patterns of aggrading, prograding and retrograding parasequence sets are easy to identify in the Wheeler domain. Recognition of these stacking patterns enabled infer changes in sediment supply and accommodations space as detailed in figures 25 and 26. Combined with information on the nature of stratigraphic surfaces (e.g. downlap, onlap etc.) and depositional processes inferred from seismic facies (see section 3.2.4 below), a sea level curve was constructed and corresponding system tracts were assigned.

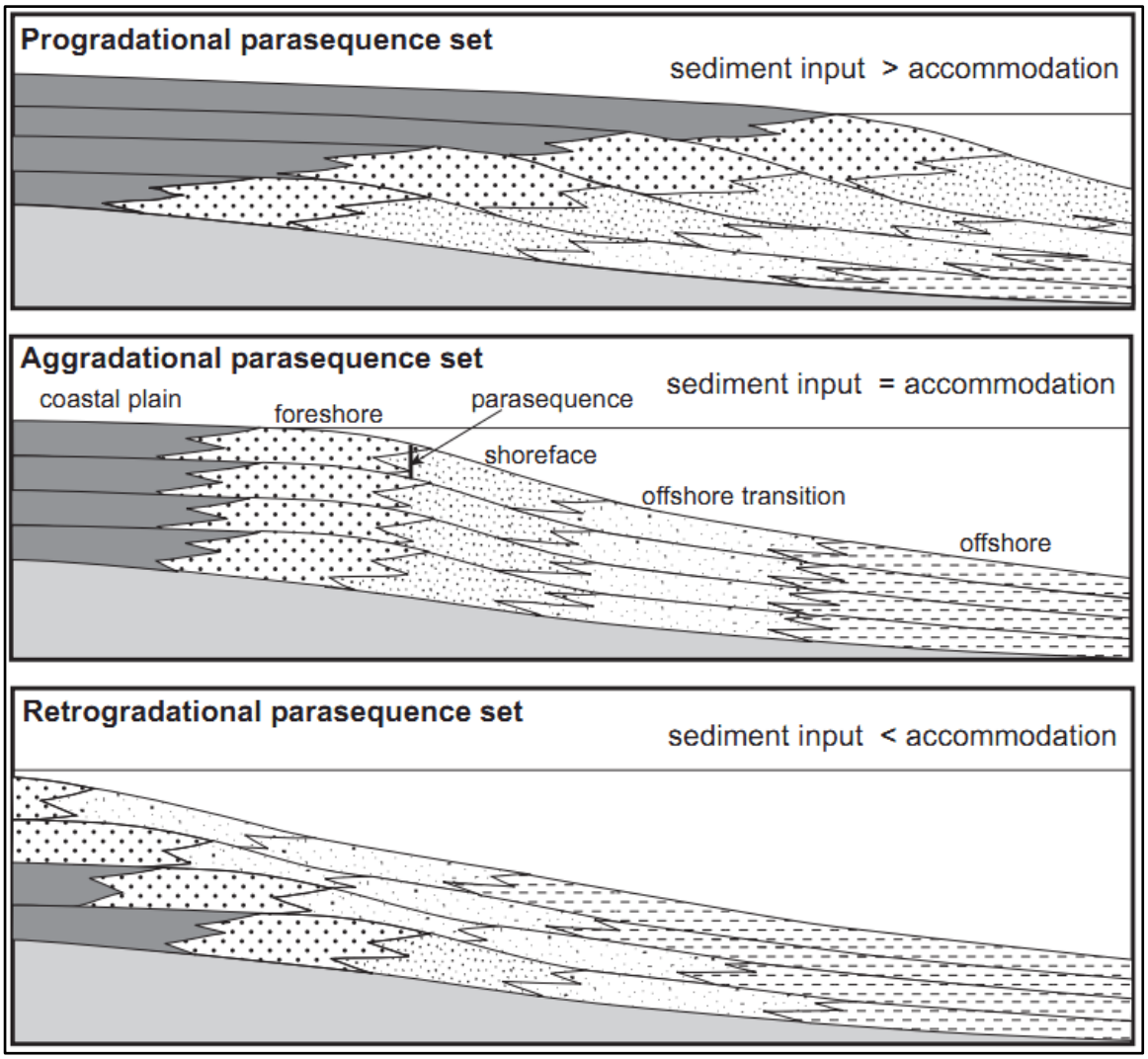

Figure 25: Stacking patterns of parasequences that forms parasequences sets (Nichols, 2009).

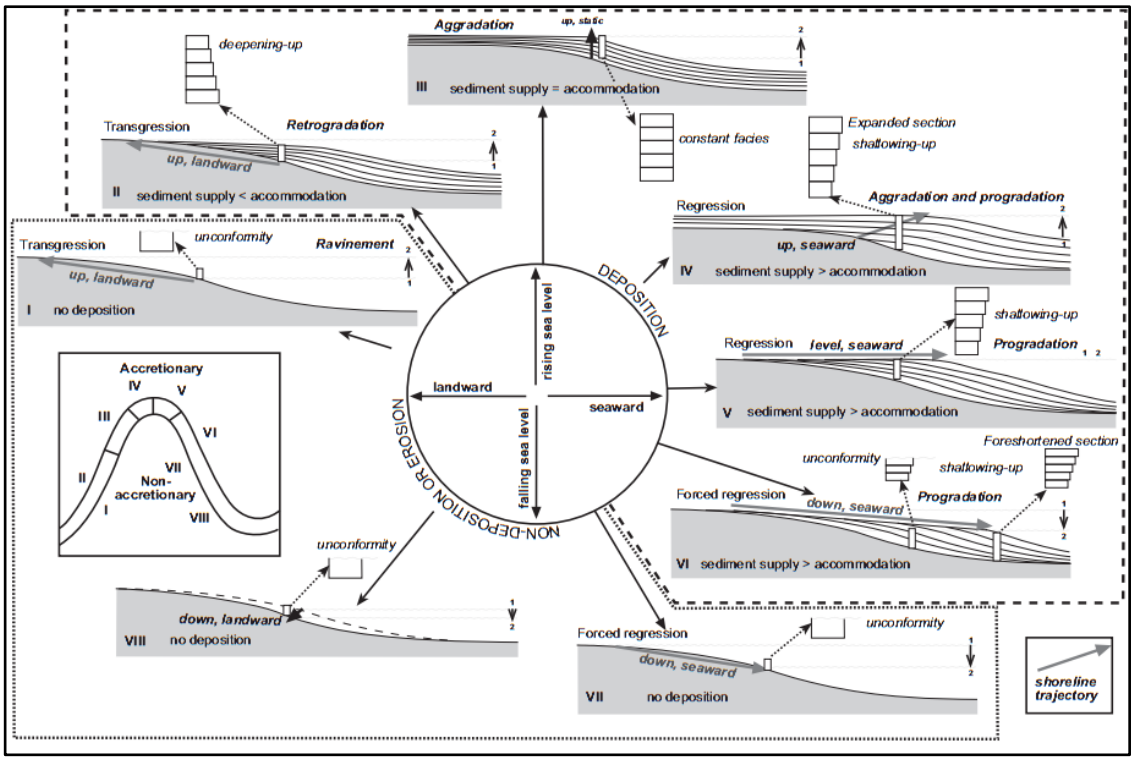

Figure 26: Possible sedimentation patterns, resulting from different relative amount of sediment supply and relative sea level change (Nichols, 2009).

3.2.4 Seismic Facies Mapping

Seismic facies are mappable, three dimensional seismic units composed of groups of reflections whose parameters are different from those of adjacent facies units. Seismic facies analysis determines as objectively as possible all variations of seismic parameters within individual seismic sequences and systems tracts in order to determine lateral lithofacies and fluid type changes (Mitchum et al., 1977). Herewith seismic facies analysis enables to quantify and interpret seismic parameter variations within the sequences and system tracts, caused by geological changes during deposition (Vail, 1987).

Thus seismic facies analysis can help in the approximation of grain size, sorting, mineralogy, porosity distribution, and permeability of the various deposition units (Mitchum et al., 1977), and herewith give hints on the presence of petroleum system elements, such as reservoir, source and seal rock lithologies.

Seismic facies analysis includes description of reflection parameters such as reflection configuration, continuity, amplitude, frequency and interval velocity (Figure 27, Table 3 & 4). The different parameters and their correlative geological interpretations are presented in table 3 below. Different types of seismic facies are diagnostic of different sedimentary environments. For example, parallel reflections can characterize some shallow-water shelf environments whilst the deeper water shelf edge and slope environments are often marked by the development of major sigmoidal or oblique cross-bedded units.

For this study a gross seismic facies classifications was carried out using reflection configuration, continuity, amplitude, and frequency. On seismic line GPN13-212M-032 domains of dominating facies were delineated and displayed as overlay polygons. Identification of particular sedimentary environments and prediction of associated lithofacies point to the location of potential source, reservoir and/or seal rocks.

Table 3: Reflection parameters for evaluation and interpretation of seismic facies. Modified from Mitchum et al. (1977).

Internal reflection parameter	**Geological interpretation**	**Seismic examples**	
Configuration	• Bedding patterns • Depositional processes • Erosion and paleotopography • Fluid contacts	Parallel	Chaotic
Continuity	• Later continuity of strata • Depositional process	Continuous	Discontinuous
Amplitude	• Velocity and density contrasts of interfaces • Bed spacing • Fluid content	Strong	Weak
Frequency	• Bed thickness • Fluid content	High	Low
Interval velocity	• Lithology estimations • Porosity estimations • Fluid content	From high to low Vp	From low to high Vp
External forms & areal association of seismic facies units	• Gross depositional environment • Sediment source • Geological setting		

Table 4: Internal reflection configurations (within sequences).

Internal Reflection configurations (within sequences)	
Most common:	Other:
• Parallel (• Subparallel • Divergent • Chaotic • Reflection-free • Prograding clinoforms - Sigmoid - Oblique - Complex sigmoid-oblique - Shingled - Tangential oblique	• Disrupted/discontinuos • Contorted • Lenticular • Hummocky • Wavy • (Even) • (Regular) • (Irregular) • (Uniform variable)

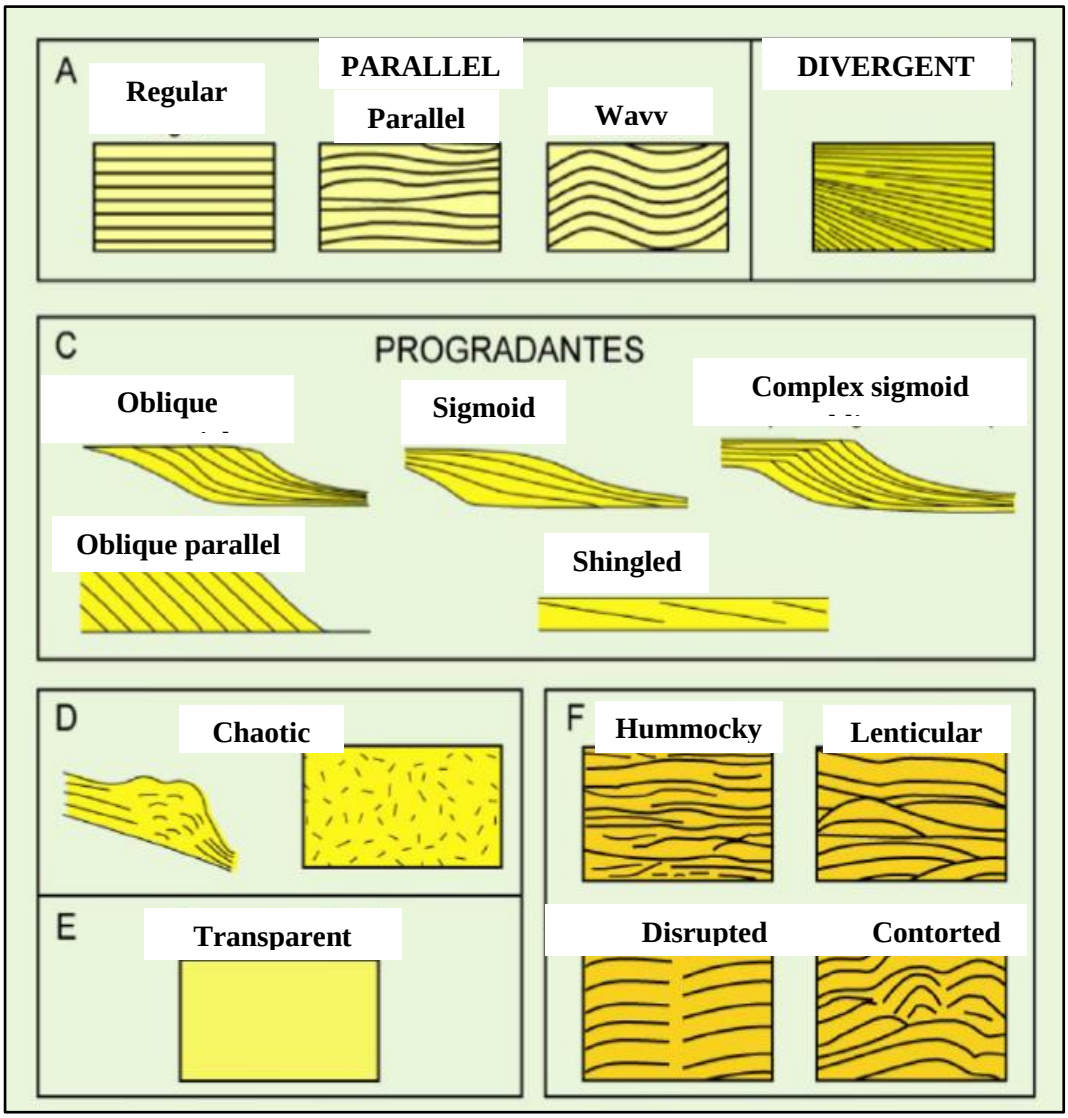

Figure 27: Typical seismic reflection patterns illustrating the concept of seismic facies. Modified from Mitchum et. al. (1977).

3.2.5 Prediction of Lithofacies

Lithofacies are referred to as the description of facies based on physical and chemical characteristic of rock/strata. Lithofacies is a result by the source material composition and the physical and chemical processes involved in the transport and deposition of

sediments. Lithofacies description and depositional environments for the shelfal sediments were extracted from the Well 2513/8-1 biostratigraphic well report as reference for the shelfal section of the interpreted seismic line on line GPN13-2012M-032.

Lithofacies were predicted from the seismic data by using an integrated approach:

Firstly, relating possible lithofacies to the seismic facies, secondly constraining proximal and distal nature of lithofacies from deduced system tracts and the position in relation to paleo-shoreline and paleo-shelf break, and lastly, the regional geological understanding of the mapped sequences.

For example, carbonate lithologies are expected to drape basement highs in the transitional megasequence, because during early basin evolution those shallow areas should have been the loci of preferential carbonate deposition. Seismic facies of strong amplitudes with sub-parallel reflection configurations affirm this interpretation. In the contrary, mass-flow deposits (turbidites/debrites) and fine-grained background suspension fallout deposits are assumed to occur in the deeper pelagic areas distant to the paleo shelf break. Continuous parallel medium amplitude and medium frequency reflections would represent suspension fallout deposits intercalated with planar turbidite sheets, while more channelized high amplitude hummocky reflections propose turbidite and debrite channel fills.

In addition, biostratigraphic information and descriptions of the texture and composition of cuttings at selected well intervals of well 2513/8 have been used as complementary information for supporting a lithofacies model for the shelfal section.

3.2.6 1D Burial History and Maturity Modelling

Two model well locations were selected, one for the shelf and the other for the lower slope of the basin. A tentative depth conversion was carried out using assumed but geological sound seismic velocities based on the predicted lithofacies for each model location. Seismic horizons, their approximate ages, unconformity surfaces and tentative but reasonable amounts of erosion, inferred lithofacies, and sound paleo water-depths were used as input for creating 1D burial history for each model well location. Paleo water-depths for the shelf were inferred from depositional facies cross checked with the biostratigraphic report for well 2513/8-1. For the model well at the base of slope paleo water-depths were estimated from inferred depositional setting alone.

The two model well locations (pseudo well 1 and 2) were selected in the actual study area on seismic line GPN13-210M-032 (Figure 28), while the burial history was also constructed for well 2513/8-1 for comparison and reference. It is important to note that well 2513/8-1 is located almost 100 kms SSE of pseudo well 1.

Pseudo well 1 is located on the shelfal area, in a similar distance from the shelf break as well 2513/8, while Pseudo well 2 has been placed in the deep water at the base of slope (Figure 28) . Well 2513/8-1 reached rocks of Barremian-Aptian age, which is the age of the lowermost source rock interval considered in this study. However, in well 2513/8 no source rock facies was encountered due to the proximal depositional facies predominating on the shelfal area. For Pseudo well 2 two potential source rocks, a Barremian/Aptian and a Cenomanian/Turonian source rock interval has been predicted and included in the 1D burial and maturity models. The presence of Lower Cretaceous source rocks in those intervals have been proven in the Wingat and Murombe wells in

the southern Walvis Basin. Both wells are located at a similar bathymetry as pseudo well 2. Thermal input parameters for maturity modelling are a geothermal gradient of 34°C/km obtained from a regional industry study (Hunt Oil, 2008). The final well report of Well 2513/8-1 did not provide calibration data (borehole temperatures provided were not corrected) and hence did not contribute to the thermal model. Geochemical source rock models (kinetics) have been chosen from previous industry studies for the southern Walvis Basin (pers. com. C Nino, Galp Energia), as no source rock studies exist for the Lüderitz Basin.

The 1D burial history and thermal modelling was carried out with PetroMod v. 2016.2 petroleum system modeling software.

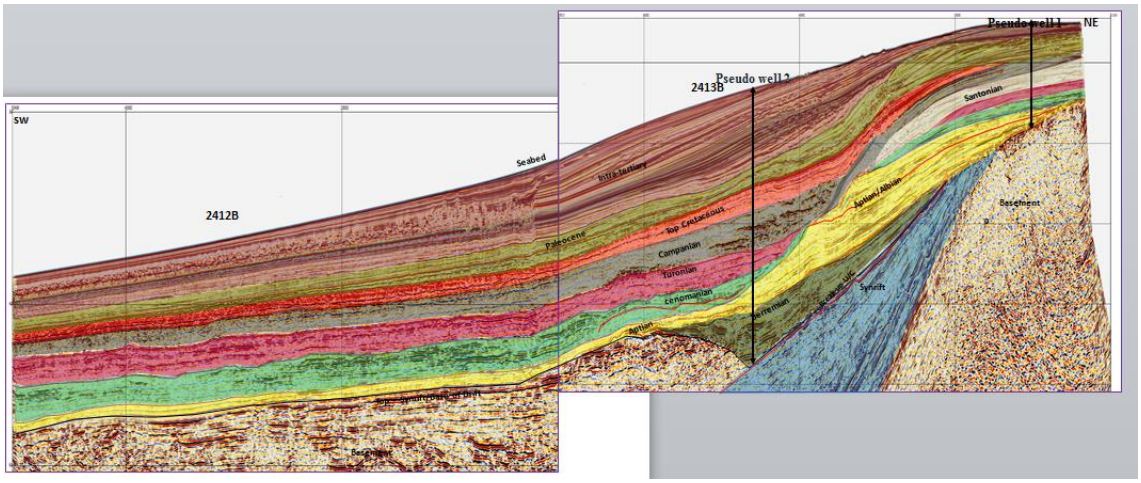

Figure 28: Locations of Pseudo well 1 and Pseudo well 2.

CHAPTER 4: RESULTS AND ANALYSIS

4.1 Seismic stratigraphic intervals and horizons

A total of nineteen stratigraphic intervals were identified on the seismic line, between top basement and the seabed (Figure 29). Appendix 1 outlines a description for each interpreted seismic interval. The characteristics of each dividing stratigraphic surface, such as sequence boundaries, are also described in this chapter.

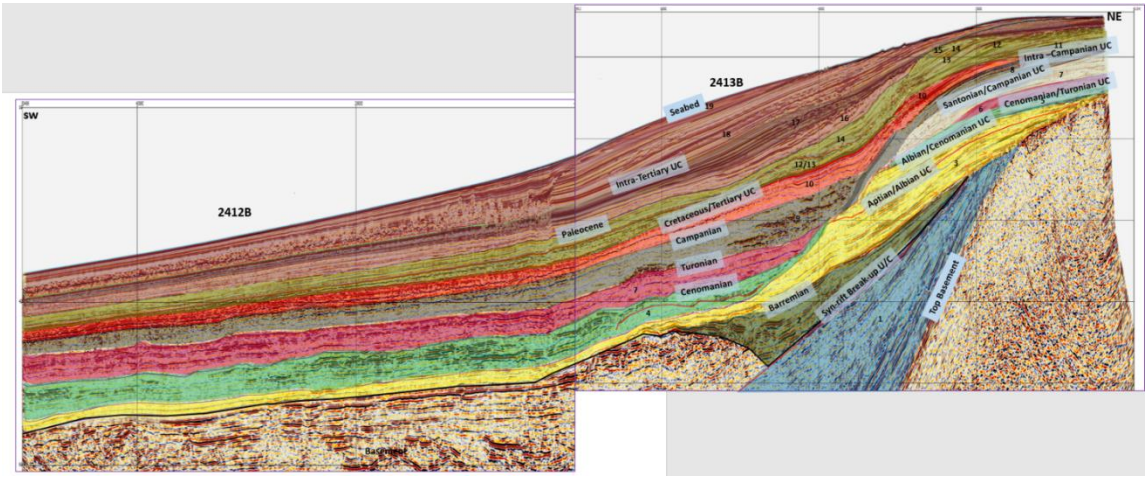

Figure 29: Dip line GPN13-212M-032 with overlay of seismic intervals and their ages and the bounding seismic surfaces. Ages had been assigned by comparison with interpreted seismic lines in industry presentations (Hunt Oil, 2008; Serica Energy, 2017) and discussions with POGC. An enlarged version of the image is given in Appendix 3.

4.2 Wheeler diagram

A Wheeler diagram was constructed to obtain better insight into the time relationships of the depositional systems, and their relationships to surfaces of non-deposition, condensation and erosion (Figure 30).

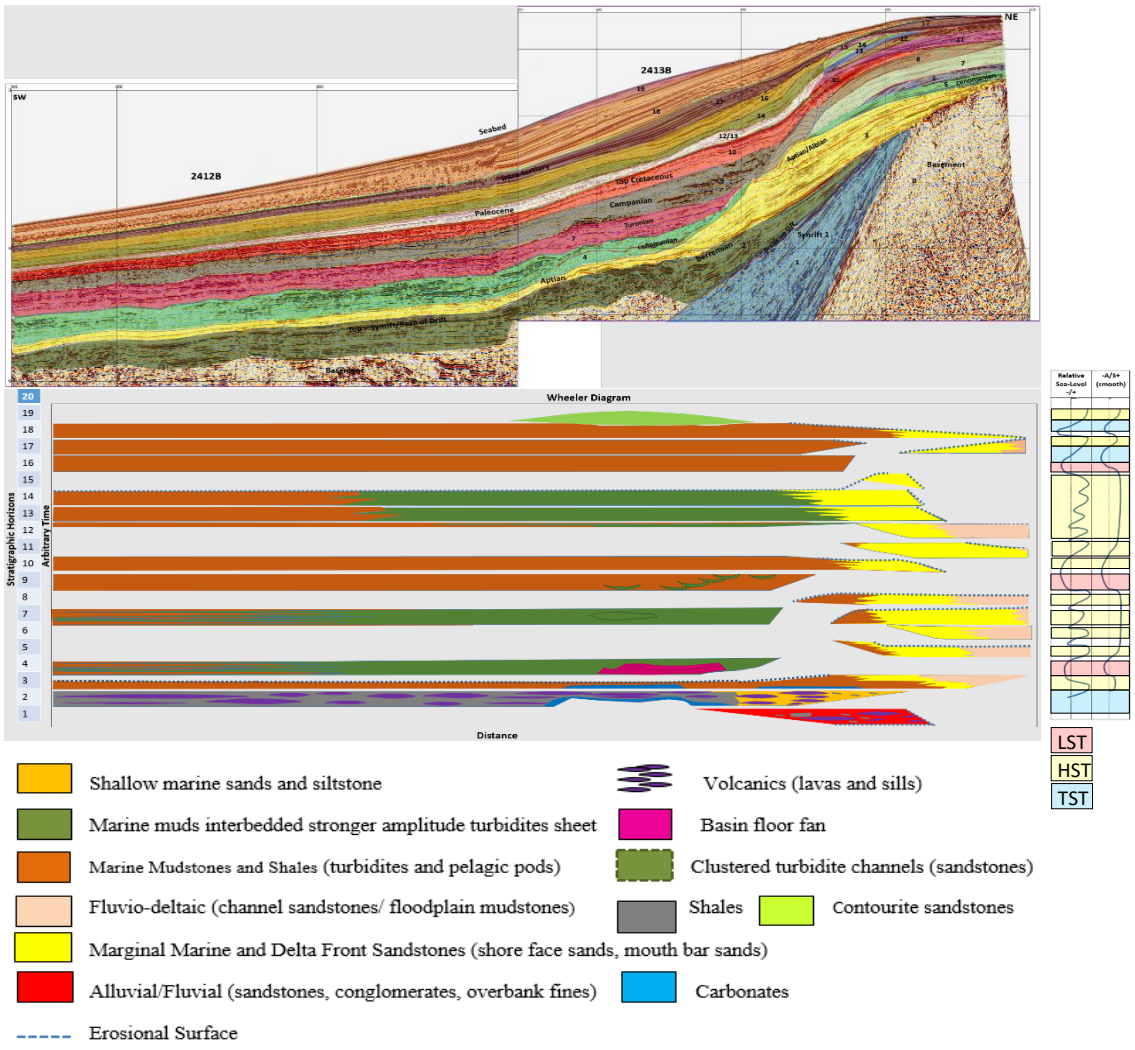

Figure 30: Wheeler diagram for line GPN13-M212-032 covering the Cretaceous to Tertiary deposits in the Lüderitz Basin, showing the relative age and distribution of the sequences. Blank areas represent areas of erosion, non-deposition, or condensed strata below seismic resolution. On the right is the relative sea level curve and the

corresponding smoothened accommodation/sedimentation ratio curve from the Aptian to the seabed.

Seismic reflectors that are considered to represent time lines that have been plotted in order of age, with an equal time increment given to each horizon. A total of 19 Seismic Intervals (SI) were identified. Figure 30 above shows the constructed wheeler diagram with the Relative Sea Level (RSL) and a corresponding smoothened curve of accommodation/ sedimentation ratio.

Lithofacies have been inferred based on seismic facies, proximity to the continent and sediment transport mechanism, complemented by the analysis of analogue sections of the Namibian margin as cited in the introductory chapters.

Seismic interval SI 1 and SI 2 are the syn-rift and transitional phase sequences, respectively. Significant volcanic deposition is known from the neighboring basins, associated with continental and later shallow marine sedimentation. The geometry of SI 3 indicates that the morphology of a passive margin with its typical division into shelf, slope and abyssal plain is fully developed. This interval is overall transgressive and fully marine deposition has been proven in boreholes in the adjacent Orange (Kudu wells, Kabeljou) and Walvis (Wingat, Murombe) basins.

A major erosion event at the end of the Albian caused a major incision removing much of the Albian strata including some of the Aptian in the deeper parts of the basin. SI 4 (Cenomanian) deposited on this erosional surface. Seismic facies show basin floor fan and subsequent stages of lowstand deposition. The following highstand deposition is

found on the shelfal progradational sequence SI 5. Major prograding phases, probably due to increased sediment input, is seen in the prograding clinoforms of SI 6 and SI 7 on the shelf to upper slope, as well the corresponding deeper water deposits further downdip. Following these two phases of deposition, some of SI 7 is truncated by the Santonian/Campanian unconformity on the shelf. This unconformity cannot be tracked further downslope due to slumped sediment on the unstable slope.

SI 8 represent a revived phase of progradation on the shelf, soon followed by deep incision at the Intra-Campanian unconformity. Subaerial exposure is evident by truncation of SI 8, further downdip erosion goes down to SI 7 likely due to submarine canyon incision. Following the Intra-Campanian unconformity, the deep water turbidites of SI 9 and SI 10 filled much of this Canyon during lowstand deposition. Channelized high-amplitude turbidites are prolific in the mid- and lower slope positions of SI 9.

At the end of the Cretaceous erosion truncates SI 8 and SI 10 on the shelf marking the Cretaceous/Tertiary unconformity, an unconformity that can be well traced across the section, and is also a major marker on other seismic lines in the Orange and Walvis basin. SI 11 to SI 15 are repeated prograding phases on the shelf during repeated highstands. High progradation allowed that significant amount of sediments arrived downdip. The slope appears to be particular unstable during this period and thus gravitative displacement of sediment packages challenges downdip correlation.

An intra Tertiary unconformity, possibly on to top of the Paleocene, causes again canyon incision as seen at the base of SI 16. SI 16 represent the lowstand fill followed by further fill during transgressive and highstand phases of SI 17. A younger intra-Tertiary

unconformity truncates SI 17 at the outer shelf and SI 15 on the upper slope. This unconformity can be traced as a correlative conformity downdip throughout the section. The succeeding SI 18 shows a transgressive onlap pattern onto the upper slope and shelf area and may therefore represent a major transgressive and subsequent highstand phase. SI 19 forms a lens-shaped local body on the slope with the updip and downdip edges truncated by the seabed. The seabed further truncates parts of SI 18 at the upper slope. Truncation of reflections at seabed level indicates strong bottom currents, and likely parts of SI 18 and entire SI 19 are contourite deposit.

4.3 Seismic Facies

Within the study area a gross subdivision into seismic facies categories has been created to augment interpretation of depositional environments. Five categories have been chosen with reference on the principal reflection configuration: Parallel, divergent, progradational, irregular, and chaotic (Figure 31). Within each category a number of seismic facies have been identified (Table 6).

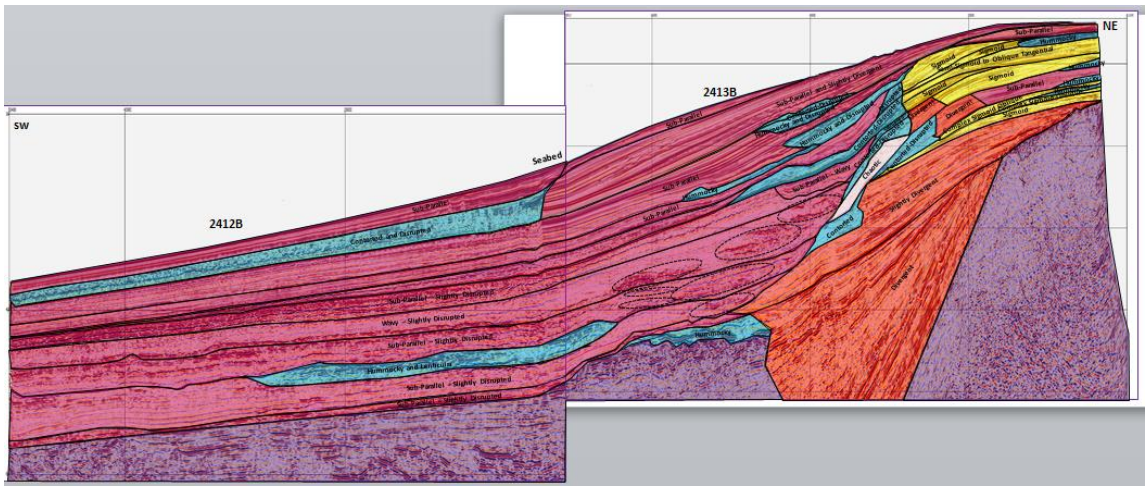

Figure 31: Seismic dip-line GPN13-M212-032 with an overlay of five seismic facies categories further subdivided in table 6. Interpretation of similar facies may vary, depending on the geological context where it occurs. Divergent seismic facies relate to growth strata in the syn-rift fill of the central graben. Up-section divergence occurs prograding in clinoforms west of the shelf edges. Hummocky facies occur towards the continent likely relating to delta top and fluvial deposition. On the slope hummocky reflections have multiple origins including slope instability and slumping, complex channel fills (central part of line), and sediment disruption likely deriving from over pressuring and dewatering and gravitational dislocation (e.g. upper Tertiary hummocky interval in western half of line). Circled areas highlight high amplitude events interpreted as channelized turbidites embedded in shales.

Table 6: Classification of seismic facies identified in seismic line GPN13-M212-032.

Seismic reflection patterns	Color Code	Internal Configurations	Amplitude	Continuity	Seismic Intervals (SI)
Divergent		Divergent	Strong to Moderate	Continuous to Sub-continuous	1, 2, 7, 8
		Slightly Divergent	Strong to Moderate	Continuous to Sub-continuous	3
Progradational		Sigmoid	Strong to Moderate	Sub-continuous	5, 7,8,10, 12, 13, 14, 15
		Complex Sigmoid Oblique	Strong to Moderate	Sub-continuous	6
		Semi-Sigmoid to Oblique Tangential	Strong to Moderate	Sub-continuous	11, 12
Irregular		Hummocky	Strong to Weak	Discontinuous	2, 5, 6, 7, 12, 14
		Contorted-Disrupted	Strong to Weak	Sub-continuous	7,10,12,13,17,18
		Disrupted	Strong to Weak	Sub-continuous	10, 14
		Hummocky and Lenticular	Strong to Moderate	Discontinuous to Sub-continuous	4
		Hummocky and Disrupted	Strong to Moderate	Discontinuous to Sub-continuous	14
		Contorted and Semi-Disrupted	Moderate	Sub-continuous	17
		Contorted	Moderate	Sub-continuous	3
		Sub-Parallel	Strong	Continuous to Sub-continuous	7, 14, 16, 17, 19
Parallel		Sub-Parallel - Wavy	Strong to Moderate	continuous to Discontinuous	10, 18
		Sub-Parallel and Slightly Divergent	Strong	Continuous to Sub-continuous	18
		Wavy – Slightly Disrupted	Moderate to Weak	Continuous to Sub-continuous	9
		Sub-Parallel – Slightly Disrupted	Strong to Weak	Continuous to Sub-continuous	3, 4, 7, 10
		Chaotic	Weak	Discontinuous	Various
Chaotic		Chaotic	Weak	Discontinuous	Various
		Undefined pre-rift and SDRs			

Divergent seismic facies

Divergent seismic facies are prominent in the syn-rift and transitional sequences, but do also occur in the post rift sequence in the shelf and slope areas. Fault controlled growth in the central half graben explains strong divergence of the strata towards the main fault. Amplitudes are partially strong, but variable. Reflection continuity is variable with continuous prominent reflections beside less continuous and erratic reflections (Figure

32). Volcanic flows of variable extent and intrusive bodies such as sills are probably abundant in both, the syn-rift and transitional sequences and can explain the presence of high amplitude reflections with variable continuity. Syn-rift faulting, especially in the western portion of the main half graben has contributed to disruption of reflections (Figure 32). Continental deposition with alluvial, fluvial and possibly lacustrine deposits is expected during the syn-rift sequence and may have passed into the transitional sequence, again explaining that much of the divergent reflections are of low continuity or hummocky. So far no well on the Namibian margin has penetrated the syn-rift sequence, hence no calibration can be made.

Divergent patterns in the post-rift are essentially not fault controlled, but the lateral change in depositional rate follows basin bathymetry with increased deposition from shallow outer shelf environments to the relatively deeper water slope environments. Reflection continuity is generally high suggesting more uniform or gradually changing deposition from shallow to deeper marine environments. The Aptian/Albian interval shows an overall, but slightly divergent pattern (Figure 33), indicating development of a shelf-slope bathymetry during a transgressive phase with high sediment supply, which explains the relative high deposition even in the deeper parts of the basin.

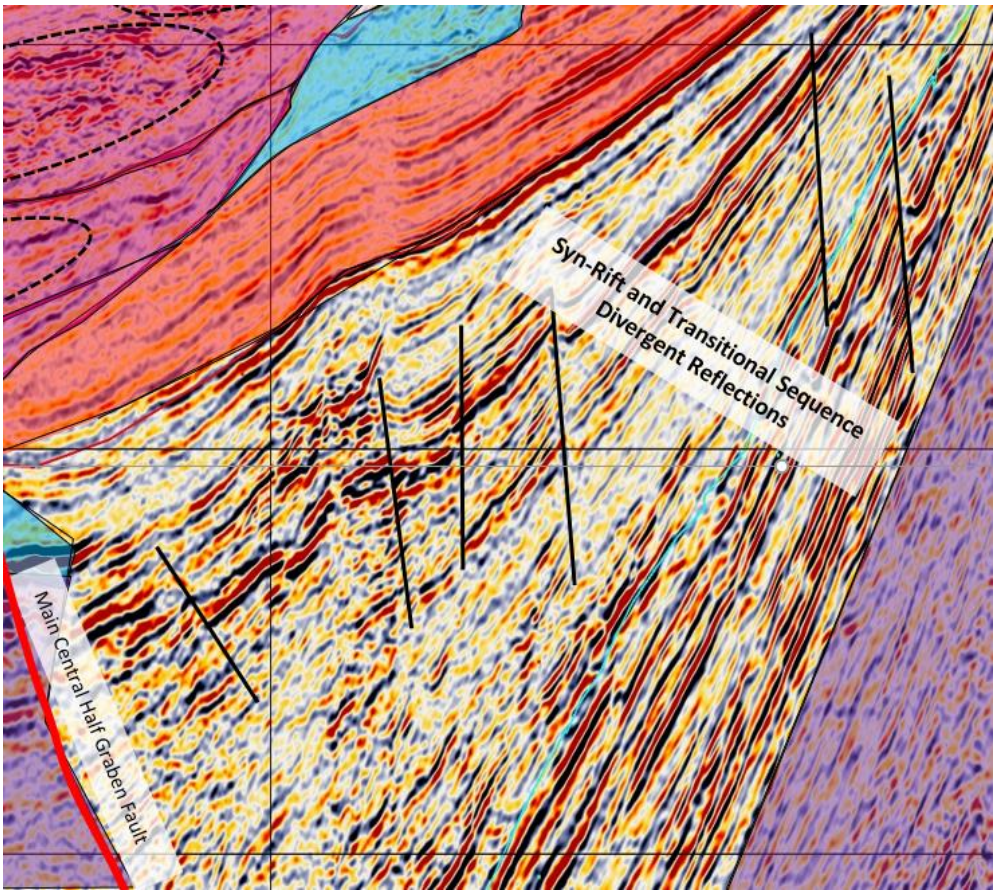

Figure 32: Divergent seismic reflections in the syn-rift and transitional sequences. Sedimentation rate increases towards the western main fault. Continental deposition accompanied by extrusive and intrusive volcanism may explain the variable amplitudes and continuity of reflection.

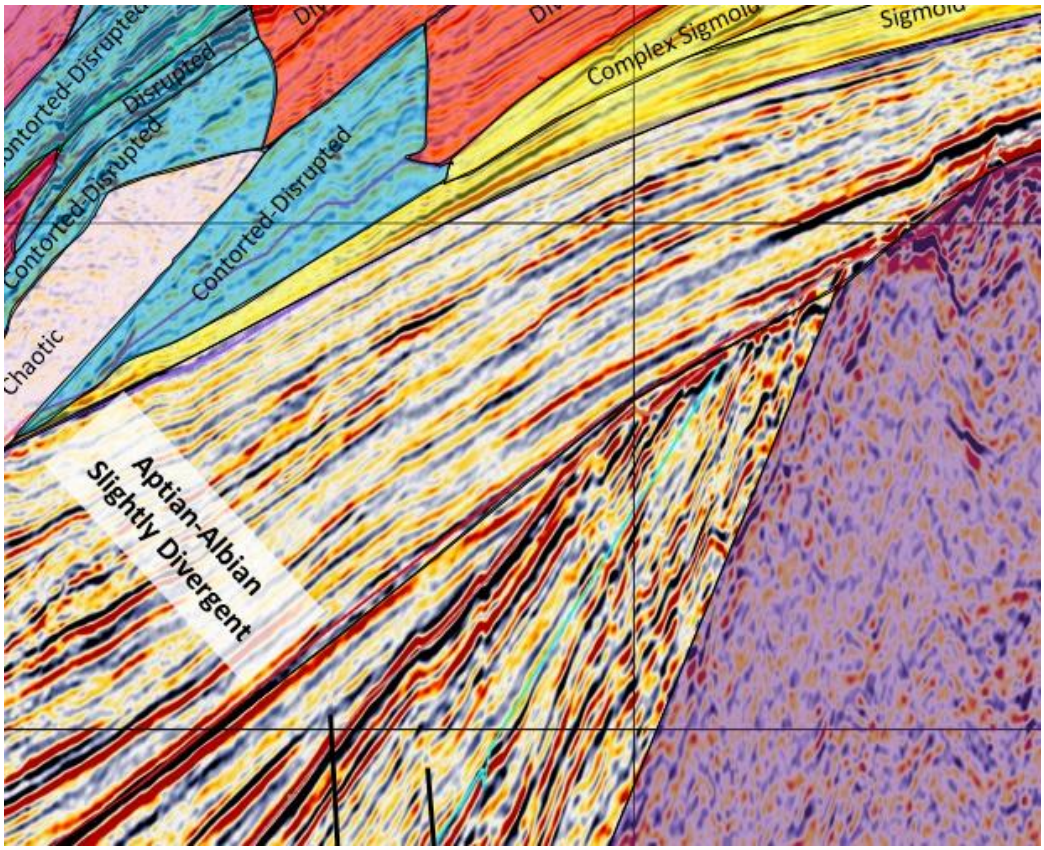

Figure 33: Slightly divergent seismic reflection in the early post-rift (Aptian/Albian) sequence. The overall downdip curvature of the reflections indicates development of a shelf-slope bathymetry with slightly increased sedimentation rate towards the deeper basin. Reflections are mostly continuous indicating more uniform depositional conditions.

Irregular seismic facies

The irregular seismic facies category includes discontinuous reflection and/or reflections of irregular geometries such has hummocky or lenticular, but excludes chaotic patterns (Figures 34 to 38). Several reflection configurations of this category have been identified as summarized in table 6 above. Seismic facies falling in this category related either to

primary depositional features, or to post depositional modification by gravity movements, fluidization and fluid escape of over pressured sediments.

Figure 34: Hummocky high amplitude reflections on the inner shelf followed by prograding patterns to the west. The hummocky pattern is interpreted as fluvial/delta top environments where coarse-grained facies of channel fills and crevasse splays associate with overbank and/or floodbasin fines resulting in strong short reflections.

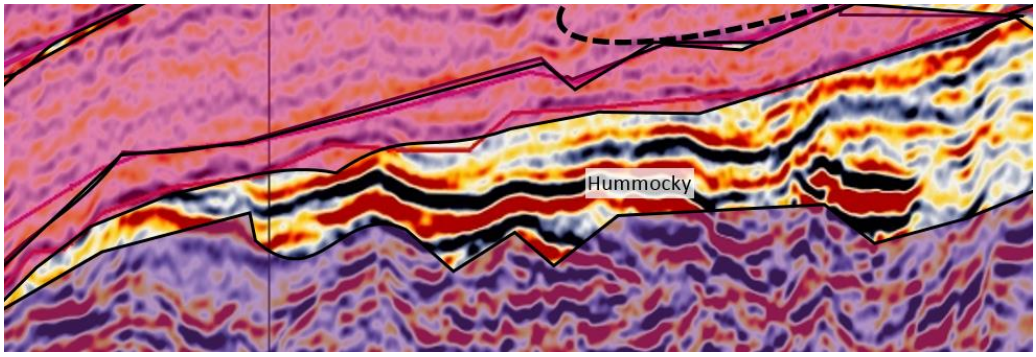

Figure 35: Hummocky reflections occurring on a structural high west of the central graben. The reflections correlate with the transitional sequence of likely Barremian age. The Murombe well in the southern Walvis Basin reached carbonates interfingering with partially altered lava flows at a similar level and at a similar position. Therefore, the high amplitude reflection may derive from carbonates intercalated with lava flows. Hummocky geometries may have derived from the interplay of carbonate and volcanic

deposition on a structural high. Carbonate deposition may have been restricted to the shallow waters at the structural high, with some talus deposits flanking it.

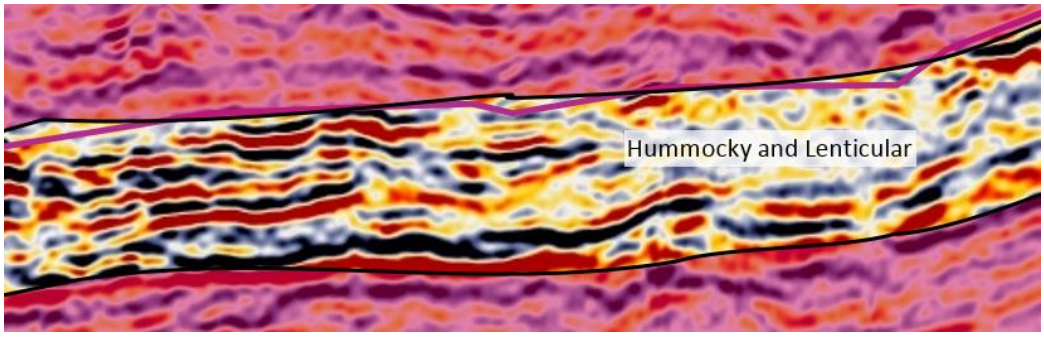

Figure 36: A combination of high to medium amplitude reflection of linear, curved, and irregular geometries dominate the Cenomanian interval immediately west of the lower slope. The high amplitude events are interpreted as turbidite deposits in both, lobes and channels on the lower slope and abyssal plain.

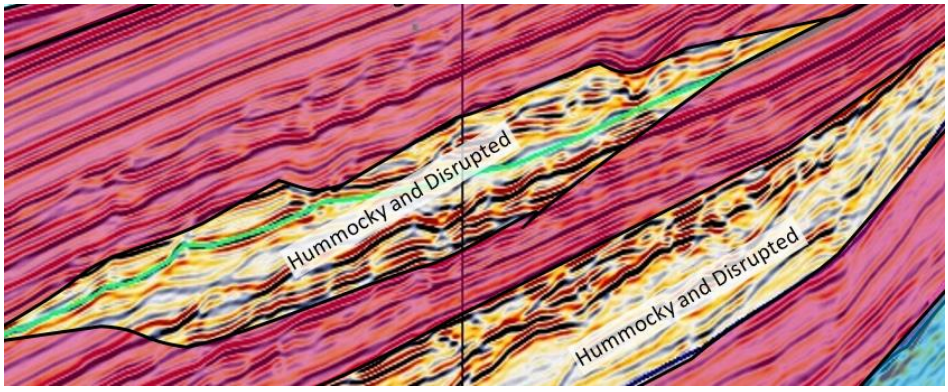

Figure 37: Reflections are hummocky with some disruptions. Amplitudes vary from moderate to low intensity. The area of the section is located in the compressional domain of gravity movement at the mid-lower slope in the Tertiary sequence. The curved shape reflections are a result of compression while the disruptions may relate to a combination of reverse faulting, thrusting and fluid escape. In the lower portion amplitudes faint, possibly as a result of homogenization during mass transport.

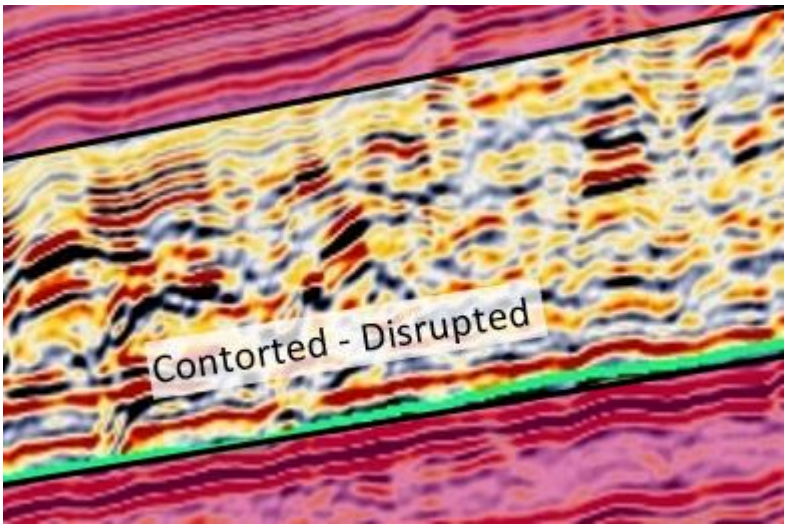

Figure 38: Moderate to high amplitude reflections show wavy and fold-shaped curvatures in the upper portion of the interval, while reflections are contorted and discontinuous in the middle part, underlain by essentially continuous reflections. The area is located high in the Tertiary sequence and correlative strata farther updip displays parallel continuous reflections patterns, probably representing distal packages of lateral extensive shale beds. The contorted middle part is interpreted as overpressured shale causing mobilization with upwards movement of fluidized material. The upwards movement causes upwraping and hence the overlying layers appear folded. Gravity induced compression with consequent folding is excluded here, as a corresponding extensional domain is absent.

Parallel seismic facies

The parallel seismic facies category includes continuous to sub-continuous reflection geometries such as sub-parallel–wavy, sub-parallel and slightly divergent, wavy–slightly disrupted and sub-parallel–slightly disrupted patterns (Figure 39-40 and Table 6 above).

Parallel seismic facies are vastly present from the lower lope and abyssal plain. There, parallel seismic facies may be interpreted to represent fine clastic sub-marine fan/sheet deposits with interbedded pelagic to hemiplegic clay, and this combination is probably responsible for the high amplitude of these seismic facies. Some intervals show transitional elements to the irregular category, e. g. in the Turonian and Campanian, where significant degrees of disruptions and clustered discontinuous high amplitude para-hummocky events occur. The latter are interpreted as stacked channelized turbidites that are prominent in the mid and lower slope.

Parallel and sub-parallel configuration occur also on the shelf representing aggrading shallow marine shoreface deposits.

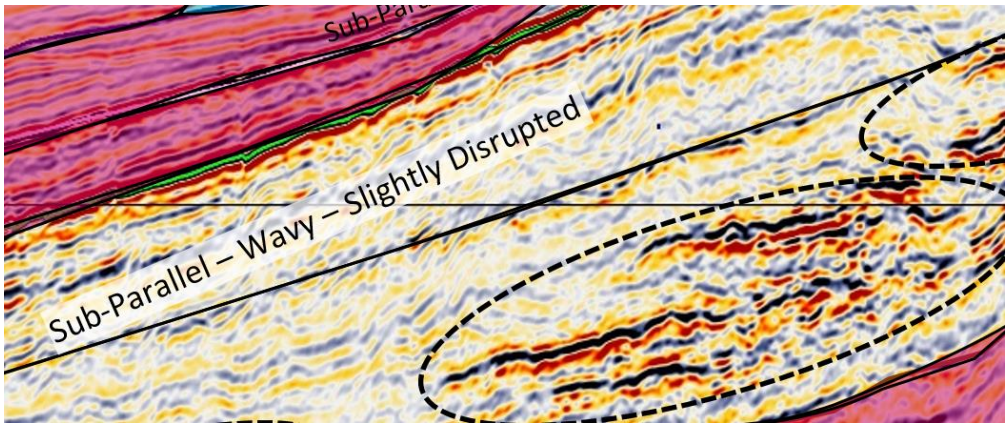

Figure 39: Seismic section displaying sub-parallel–wavy-slightly disrupted seismic facies of moderate to low reflectivity. Most reflection are continuous enough to be traced laterally as disruptions are of limited offset. The circled fields highlights stacked high amplitude events of limited continuity and some irregular (hummocky) patterns. The sequence is an Upper Cretaceous canyon infill located on the lower slope. Post-depositional deformation during dewatering may have led to the wavy partially

disrupted reflections. The high amplitude events are interpreted as channelized turbidites embedded in shale dominated pelagic suspension fallout and fan sheet deposits.

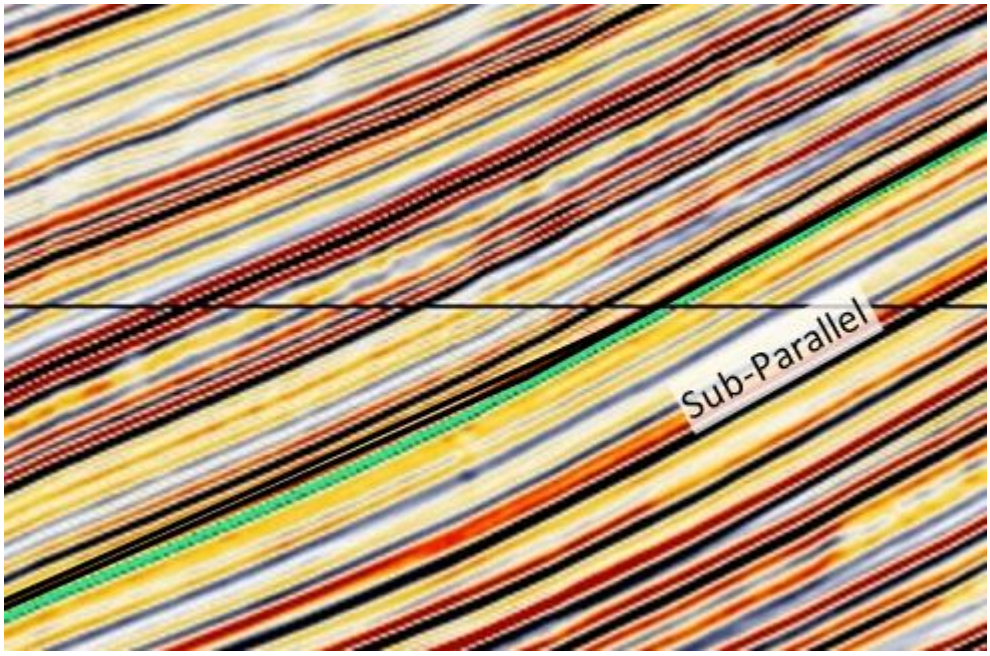

Figure 40: Seismic section displaying sub-parallel to slightly divergent seismic facies, consisting of high to moderate amplitude entirely continuous reflections. The area of the section is located mid-slope of the Upper Tertiary sequence. These facies may be interpreted to represent fine clastic sub-marine fan/sheet deposits with interbedded pelagic to hemiplegic clay, explaining the moderate to high amplitudes reflection of good continuity.

Progradational seismic facies

The progradational seismic facies category includes continuous to sub-continuous reflections of high to moderate amplitude with geometries such has sigmoid, complex sigmoid oblique, semi-sigmoid to oblique tangential (Figure 41-42 and Table 6).

Progradational facies have been identified on the shelf and upper slope, and most are of the sigmoidal type. On the shelf some prograding sequences are truncated by regional unconformities, hence top-sets are absent and the recognition of the reflection configurations is tentative. The configuration of prograding reflections gives a hint to the accommodation/sedimentation ratio as well the energy of the environment.

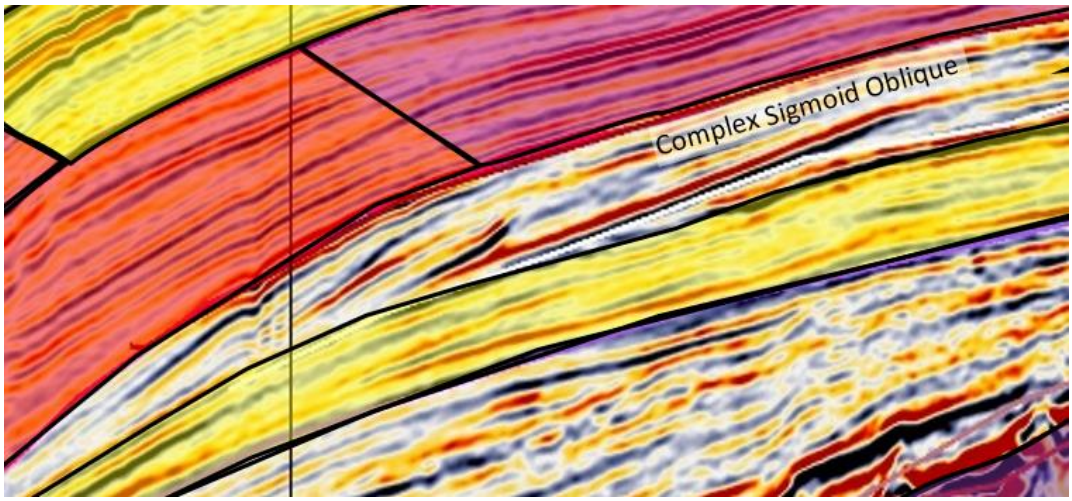

Figure 41: Seismic section displaying seismic Complex Sigmoid oblique facies, consisting of high to moderate amplitude reflections with sigmoid geometries. The seismic interval is located in the inner shelf in the Turonian sequence. The internal dipping reflections are terminated by toplap at or near the upper surface, and by downlap at the base. The downlapping reflector terminations represent outbuilding of sediments from relatively shallow into relatively deep waters. Toplap surfaces at least three levelds occur in this seismic interval. This implies a history of alternating upbuilding and depositional bypass in the topset segment, probably within a high-energy depositional regime.

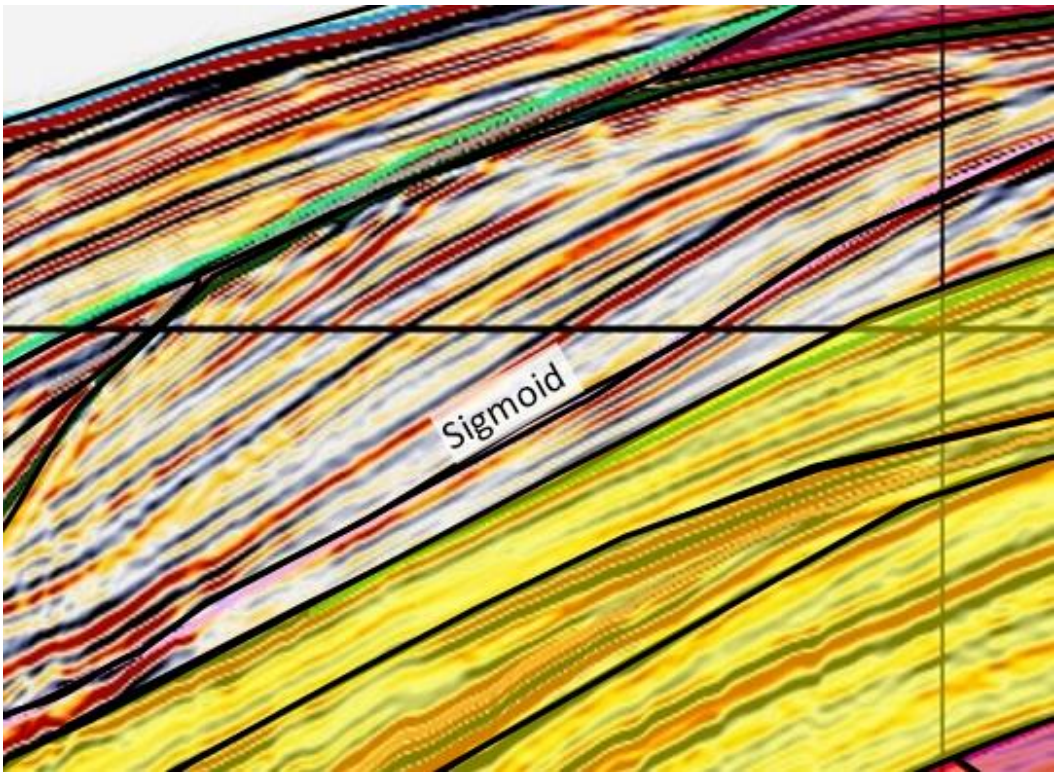

Figure 42: Seismic section displaying seismic sigmoid facies, consisting of high to moderate amplitude continuous reflection with sigmoid geometries. The section is located on the outer shelf in the Tertiary. This interval has shown some complexity as five sets of sigmoid-shaped foresets occur in this seismic interval with an overall outward (prograding) and minor upward building pattern. The lower (bottomset) segments of the strata approach the lower surfaces at low angles, however an incision truncates the bottom sets to the west. The preservation of the topsets may indicate low energy deposition during slowing relative sea level rise. The presence of five sets of foresets may derive from high frequency (3rd or higher order) fluctuations in relative sea level, or lobe switching in a delta front setting.

Chaotic seismic facies

The chaotic seismic facies category includes discontinuous reflection of low amplitude and no systematic geometries in a unit (Table 6 above and Figure 43). Chaotic facies is commonly adjacent to disrupted and contorted reflection configuration caused by post depositional transport (slumping). Therefore, chaotic facies represents the highest level of post depositional sediment disturbance.

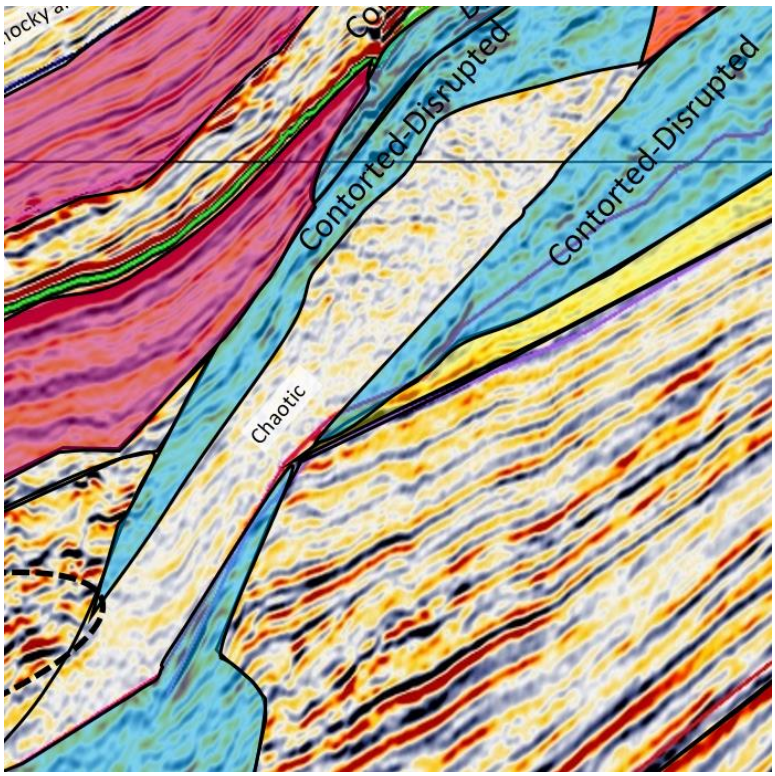

Figure 43: Seismic section in the Cretaceous post rift displaying seismic chaotic facies, consisting low reflectivity, low amplitude and no continuity with chaotic reflection geometries, indicative of slumping and homogenization of soft sediments at an unstable slope.

4.4 Burial History

Three well locations (2513/8-1, Pseudo well 1 and 2) have been modelled in 1D to understand the burial and thermal history in order to predict thermal maturation and timing of petroleum generation in the Lüderitz Basin. Appendix 4 shows tables with the input information used for the three 1D models. Input parameters were tops of stratigraphic intervals (in depth), lithology (PetroMod categories), tentative paleo-water depth, and the default McKenzie Heat flow model for passive margins, assuming a syn-rift phase from 130 to 120 Ma followed by post-rift subsidence. The paleotemperatures for the sediment-water interface was automatically calculated following Wygrala (1989). Where applicable, amounts of erosion where estimated for unconformities in the Cretaceous and towards the top of the Paleocene.

The burial history reconstruction of the Lüderitz basin for the respective wells locations is shown in Figure 44, 45 and 46 below.

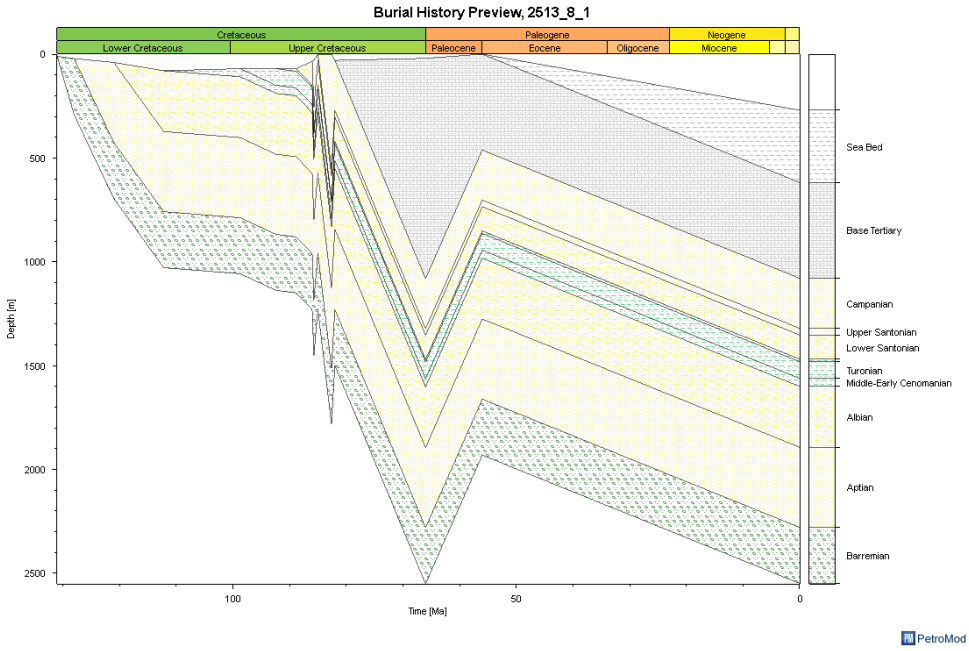

Figure 44: Burial history for well 2513-8-1, located on the shelf ca 100 km south of the study area. Paleo water depths were estimated on the micro fauna interpretation given in the biostratigraphy report for this well. Estimates for two Cretaceous unconformities derive from tentative depths of erosive incisions seen in seismic, while erosion amount in the Paleogene (Paleocene unconformity) follows carefully a suggestion of an industry presentation by Hunt Oil (2008). This Paleogene erosion on the shelf coincides with an onshore uplift event deduced from apatite fission track data (AFTA) (Brown et al., 2014).

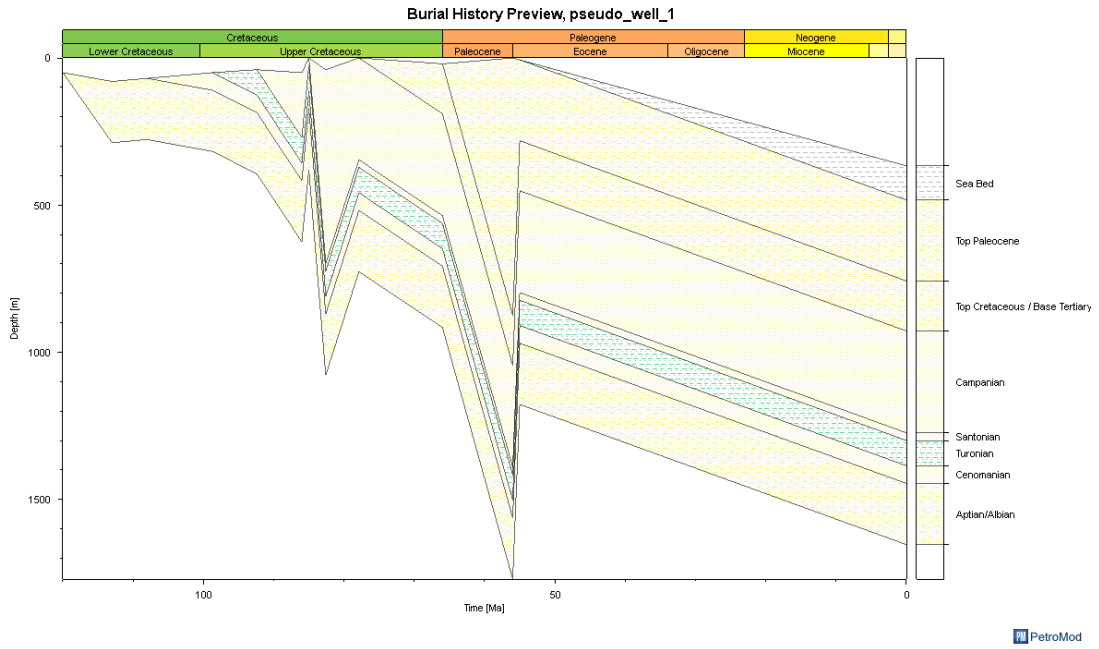

Figure 45: Burial history for Pseudo Well 1, located on outer shelf within the study area. This model resembles much the burial history of well 2513/8-1, but less information has been available for input. Stratigraphic tops were taken from seismic line GPN13-212M-032 at the model well location. Lithologies and tentative paleo-water depth were derived on seismic facies and sequence stratigraphic context. In the model location minimum erosion could be estimated for two Cretaceous unconformities (Santonian, and Intra Campanian U/C) by extrapolating truncated reflections. For the Paleogene unconformity the same amount as for well 2513/8-1 was chosen.

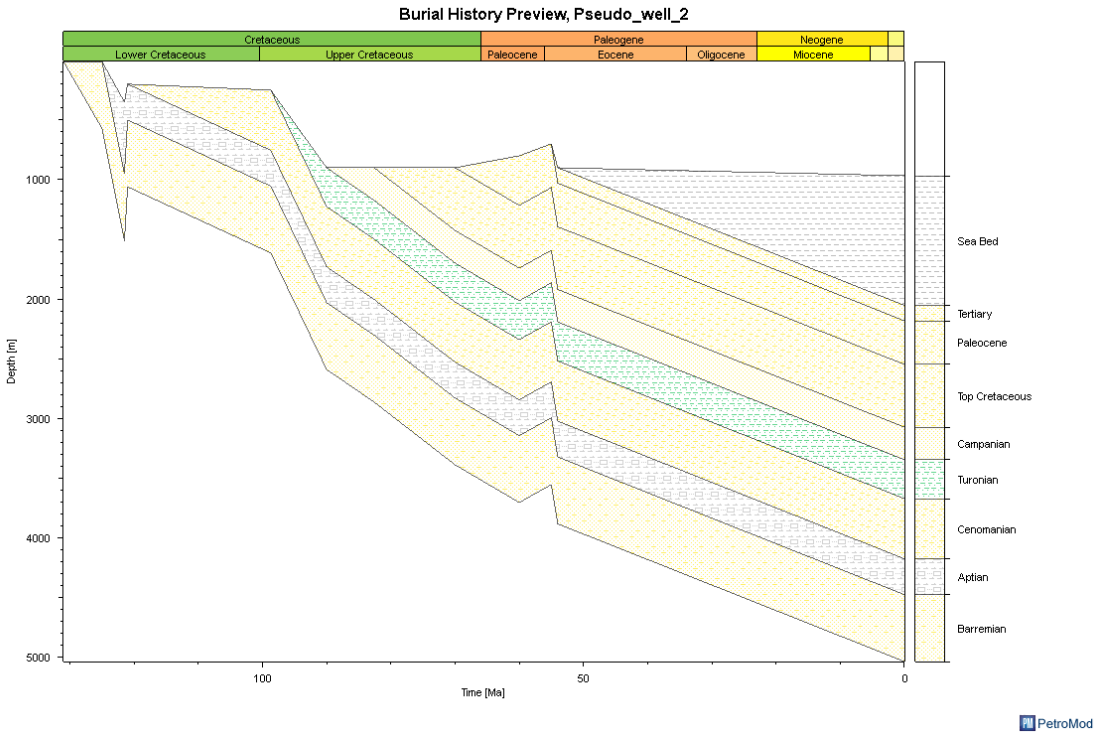

Figure 46: Burial history for Pseudo Well 2, located at the base of slope in the study area. Stratigraphic tops were taken from seismic line GPN13-212M-032 at the model well location. Lithologies and tentative paleo-water depth were derived on seismic facies and sequence stratigraphic context. Most unconformities do probably not involve any or no significant amounts of erosion, due to the deep water location of the model well location. A minimum erosion of 300m could be estimated for the Albian unconformity by extrapolating truncated reflections, probably caused by submarine canyon erosion and not by subaerial exhumation. For the Paleocene unconformity erosion is not obvious in seismic, therefore only a small amount of 50m has been chosen accompanied by a low sea level.

The shelf area (Figure 44 and 45) experienced similar periods of deposition, non-deposition and/or erosion for both she;fal well locations. The first clear erosional event is the Santonian/early Campanian unconformity, which led in the removal of an estimated 195 m of strata in the study area. The second obvious erosional event is at the Intra-Campanian erosional unconformity that began during mid-Campanian and eroded an estimate of 312 m obtained from estimated vertical canyon depth in seismic strike sections. The last erosional event began in the early Tertiary and an estimate of 600m eroded strata is given. AFTA data from the coastal region onshore Namibia indicates an early Tertiary uplift that coincides with Tertiary incisions into the shelf.

Pseudo well 2 at the base of slope (Figure 46) also experienced periods of erosion. The first major erosive surface is the Albian/early Cenomanian unconformity, where at the model location an estimate of 300 me of Aptian/Albian strata was eroded by the incision of a submarine canyon. Other Cretaceous unconformities show conformable relationships in this downdip position, and hence no removal of strata is inferred. The Paleocene unconformity shows some subtle truncation associated with a see level drop, therefore a minor erosion amount of 50m was included in the model.

Thermal History and maturity

Thermal history models were created for all three well locations. As no thermal calibration data was available from boreholes, a geothermal gradient of 34°C/km was used for calibration, following a suggestion in an industry presentation by Hunt Oil (2008).

In general, burial histories show a direct relationship between the burial depth of the formations and their temperatures. The maximum temperatures are reached when the layers are at deepest burial. In Pseudo well 2 the Early Cretaceous strata reaches a remarkable high temperature peak prior to erosion at the Albian unconformity, despite relatively shallow burial during this time. The higher heat flow during the late syn-rift and early post rift stage explains this early peak in temperature. The temperature charts for wells 2513/8-1 and Pseudo well 1 show that potential source rocks in the Barremian to Aptian/Albian interval reach temperature values in the range from 70 to 90 °C for 2513/8-1 and 50-60 °C for the shallower Pseudo well 1 (Figure 48 and 49). In Pseudo well 2 peak temperatures of potential source rocks in the Barremian to Aptian interval range from 80 to 100 °C (Figure 50). For the shelfal wells peak temperatures were reached in the beginning of the Tertiary, while for the deeper Pseudo well 2 the present-day temperature is the peak temperature.

The none-calibrated vitrinite reflectance chart created by PetroMod show for the shelfal wells 2513/8-1 and Pseudo well 1 that a potential Aptian/Albian source rock reach Ro values in the range from 0.42 to 0.50 %Ro for 2513/8-1 and 0.34-0.37 %Ro for the slightly shallower Pseudo well 1 (Figure 487 and 49). The modelled vitrinite reflectance for Pseudo well 2 indicates that a potential Barremian to Aptian source rock is in the range of 0.50 to 0.66 %Ro (Figure 50). Following the general maturity chart by Collins (1991) (Figure 47), the Lower Cretaceous source rock is essentially immature to early mature on the shelf, while early to middle stages of maturity are reached at the base of slope at Pseudo well 2.

Hydrocarbon generation zones	SCI	% *St*	% *Ro*
Immature	< 3.5	< 3	< 0.35
Early mature	3.5–5	3–5	0.35–0.5
Middle mature	5–7	5–7	0.5–0.75
Late mature	7–8.5	7–10	0.75–1.3
Post mature	8.5–10	> 10	> 3

Figure 47: Vitrinite reflectance (Ro) as common proxy for maturity (Collins, 1990).

The conclusion on maturity should be treated with caution as no actual thermal well data or measured Ro values had been available for calibrations. In addition, actual maturity depends much on source rock kinetics, which has not been established for the Lüderitz Basin. Potential deep marine source rocks are expected to contain a large ratio of type II kerogen, while potential shelfal source rock may contain substantial amounts of more gas-prone type-III kerogen deriving from continental input.

Considering that the Namibian margin is a volcanic margin with possibly enhanced heat flow history, temperature and maturity estimations should be regarded as minimum values.

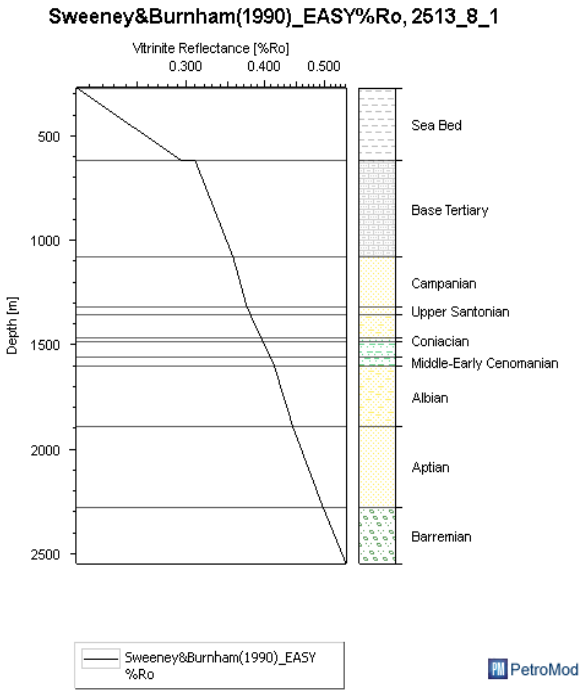

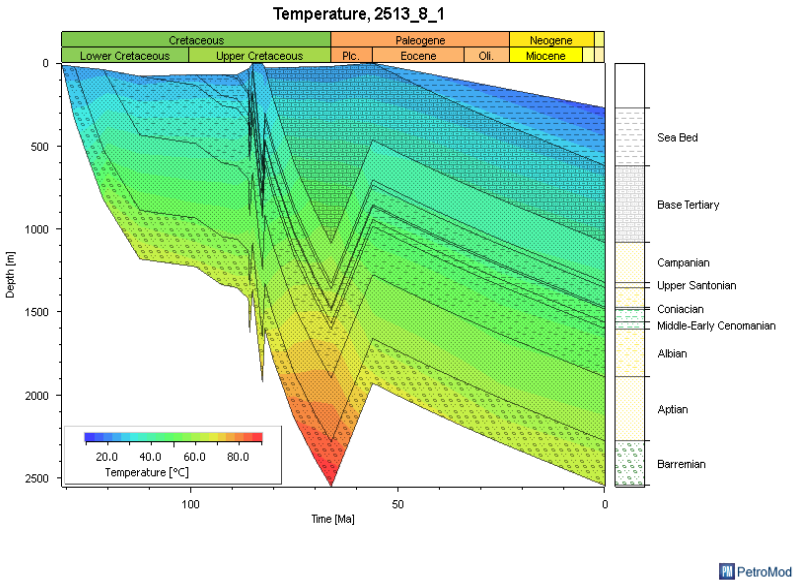

Figure 48: None Calibrated Vitrinite Reflectance and Modelled temperature history for well 2515/8/1.

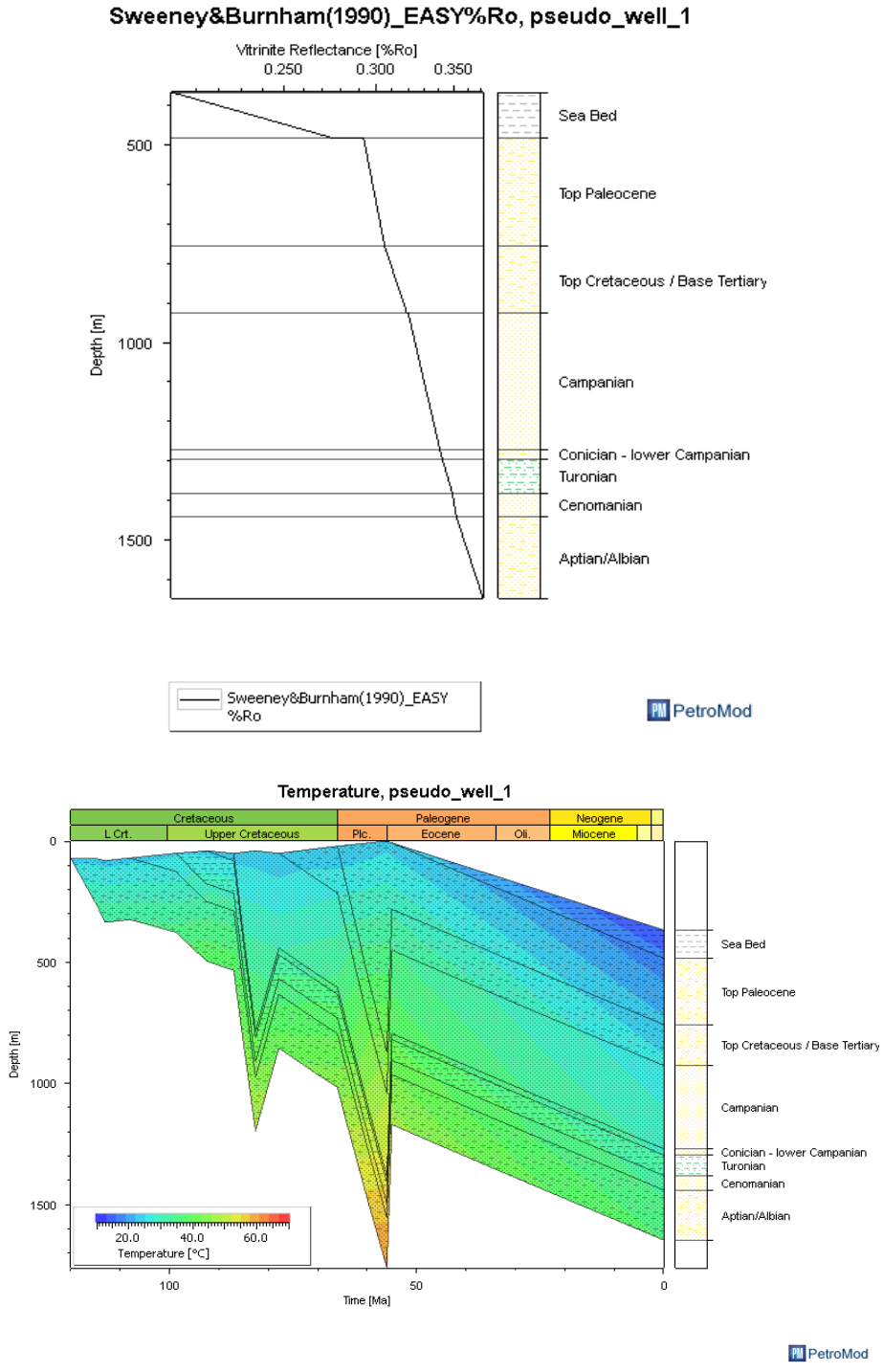

Figure 49: None Calibrated Vitrinite Reflectance and Modelled temperature history for Pseudo well 1.

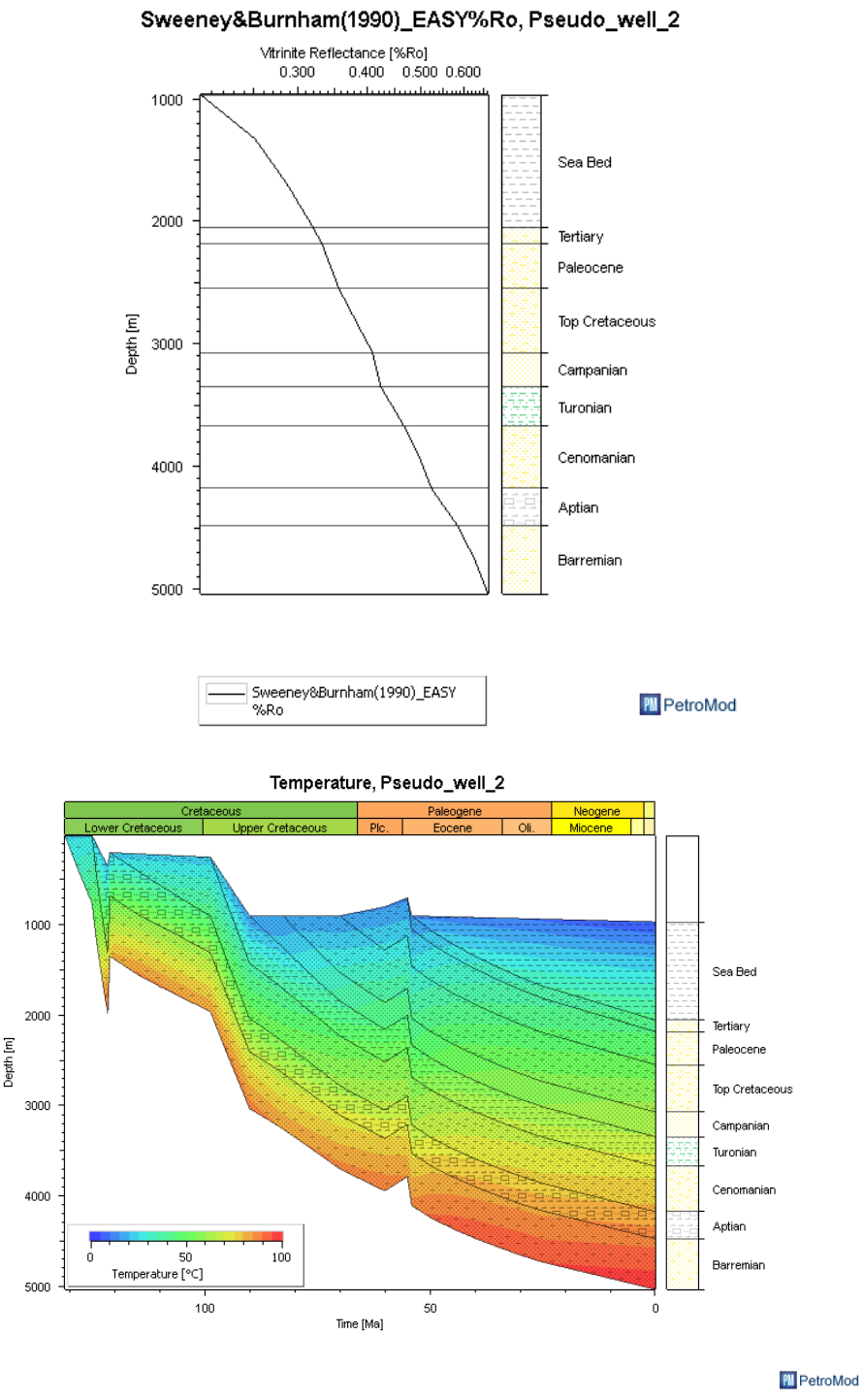

Figure 50: None Calibrated Vitrinite Reflectance and Modelled temperature history for Pseudo well 2.

Aspects of Uncertainty

The burial and thermal history models are based on a number of assumptions of various levels of uncertainty. The heat flow evolution has been modelled using the McKenzie modell for passive margins. The timing of the syn-rift and thermal subsidence phases are well known (Appendix 4), and apart from some uncertainty about basal heat flow and stretching factor, the model is well constrained. The geothermal gradient of 34°C/km was taken from Hunt Oil (2008), but no information on how this gradient was estimated was available. A small change in geothermal gradient, just by a few °C/km difference, will significantly change the thermal models.

The biggest uncertainties in the burial history models are the extent of stratigraphic gaps and amount of eroded strata. Tentative depths of erosion for two main Cretaceous unconformities were derived from incisions seen in seismic. The resulting amounts of eroded strata are minimum values, but do not exclude larger values. The amount of erosion in the Paleogene (Paleocene unconformity) considered a suggestion of an industry presentation by Hunt Oil (2008), but was judgted as too large for the choosen Pseudo well positions, but no constraints for minimum amounts were found. Therefore, the chosen value for intra Tertiary erosion is speculative.

Paleo-water depths were tentatively estimated solely on sequence stratigraphic context for Pseude Well 2, located at the base of slope. Norsk Hydro's (1998) micro fauna interpretation for paleobathymetry was applied for Pseudo well 1 located on the shelf. Errors in paleo wather depths will also effect the burial history models, but to a lesser extent than wrong estimates of stratal gaps and erosive events.

Petroleum System Element Chart

Petroleum System Element (PSE) charts are helpful in recognizing the presence or absence of petroleum system elements and their relative timing.

A PSE chart was only created for Pseudo well 2 (Figure 51), as therein source rock presence is likely and the thermal history indicates that source rock maturity is achieved.

The PSE chart of figure 51 below shows the time interval of occurrence of the various elements and processes for Pseudo well 2 location. As shown, potential source rock deposition occurred during the Lower Cretaceous interval from the Barremian to the Aptian as known from the Orange and Walvis basins (See chapter 2; Literature Review). Another regional developed source rock may occur in the Upper Cretaceous (Cenomanian/Turonian). As reservoir rocks all potential porous lithologies, including Barremian to Aptian Carbonates, and Upper Cretaceous turbidite sandstones are considered. The carbonate reservoirs are located beneath and laterally adjacent to the Lower Cretaceous source rock, while all siliciclastic reservoirs occur above it. Seal rocks are ubiquitous with shale intervals occurring from the Lower Cretaceous to Paleocene. Migration pathways have not been mapped, but in general reservoir rocks in proximity to matured source rocks are more likely to receive charge. Traps have been considered to be mainly stratigraphic, therefore trap formation equals seal deposition.

Peak temperatures have been associated with the generation of petroleum followed directly by migration and accumulation. Maturity levels of the Lower Cretaceous source rocks attained higher levels than the shallower Cenomanian/Turonian source rocks. Temperatures in the maturity range have been reached from the later Tertiary. Hence, petroleum generation and subsequent migration, accumulation and preservation may still

be an ongoing process. The underburden Barremian carbonate reservoirs will only have received charge if an according pressure gradient allowed for downward migration. Cracking of oil into gas may occur due to enhanced temperatures beneath the source rocks.

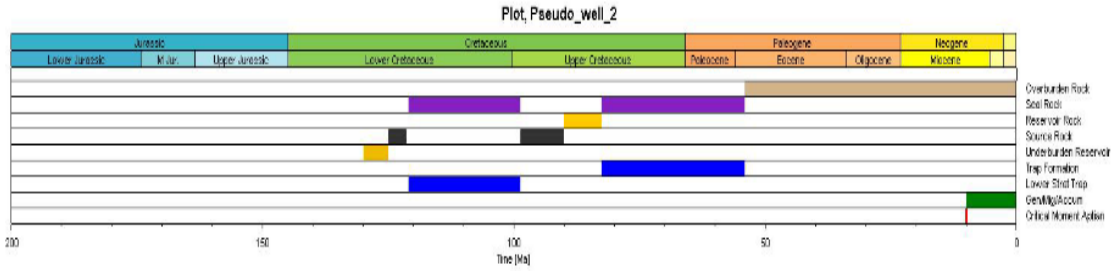

Figure 51: Chart of petroleum events for Pseudo well 2 location. The critical moment for hydrocarbon generation is well after the deposition of all potential source, reservoir and seal rocks, indicating that the area has a potential to host hydrocarbons.

CHAPTER 5: SYNTHESIS AND DISCUSSION

5.1 Sequence recognition and lithofacies prediction

This study has divided the Cretaceous and Tertiary succession into 19 Seismic Intervals (SI) based on the recognition of 11 seismic stratigraphic surface. Ages had been assigned by comparison with interpretations contained in previously cited work (e.g. (Light et al., 1993, Bagguley et al., 1999) (Figure 52) and industry presentations, supported with a tentative correlation with the far off well 2513/8-1, located 100 km south of the study area.

A lithofacies model has been created for seismic line GPN13-212M-032 (Figure 53), based on seismic facies, system tracts, and analogue interpretations presented in publication, e.g. Light et al., (1993), Bagguley and Prosser (1999), Baby et al (2018), as well in unpublished industry presentations. None of the previous interpretations used the GPN13 data set.

Period	Epoch	Age	Seismic Intervals	Seismic Surfaces	Horizons Light et al. (1993)	Megasequences Bagguley &Prosser (1990)
Tertiary Paleogene &	Paleocene to Miocene	Upper Tertiary	SI 18, SI 19	-UT UC-		MS50b
		Lower-Mid Tertiary	SI 16, SI 17			
		Paleocene	SI 11, SI 12, SI13, SI 14, SI 15	-P UC-		
Cretaceous	Late	Maastrichtian	SI 10	-CT UC-	-Horizon L-	MS50a
		Campanian	SI 8, SI 9	-IC UC-		
		Santonian	SI 7	-SEC UC-	-Horizon N-	
		Turonian	SI 6	-T UC-		
		Cenomanian	SI 4, SI 5	-TAEC UC-		
	Early	Albian	SI 3			
		Aptian	SI 3		-Horizon P-	MS40
		Barremian	SI 2		-Horizon Q-	
Jurassic	Late		SI 1		-Horizon R-	MS 20 and MS 30
					-Horizon T-	

UT UC - Upper Tertiary Unconformity; **P UC** - Paleocene Unconformity

CT UC - Cretaceous/ Tertiary; **SEC UC** - Santonian/Early Campanian Unconformity

T UC - Turonian Unconformity; **TAEC UC** - Top Albian/early Cenomanian Unconformity

Figure 52: Summary table showing the seismic intervals and bounding surfaces identified in study compared with those of Light et al. (1993) and Bagguley & Prosser (1999).

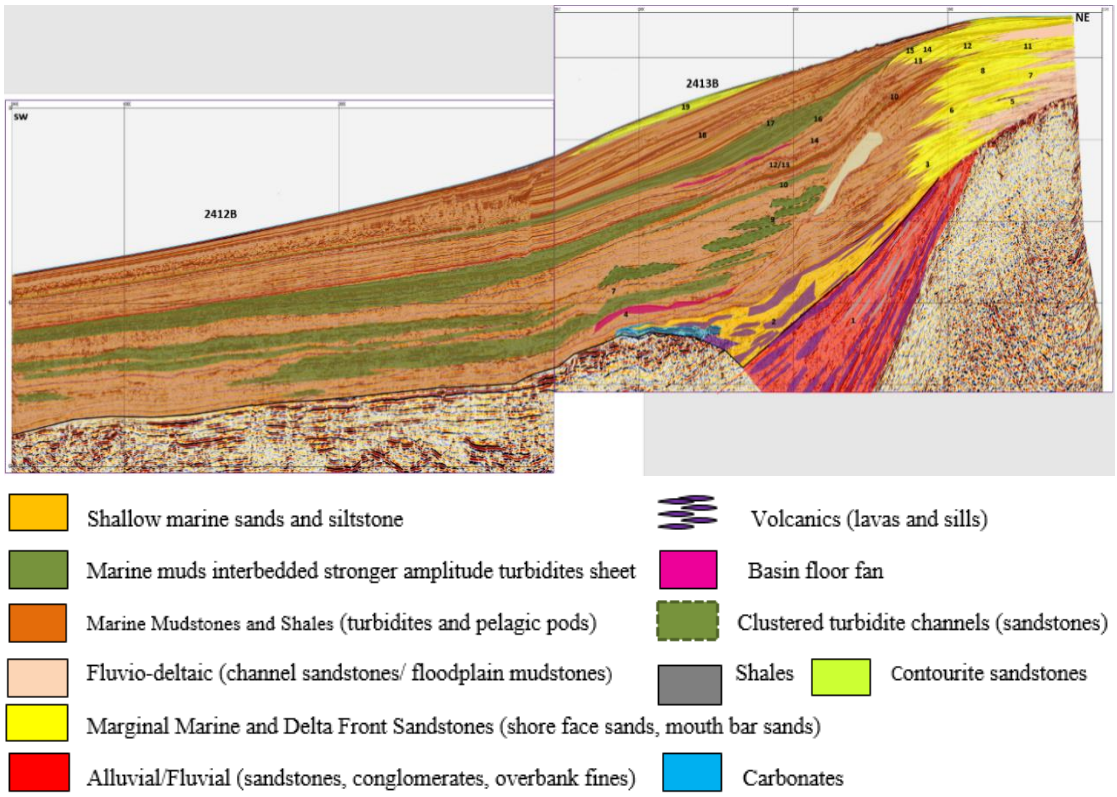

Figure 53: Lithofacies model for seismic dip line GPN13-212M-032. Numbers refer to identified Seismic Intervals (SI). For details see text below.

SI 1

SI 1 represents the Syn-rift and it was deposited in the Late Jurassic to Hauterivian (Light et al., 1993), and has a thickness of 1275ms at Pseudo well 2 location. Divergent internal configurations seismic reflectors with occasional fanning geometry is diagnostic for its syn-tectonic deposition. Continental deposits of a syn-rift settings are inferred. These include alluvial/fluvial (sandstones, conglomerates, overbank fines) lithologies and possibly lacustrine shales (more in the rift center). Volcanics deposits, both

extrusive (lavas) and intrusive (sills/dykes) are expected to be widespread, as the Namibian margin is regarded as a volcanic passive margin (Gladczenko et al., 1998).

SI 2

SI 2 was deposited in the timespan from within the Hauterivian to the end of Barremian, and has an average thickness of 415 ms at Pseudo well 2 location. This interval onlaps SI 1 with a low angle at a regional well-recognized unconformity which marks the transition from the rift phase to the drift (thermal sag) phase. Reflections in SI 1 are of high to medium amplitude, continuous to discontinuous, and divergent. Divergence is lower than for SI 1 indicating subsiding growth. During this interval probably marine conditions started to establish. Continuous reflections are interpreted as shallow marine sandstones and siltstones. In the Orange Basin shallow marine and aeolian sandstones have been found between Barremian lavas, but no deeper deposits are described. In addition, shallow marine clayey siltstones topped by organic-rich levels are described (Hodgson & Intawong, 2013).

High amplitude events are likely volcanics and carbonates. Platform carbonates have been probably restricted to the central basement high that provided a substrate for reef growth. Carbonates resting on mafic volcanics have been intersected in the Murombe well in the southern Walvis Basin at a similar position in relation to a basement high.

SI 3

SI 3 was deposited in the Aptian and Albian (approx. 100.5 -125 Ma) and has an average thickness of 283 ms at Pseudo well 2 location thinning to 172 ms at well Pseudo well 1 location. The entire interval onlaps on SI 2 and SI 1, and closer towards the continent,

also the basement. The overall downdip curvature of the reflections indicates development of a shelf-slope bathymetry with slightly increased sedimentation rate towards the deeper basin. Characteristic are medium to low-amplitude mostly continuous and slightly divergent reflections. On the shelf in well 2513/8-1 fluvio-deltaic sandstones dominate this interval. This coincides with slight hummocky configuration of reflections on the shelf. Towards the poorly defined offlap break subtle small scale clinoforms are recognizable that could coincide with sandy deltafront deposition. Farther downdip reflections are essentially continuous proposing uniform deeper marine shale deposition. This coincides with findings from wells in the Orange (Kudu wells) and Walvis (Wingat, Murombe) basin, where shales including the kerogenous shales referred to as the Aptian-Albian source rock (Mello et al., 2012; Hartwig et al., 2012), as well as calcareous intervals (marlstones) have been drilled.

SI 3 is overall aggradational with a subtle downlap surface occurring in its lower upper half. This surface could represent the MFS near the Aptian/Albian boundary described in Baby et al. (2018). The overall transgressive development has probably restricted coarser siliciclastic deposition to the shelf, with few mass flows (turbidites/debrites) reaching the deeper basin. Widespread carbonate deposition has been proposed by Hodgson & Intawong (2013) and Baby et al. (2018), however there are no distinct seismic features supporting this scenario in the section studied. A stronger amplitude occurs where the Aptian drapes SI 2 on the basement high, and this has been interpreted as a continuation of carbonate deposition at this location. SI 3 is overall transgressive indicated by its onlap pattern. Its relative high thickness associated aggradational

stacking at the offlap break suggests a relative high sediment input largely balanced by relative sea level rise, probably caused by a phase of strong thermal subsidence.

The bounding surface at the top of the SI 3 is a prominent seismic marker representing the top-Albian/early-Cenomanian Unconformity, varying locally in character, with a local downlap surface towards the South-West, followed by a deeply incised canyon visible from the mid-slope position.

SI 4 and SI 5

SI 4 and SI 5 follow both the top Albian/early Cenomanian unconformity, while SI 4 is deposited on the floor of a deeply incised canyon, SI 5 is deposited on the shelf. Both intervals are believed to be of Cenomanian age (approx. 93.9 -100.5 Ma). SI 4 is characterized by medium amplitude sub-parallel with a shallowly mounded areas of slightly hummocky internal configurations. SI 4 is interpreted as a Low System Tract (LST) with onlap against the canyon flanks in the North-East. The slightly mounded feature immediately downdip of the base of slope is interpreted as a basin floor fan, while the other more parallel reflections are more or less continuous turbidite sheets interbedded with deep marine hemipelagic mudrocks and shales. The turbidites may consist largely of sandstones, especially if the canyon was attached to an onshore fluvial system.

Following the SI 4 LST deposited in the deeper part of the basin, SI 5 deposited on the shelf as the subsequent High System Tract (HST). SI 5 is composed of shallow sigmoid clinoforms delineated by a clear toplap and downlap surface. Slight hummocky features in the east point to a fluvial/delta top system passing into delta front deposits of the

clinoform foresets. Proximity of delta top and strong progradational pattern suggest high sediment input of sand rather than mud.

SI 6

SI 6 is believed to be of essentially of Turonian age and follows with a downlap surface on the previous unit SI 5. Its thickness is similar to SI 5 with 152 ms at well Pseudo well 1 location. Seismic facies is similar as well, but the sigmoid clinoform is more oblique and complex. SI 6 is again regarded as High System Tract (HST) and, considering the pronounced progradation and complex sigmoid pattern, a high energy shallow marine environment promoting sand deposition is proposed. In the east clear hummocky reflections are developed relating to fluvial and/or delta top deposition. The downlap surface defining the base of this unit may correspond to the Cenomanian/Turonian unconformity (93Ma Sequence boundary) identified in well 2513/8-1 (Norsk Hydro Biostrat Report). Following lowstand and transgressive units were not identified as incisions and slumping at the shelf edge hampered downdip correlation.

SI 7

Following SI 6 the rather aggradational SI 7 follows. The age of the boundary between SI 6 and SI 7 is unknown. SI-7 is with 272 ms thickness thicker than the previous units at Pseudo well 2 location. It is characterized by low- medium amplitude, parallel continuous reflections forming a sigmoid clinoform. Bottomsets and topsets are largely absent due to downdip truncation by slope instability and truncation by a major probably Santonian/Campanian unconformity on the shelf. Baby et al. (2018) propose for the Lüderitz Basin inner margin deposition of prodelta and deltafront claystones interbedded

with siltstones and sandstones during the Turonian – Campanian interval. This interpretation is in line with the uniform sigmoid clinoform configuration suggesting deltaic low energy deposition of probably somewhat finer sediments. Finer grained lithologies, i.e. siltstones and argillaceous sandstones have also been observed in well 2513/8-1 located 100 km further SSE.

The relative higher thickness of SI 7 may correspond with Baby et al.'s (2018) observation that the Lüderitz Basin became a major depocenter in the Upper Cretaceous, probably caused by a new drainage trunk leading into the southern part of the basin.

SI 8

SI 8 rest on SI 7 on a slightly seaward dipping unconformity. The unconformity cannot be traced downdip due to slope instability, and it is unclear whether it corresponds to a regional unconformity. SI 8 is of similar seismic character as the previous interval SI 7. Strong hymmocky reflections in the east are interpreted as fluvial/deltatop while the forsets may represent finer grained (silt and sandstones) deltafront and prodelta deposits. As with the previous interval, primarily highstand deposition is inferred from the aggrading, slightly prograding character.

Downdip tracing of SI 7 and SI 8 is difficult, but it seems that SI 7 and possibly some of SI 8 can be found in the deep basin on top of SI 4. This order implies that either the downdip segments of SI 5 and SI 6 have been eroded at the end of SI 6 or they are below seismic resolution. The basinal part of SI 7 is interpreted of paleagic mustones interbedded with turbidite sheets. The turbidite sheets are predicted to be finer grained in case they are sourced from the shelfal lower energy deposits of SI 7.

On the inner shelf SI 8 is truncated by a major erosional unconformity, which corresponds to the regional well developed Cretaceous/Tertiary unconformity. On the upper slope the top of SI 8 is defined by a downlap surface, which can, with some uncertainty, be traced to pass into a major incision down the slope that levels on top of SI 7 near the base slope. This incision is interpreted as a submarine canyon deepening that may correspond to a major erosion event during the early Campanian (Baby et al., 2018) and is therefore termed Intra Campanian unconformity.

SI 9

SI 9 is the lowstand system tract following the presumed Intra-Campanian unconformity. Five sets of seismically well-defined stacked high amplitude clusters are chracterising this unit. They are interpreted as stacked channeled turbidites that successively migrate from base of slope to mid of slope positions. Proximal sediment input associated with the lowstand should have promoted coarser-grained (sand prone) sediment source for the turbidites.

SI 10

SI 10 is represented by clinoform bottomsets downlaping on SI 8 on the outer shelf. Downdip SI 10 can be traced through an area of slope instability into the deep basin. There, it forms subparallel slightly disrupted reflections of medium amplitudes, interpreted as pelagic mudstones and turbidite sheets. Highstand deposition is inferred due to shelf progradation evident by the downlap surface. Consequently, sandstones are expected in the clinoforms, while the downdip turbidites are presumably less sand prone than the previous lowstand turbidites.

SI 10 reaches into the upper Cenomanian and is truncated by the top Cretaceous/base Tertiary unconformity. This angular unconformity is recognized in the Orange and Lüderitz basins. Tertiary strata overlay tilted Late Cretaceous strata with a degree of truncation that increases toward the coast. Aizawa et al. (2000) recognize a pronounced coastal uplift with associated shallow marine erosive beveling on the shelf leading to an estimated erosion of 1 km at the inner southern Namibian margin.

SI 11 to SI 15

SI 11 to SI 15 are 5 sets of sigmoid clinoforms that downlap progressively the outer shelf and upper slope. Baby et al. (2018) describe the Paleogene interval as essentially fine-grained. Preservation of topsets may relate to low energy deposition, suggesting that muddy sands prevail in the delta front. East of the well-defined continuous high amplitude clinoforms strong hummocky reflections occur in SI 12, interpreted as fluvial/delta top deposits.

The presence of five sets of foresets may derive from high frequency (3rd or higher order) fluctuations in relative sea level, or lobe switching in a delta front setting. The thinning of the topsets indicates waning of relative sea level rise during late highstand, soon followed by a major unconformity. This Tertiary unconformity is likely the regionally recognized unconformity positioned at the end of the Paleogene (Rupelian to Chattian) (Baby et al., 2018).

SI 16 and SI 17

Following the Paleogene unconformity SI 16 deposited as a lowstand system tract in the deeper basin. The associated sea level fall led to slope instability causing deformation

and slight contortion of the deposit on the slope. Near the base of SI 16 is a basin floor fan characterized by its low amplitude irregular internal reflections. Otherwise continuous reflections indicate deep marine pelagic suspension fallout and turbidite deposition. SI 17 is of similar seismic character as SI 16. This interval onlaps SI 16 on the upper slope and is therefore interpreted as a transgressive deposit that ultimately inundated the shelf. Clinoforms are absent on the shelf, either they have been eroded by the succeeding unconformity, or they occur east of the seismic section. Lithofacies is unclear as there is no calibration, but shelfal deposits are likely sand prone while deeper deposits are likely shales.

On the shelf SI 17 is truncated by an unconformity that passes downdip into its correlative high amplitude conformity. This unconformity is the youngest in the Tertiary section and is therefore assigned as the regionally mapped Miocene (Tortonian) unconformity, the youngest erosional unconformity recognized in the Walvis, Lüderitz, and Walvis Basins (Baby et al., 2018)

SI 18 and 19

SI 18 and SI 19 are the youngest deposits of the upper Tertiary. They are characterized by moderate to high amplitude, medium to high frequency, and sub-parallel to parallel reflections. In the deep offshore seismic character of SI 18 suddenly changes into a disrupted and contorted reflection configuration interpreted as sediment fluidization caused by retarded dewatering and ensuing hydrostatic overpressure.

SI 19 follow with a para-unconformity on SI 18. It forms a shallow mounded body with sub-parallel continuous internal reflections that stretches from the lower to the upper middle slope.

SI 18 and 19 are aggradational. SI 18 onlaps the upper slope and must have been deposited during a phase of sea level rise. The high sediment thickness on the slope may be explained by increased sediment input from coast parallel bottom currents. A sand prone facies of contourites is therefore likely to occur. However, the fluidization of the sediments in the deeper basin points to substantial clay content to decrease the rate of dewatering as required for sediment instability. SI 19 has no obvious updip sediment source and is therefore interpreted as a pure contourite deposit. Truncation of SI 18 and SI 19 at the seabed gives evidence for recent bottom currents that are strong enough to be erosive.

5.2 Petroleum System Elements

A model for the distrinution of source rock, reservoir rock and seal rock lithologies has been created for seismic line GPN13-212M-032 (See figure 54 below and discussion below).

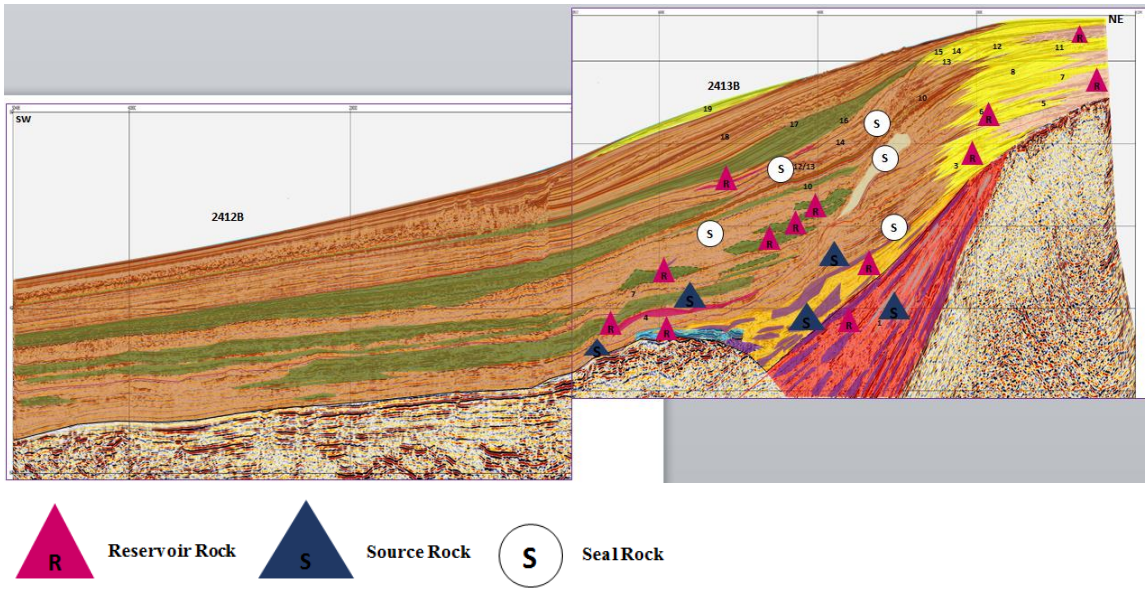

Figure 54: Conceptual illustration of the distruibution of source rocks, reservoir rocks and seal rocks may have developed in the Lüderitz Basin. See text below for discussion.

5.2.1 Source Rocks

Several pods of lacustrine and restricted marine shales are speculated to occur within the lower and upper sections of the syn-rift respectively (Figure 54; Bray et al., 1998; Mello et al., 2011; Hartwig et al., 2012). These units are capable of sourcing hydrocarbons given that they contain sufficient amounts of Total Organic Content (TOC) present as reactive kerogen. The syn-rift sequence is well developed in the study area; however, it has not been tested offshore Namibia. Lacustrine syn-rift source rocks and associated oil

in Hauterivian sandstones were discovered in the AJ-1 well in the South African Orange basin (Jungslager, 1999).

Passing into the early post-rift, Bray et al. (1998) refer to numerous organic rich shale intervals intersected in late Barremian and Aptian/Albian intervals of the Kudu wells in the Orange Basin. These source rocks were deposited when the circulation in the slowly widening South Atlantic was still restricted facilitating anoxic bottom waters (McDonald et al., 2013). A thick Aptian source rock was found to be rich and mature in the Wingat well in the southern Walvis basin (Hodgson and Intawong, 2013). Thus, Lower Cretaceous mature source rocks have been discovered in the Orange and Walvis basins, suggesting that these source rocks may also be present in the Lüderitz Basin, located in between. In the study area, continuous reflections occur in SI 2 and SI3 (transitional and early post rift seismic units), consistent with laterally extensive shale intervals. SI 3 is overall transgressive and contains a preserved MFS and is herewith a good candidate to contain organic rich shales qualifying as good source rocks.

A regional extensive Cenomanian/Turonian source rock has been intersected in the Kudu wells (Bray et al., 1998) and in the Mooshead well in the Orange basin (Hodgson and Intawong, 2013), and it has also been described from the Walvis basin. This Cenomanian/Turonian source rock is possibly related to an eustatic higstand in the late Turonian (Haq and Shutter, 2008). In the study area SI 4 (Cenomanian) and SI 7 (Turonian) are interpreted as deep marine mudstones and shales interbedded with turbidite sheets. SI 4 is interpreted as a lowstand system tract, containing a basin floor fan and numerous high amplitude turbidite sheets, suggesting that potential source rock intervals are of limited vertical extent. Reflections in SI 7 are wider spaced (lower

frequency) and more continuous, hence the presence of thick continuous source rock intervals is more likely (Figure 54).

5.3 Reservoir Rocks

Within the syn-rift, Nepembe (2016) proposed several siliciclastic reservoir facies including aeolian pinch-outs, fluvial conglomerates and sandstones; and alluvial outwash clastics (figure 54). In the transitional sequence (SI 2) he further proposes volcanic-interbedded gravels as well as fluvial deposits. In the post-rift (SI 3 to 19) numerous turbidites are present from the slope to the deep basin, while on the shelf marginal marine and deltaic sandstones are widely distributed. Channelized fluvial sandstones are expected to occur east of the marginal marine and delta from facies. In the transitional and early post-rift sequences (SI 2 and SI 3) platform carbonates, probably most prolific on the basement high west of the centreal graben, can be of good reservoirs.

Trends in reservoir quality can be predicted from the energy of environment and proximity of sediment source. For example, lowstand turbidites (SI 4, SI 9, SI 16) may provide better reservoirs than late transgressive of highstand turbidites. On the shelf, cleaner sandstones are deposited in higher energy delta front setting that may cause more oblique tangential or complex shaped clinoforms (SI 5, SI 6) (Veeken & van Moerkerken, 2013). Diagenetic porosity loss is more likely in older and deeper reservoirs than in shallower ones (Bond & Kominz, 1984).

5.4 Seal Rocks

Possible seals in the syn-rift sequence (SI 1) are lacustrine shales, thin playa evaporites, and tight igneous units (lava flows, sills and dykes) (Figure 54). In the Barremian-Aptian (SI 2 and SI 3) marine shales, including those that are source rocks, can be efficient seals. Extensive shales are predicted to occur throughout most of the deep marine post-rift section (SI 4, 9-10, 12-14, 16-19). The highly contorted slumps on the slope can also be good seals, as possible sand layers have been mixed with mud during slumping. On the shelf seals are thin veneers of flooding surfaces, as far these are not eroded, and fluvial overbank/delta top fines.

5.5 Traps

Opportunities for stratigraphic trapping mechanisms are numerous (Figure 54). First, the identified Lower Cretaceous carbonate unit resting on the basement high are surrounded by fine-grained units, such as the Aptian shales, providing effective sealing (a in Figure 54). This setup therefore constitutes a stratigraphic trap for hydrocarbon accumulation. Second, lateral termination of syn-rift to early post-rift (SI 1-3) clastics units against the basement up-dip constitutes a trap mechanism (b in figure 55). Third, turbidites, especially when channelized, are mostly capped by deep marine shales forming a good stratigraphic trap, a scenario seen in the Cenomanian to Campanian interval (SI 4,7, 9) (c in Figure 55). Unconformity traps, e.g. those formed by the top Cretaceous unconformity provide another option of stratigraphic traps (d in Figure 55). Smaller stratigraphic traps may occur on the shelf where fluvial channels are sealed by floodplain fines.

The presence of stratigraphic traps requires a complete closure of the reservoir, which can only be confirmed in depth sections, ideally in 3D.

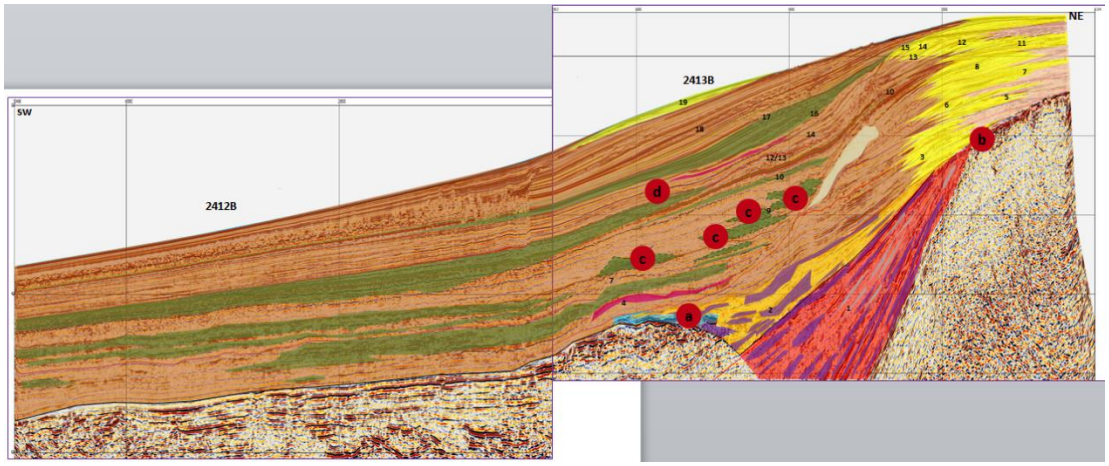

Figure 55: Conceptual illustration of stratigraphic traps that may have developed in the Lüderitz Basin. See text above for discussion.

5.6 Maturation

Hydrocarbon generation and maturation strongly depend on thermal evolution within the basin. Due to the absence of available vitrinite reflectance values and other calibration data within the basin, the following discussion on thermal evolution and maturation is based on a PetroMod simulation using a geothermal gradient of 34 °C/km as proposed for the Lüderitz Basin in an industry presentation by Hunt Oil (2008). The simulation further used standard parameters for the McKenzie passive margin thermal evolution model integrated in the software. Result are displayed in 1D thermal history charts and diagrams of calculated vitrinite reflectance values for each well location.

These results are herein compared with thermal models created for the neighboring Orange Basin by Hirsch et al. (2008).

The burial history chart at the well 2513/8-1 well location shows a shallow burial, with maximum temperatures reaching 70°C at total depth of 2550 m (Figure 44 above) prior to Tertiary uplift and erosion. The corresponding Ro reaches 0.55%, which is marginal for early hydrocarbon generation. To conclude, at well 2513/8-1 the maximum burial would have been insufficient for notable hydrocarbon generation in case a source rock facies would have been present there. The same applies to Pseudo well 1, while being shallower, even marginal maturity would not have been reached. Downdip, at Pseudo well 2 the situation is much more favorable for hydroicarbon generation for three reasons: (1) Analogue to the neighboring basins, source rocks at different levels (syn-rift, Barremian to Aptian, Cenomanian/Turonian) are likely to be well developed at the base of slope location, (2) with significant deeper burial calculated Ro for the Barremian with 0.66% is much higher falling into the early oil mature window of Collins (1991), and (3) maximum temperatures are reached not be before the late Tertiary with possible ongoing maturation.

The corresponding temperatures for Barremian to Aptian source rocks lie between 80-100°C, while the calculated non-calibrated vitrinite reflectance values for Cenomanian/Turonian source rocks reach Ro 0.52% corresponding to 65°C. The above temperatures/ Ro values are sufficient to mature the Early Cretaceous source rocks, but may only cause incipient maturity of the Cenomanian/Turonian interval. A main uncertainty factor is the actual source rock kinetic for the Lüderitz Basin. The actual kerogen transformation of source rocks is not only strongly dependent on the thermal history, but also on the geochemistry and texture of the kerogen and the mineral matrix (Selley & Sonnenberg, 2015).

A study done by Hirsch et al. (2008) indicates that the syn-rift in the Orange Basin experienced maximum temperatures of 165°C during maximum burial at 16 Ma leading to complete reactive kerogen transformation. This finding implies that potentially occurring syn-rift source rocks in the Lüderitz Basin will also have reached maturity, as the syn-rift depth in the Lüderitz basin is similar to that in the Orange Basin. Hirsch et al. (2008) further state that the Hauterivian and the Barremian/Aptian source rock intervals enter the maturity window for oil and gas generation when overstepping Ro 0.5% at 95.5 and 93 Ma, respectively (Figure 56). These findings are similar with the observations at Pseudo well 2, where from about 85 Ma temperatures steadily increase from 65°C to current 100°C. The Tertiary erosion event at the end of the Paleogene did not significantly change this trend in the base slope position of the basin.

The cracking of oil to gas commences at a vitrinite reflectance value of Ro 0.8% (Tayler et al., 1998). These values have not been reached in the study area, except for possible syn-rift source rocks. Therefore, depending on source rock characteristics, the study area should be rather regarded as oil than gas prone. This in in contrast to the Orange basin, where Barremian/Aptian source rocks exceed Ro values of 1.0%, while the shallower Cenomanian/Turonian source rock remained in the oil and gas generation window (Hirsch et al., 2008).

The differences in thermal history between the study area and Orange Basin can be attributed to two main factors: (1) the geothermal gradient in the Orange Basin is with 35 to 37°C higher than in the Lüderitz Basin (Hunt Oil, 2008), and compared with the Lüderitz Basin, the Cretaceous sequence is in general thicker while the Tertiary is poorly developed.

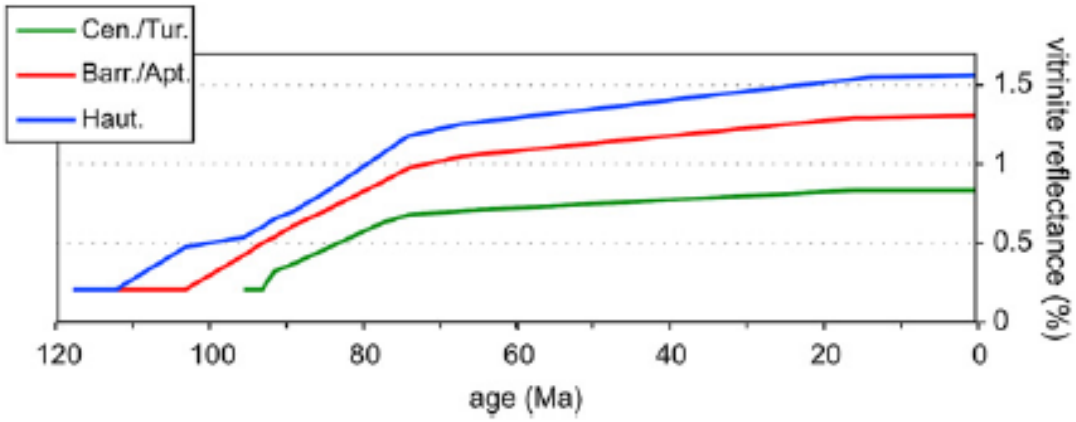

Figure 56: Transformation ratio of the three main source rocks within the Orange Basin: Cen/Tur – Cenomanian/Turonian; Apt/Barr – Aptian/Barremian; and Haut – Hauterivian source rock. Copied from Hirsch et al. (2008).

5.7 Timing, Migration and Petroleum Potential

According to the basin Modelling studies done for the Orange Basin by Hirsch et al. (2008), it is revealed that the syn-rift source rocks started to expel hydrocarbons around 80 Ma and the Barremian/Aptian source rock interval enter the maturity window of oil and gas generation when overstepping 0.5 in vitrinite reflectance at 93 Ma. According to the results obtained from the burial history of Pseudo well 2, the Barremian/Aptian Source rock started to generate hydrocarbons from earliest 85 Ma but as temperatures increased till today the peak in hydrocarbon generation may have just been reached in more recent times.

To conclude, the modelled thermal history suggests that potential Lower Cretaceous source rocks may have generated petroleum only at locations of thick overburden, such as the base of slope location chosen for Pseudo well 2. Peak hydrocarbon generation is

expected to be relatively young, enhancing the chance for trapping and preservation as the other petroleum system elements, such as reservoir and seal and trapping configurations had been in place before (Figure 51).

CHAPTER 6: CONCLUSIONS AND RECOMMENDATIONS

Seismic interpretation was used to build a seismic stratigraphic framework for the northern Lüderitz Basin. A Wheeler transformation assisted in sequence recognition, and in combination with seismic facies mapping, in lithology prediction. The resulting framework of stratigraphic and lithologic units formed a new basis for targeting reservoir, source and seal rocks away from well control.

The stratigraphic evolution of the Lüderitz Basin lead to the formation of 19 recognized Seismic Stratigraphic Intervals (SI), separated 11 seismic stratigraphic surface. In absence of direct well control stratyigraphic ages were assigned by comparison with interpretations from neigbouring areas. Lithofacies were predicted based on seismic facies, system tracts, position in relation to the paleo-shelf breaks, and as well as from analogue interpretations from adjacent areas in the Lüderitz and Walvis Basin.

Prediction of petroleum system elements such as source, reservoir, and seal, followed the lithofacies model. In the study area the presence of of at least three source rocks, namely; lacustrine shales in the syn-rift, Barremian and Aptian/Albian marine shales and younger Cenomanian/Turonian deep marine mudstones and shales interbedded with turbidites sheets. The model also proposed several reservoir rocks; siliciclastics continental deposits in the syn-rift, transitional to early drift stage platform carbonates, and post rift phase lowstand turbidides (lower slope) and sandstones on the shelf in the post rift. It further proposed seal rocks comprising of lacustrine shales, evaporites and igneous units in the syn-rift and in the post rift the ubiqitioius marine shales in the

deeper basin, and contorted slumps on the slope. Finally, the model proposed that the traps present in the area are predominantlty stratigraphic.

The modelled thermal history suggests that potential Lower Cretaceous source rocks may have generated petroleum only at locations of thick overburden, such as the base of slope location chosen for Pseudo well 2. Peak hydrocarbon generation is expected to be relatively young, enhancing the chance for trapping and preservation as the other petroleum system elements, such as reservoir and seal and trapping configurations had been in place before.

It is highly recommended that additional geological work is required to fully understand and acknowledge the full petroleum potential of the Lüderitz Basin. Based on the untested 2D interpretation in this study, the area at the base of slope appears most prospective, because of a better chance of source rock maturation and presence of channelised turbidites located above likely Lower Cretaceous source rock intervals. A 3D seismic survey in the depth domain will be required to confirm closures of potential traps. Hydrocarbon transformation and migration shall be modelled taking into account realistic source rock geochemical parameters.

REFERENCES

1. Aizawa, M., Brian, B., Cartwright, J., Milner, S., & Ward, J. (2000). Constraints of Namibia from the offshore stratigraphic record. Communions of Geological Society of Namibia, 12, 383-393.
2. Allen, P. A., & Allen, J. R. (2013). Basin Analysis: Principles and Applications. Blackwell Science, 335-397.
3. Austin, J. A., & Uchupi, E. (1982). Continental-oceanic transition of southwest Africa, Am. Assoc. Petrol. Geol. Bull., 66, 1328-1347.
4. Bagguley, J., & Prosser, S. (1999). The interpretation of passive margin depositional processes using seismic stratigraphy: examples from offshore Namibia. The Oil and Gas Habitats of the South Atlantic: Geological Society, London, Special Publication, 153, 321-344.
5. Baby, G., Guillocheau, F., Morien, J., Ressouche, J. Robin, C., Broucke, O., Dall'Asta, M. (2018). Post-rift stratigraphic evolution of the Atlantic margin of Namibia and South Africa: Implications for the vertical movements of the margin and the uplift history of the South African Plateau, Marine and Petroleum Geology 97 (2018) 169–191.
6. Bond, G. C., & Kominz, M. A. (1984). Construction of tectonic subsidence curves for the early Paleozoic miogeocline, southern Canadian Rocky Mountains: implication for subsidence mechanisms, age of breakup, and crustal thinning. Geological Society America Bulletin, 95, 155-173.

7. Bray, R., Lawrence, S., & Swart, R. (1998). Source rock, maturity data indicate potential off shore Namibia. Oil & Gas Journal, 1-10.
8. Brown, L.F Jr.,& Fisher, W. L. (1997). Seismic stratigraphic interpretation of depositional systems: examples from the Brazilian rift and pull-apart basins. Payton 1977, pp.213-248.
9. Brown, R., Summerfield, N., Gleadow, A., Gallagher, K., Carter A., Beucher, R & Wildman, M. (2014). Intracontinental deformation in southern Africa during the Late Cretaceous. Journal of African Earth Sciences, 100, 20- 41.
10. Collins, A. (2010). The 1 – 10 spore colour index (SCI) scale: a universally applicable colour maturation scale, based om graded, picked palynomorphs. In: Fremont, W.J.J., Weegink, J.W. (eds). Proceedings International Symposium on Organic Petrology, Zesist, The Netherlands, 7-9 Jan 1990, Meded Rijks Geol Dienst, 45, 39-48.
11. Conti, B. (2013). The Petroleum habitats and exploration new frontiers in the South Atlantic basins. In E. Morales (Chair), The Southern South Atlantic petroleum systems. Symposium conducted at the meeting of World Petroleum Council, Montevideo, Uruguay.
12. Clemson, J. (1997). Structural segmentation and the influence of basement structure on the Namibian passive margin. Journal of Geological Society of London. (Unpublished dissertation). University of London, England.
13. Dingle, R. V. (1992/1993). Structural and sedimentary development of the continental margin off southwestern Africa. Communications geological survey of Namibia, 37-46.

14. Embry, A.F. (2009. Practical Sequence Stratigraphy. Canadian Society of Petroleum Geologists, Online at www.cspg.org, 79 p.
15. Nepembe, E. (2017). Structural styles and implication on the hydrocarbon potential in the syn-rift mega-sequence within the Luderitz basin, offshore Namibia. (Unpublished dissertation). University of Namibia, Namibia.
16. Gahlla, S.S. (1998). Final Well Report Well 2513/8-1 Licence 008 Namibia. Stabekk, Norway: Norsk Hydro.
17. Gerrard, I., & Smith, G.C. (1982). Post-Palaeozoic succession and structure of the Southwestern African continental margin, in Studies in Continental Margin Geology, AAPG Memoir, 46, pp. 49-74, eds Watkins, J.S. & Drake, C.L., AAPG, Tulsa, OK.
18. Gladczenko, T.P., Hinz, K., Eldholm, O., Meyer, H., Neben, S. & Skogseid, J. (1997). South Atlantic volcanic margins, J. geol. Soc. Lond., 154, 465-470.
19. Gladczenko, T., Skogseid, J., & Eldhom, O. (1999). Namibia volcanic margin. Marine Geophysicals Researches, 20, 313-341.
20. Haq, B. U., & Shutter, S. R. (2008). A chronology of Paleozoic sea-level changes. Science, Vol. 322, p. 64-68.
21. Hunt Oil (2008). Namibia Farm Out Presentation Dec 2008 (unpublished)
22. Hodgson, N., & Intawong, A. (2013). Derisking deep-water Namibia. Petroleum Geology and Basins, 31, 91-96.
23. Intawong, A., & Hodgson, N. (2015). De-risking deep-water Namibia: Petroleum geology and basins. First Break, 31, 91-96.
24. Jungslager, E. H. A. (1999). Petroleum habitats of the Atlantic margin of South Africa. The Oil and Gas Habitats of the South Atlantic, 153-168.

25. Kuhlmann, G., Adams, S., Anka, Z., Campher, C., di Primio, R., & Horsfield, B. (2011). 3D petroleum systems modelling within a passive margin setting, Orange basin, blocks 3/4, offshore South Africa- implications for gas generation, migration and leakage. South African Journal of Geology, 114, (3-4), 387 – 414.
26. Kirkpatrick, L.H., Green, A. N., & Pether, J. (2019). The seismic stratigraphy of the inner shelf of southern Namibia: The development of an unusual nearshore shelf stratigraphy. Marine Geology 408, 18–35.
27. Light, M. P., Maslanyj, M. P., & Banks, N. L. (1992). New geophysical evidence for extensional tectonics on the divergent . Geological Society Special Publication:, 257-270.
28. Light, M.P.R., Maslanyj, M.P., Greenwood, R. J., & Banks, N. C. (1993). Seismic sequence stratigraphy and tectonics offshore Namibia. Tectonics and Seismic Sequence Stratigraphy, (71), 163-191.
29. Martínez, D. T. (2013). Interpretation and recognition of Depositional Systems using seismic data. Universidade de Brasília, Instituto de Geociências, Programa de Pós-graduação em Geologia.
30. Maslanyj, M., Light, M. P. R., Greenwood, R. J., & Banks, N. L. (1991). Extension tectonics offshore Namibia and evidence for passive rifting in the South Atlantic. Intera Information Technologies, Highlands Farm, Greys Road, Henley on Thames, Oxon RG9 4PS, UK.
31. Mc Dermott, K., Gillbard, E., Clarke, N. (2015). From basalt to skeletons – the 200 million-year history of the Namibian margin uncovered by new seismic data. Petroleum Geology and Basins, 33, 77 – 85.

32. McMillan, I. K. (1990). Foraminiferal biostratigraphy of the Barremian to Miocene rocks of the Kudu 9A-1, 9A-2 and 9A-3 boreholes, Comm. geol. Surv. Namibia, 6, 23-29.
33. Mitchum, R. M Jr. (1977). Seismic stratigraphy and global changes of sea level, part 11: glossary of terms used in seismic stratigraphy. In: Payton, C. E. (ed.), Seismic Stratigraphy – Applications to Hydrocarbon Exploration. American Association of Petroleum Geologists Memoir 26, 205–212.
34. Mitchum, R. M Jr., Vail, P. R., Thompson, S III. (1977a). Seismic stratigraphy and global changes of sea level: part 2, The depositional sequence as a basic unit for stratigraphic analysis. AAPG Mem 26, 53–62.
35. Mitchum, R.M Jr., Vail, P.R., Sangree, J.B., (1977b). Seismic stratigraphy and global changes of sea level: part 6, Stratigraphic interpretation of seismic reflection patterns in depositional sequences. AAPG Mem 26, 117–133.
36. Nanda, N.C. (2016). Seismic Data Interpretation and Evaluation for Hydrocarbon Exploration and Production. A Practitioner's Guide. Springer Cham Heidelberg New York Dordrecht London. Springer International Publishing Switzerland.
37. Nepembe, E. (2017). Structural styles and implication on the hydrocarbon potential in the syn-rift mega-sequence within the Lüderitz basin, offshore Namibia. Master of Science (Petroleum geology). The University of Namibia.
38. Nürnberg, D., & Müller, R. D. (1991). The tectonic evolution of the South Atlantic from Late Jurassic to present. Elsevier Science Publishers B.V., Amsterdam. Tectonophysics, 191, 21-53.

39. Paton, D. A., di Primio, R., Kuhlmann, G., van der Spuy, D., & Horsfield, B. (2007). Insights into the petroleum system evolution of the southern Orange basin, South Africa. Journal of Geology, 110, 261 -274.
40. Serica Energy (November, 2014). The Namibian Atlantic margin south of the Walvis ridge: Piecing together the jigsaw of a potentially prospective new frontier. In PETEX. Conference conducted at the meeting of PETEX, London, England.
41. Selley, R.C., & Sonnenberg, S.A. (2015). Elements of petroleum geology. 3rd ed. San Diego, Calif: Academic Press.
42. Sibuet, J. C., Hay, W.W., Prunier, A., Montadert, L., Hinz, K., and Fritsch, J. (1984). The Eastern Walvis Ridge and adjacent basins (South Atlantic): morphology, stratigraphy, and structural evolution in light of the results of Legs 40 and 75, in W.W. Hay, J.-C. Sibuet et al. (eds). Initial Report Deep Sea Drilling Project, 75, 483–508.
43. Spectrum Newsletter (3rd Quarter, 2012).
44. Stewart, J., Watts, A. B., &. Bagguley, J.G. (2000). Three-dimensional subsidence analysis and gravity modelling of the continental margin offshore Namibia. Geophys. J. Int. 141, 724-746.
45. Summons, R. E., Hope, J.M., Swart, R.,& Walter, M. R. (2008). Origin of Nama Basin bitumen seeps: Petroleum derived from a Permian lacustrine source rock traversing southwestern Gondwana, Organic Geochemistry, 39, 589–607
46. Tayler, G.H., Teichmüller, M., Davis, A., Diessel, C.F.K., Littke, R. & P. Robert (1998). Organic Petrology, Gebrüder Bornträger.

47. Vail, P.R., Todd, R. G., Sangree, J. B., (1977a). Seismic stratigraphy and global changes in sea level. In: C. Payton, (ed.), Seismic stratigraphy: applications to hydrocarbon exploration, AAPG Memoir 26, p. 49-212.
48. Vail, P.R. (1987). Seismic stratigraphy interpretation procedure. Part 1: Seismic stratigraphy procedure. In Atlas of Seismic Stratigraphy, v. 1, AAPG Studies in Geology 27, ed. A.W. Bally, 1–10. Tulsa, OK: American Association of Petroleum Geologists.
49. Van Wagoner, J.C., Mitchum, R.M., Campion, K.M., & Rahmanian, V. D. (1990) Siliciclastic Sequence Stratigraphy in Well Logs, Cores and Outcrop: Concepts for High Resolution Correlation of Time and Facies. Methods in Exploration Series 7, American Association of Petroleum Geologists, Tulsa, OK.
50. VanWagoner, J.C., Posamentier, H.W., Mitchum, R.M., Vail, P. R., Sard, J.F., Loutit, T.S. & Hardenbol, J. (1988). An overview of sequence stratigraphy and key definitions. In: Sea Level Changes: an Integrated Approach (Eds C.K. Wilgus, B.S. Hastings, C.G.St.C. Kendall, H.W. Posamentier, C.A. Ross and J.C. Van Wagoner). Special Publication 42, Society of Economic Paleontologists and Mineralogists, Tulsa, OK, 39–45.
51. Veeken, P., & Van Moerkerken, B. (2013). Seismic Stratigraphy and Depositional Facies Models, EAGE Publications.
52. Wygrala, B. P. (1989). Integrated study of an oil field in the Southern Po Basin Northern Italy. Ph.D. dissertation, University of Cologne, Germany.

APPENDICES

Appendix 1: Table of stratigraphic interval description

Unit/ Surface	Main characteristics	Seismic facies Inner shelf	Seismic facies outer shelf/upper slope	Seismic facies Slope	Seismic facies lower slope/ basin floor	Tentative correlation with well 2513-8 (ages, SBs, MFS)	Lithology in well 2513-8	Interpretation of unit/surface	Lithology prediction Inner Shelf	Lithology prediction Outer Shelf/upper slope	Lithology prediction Lower slope/basin floor
1	Synrift, subtle onlapping on basement/pre-rift, Divergent pattern	Absent	Absent	Absent	Absent	Absent		Continental early syn-rift fill; likely alluvial, fluvial, lacustrine and volcanic deposition; coarse siliciclastics of alluvial fans, fluvial arenites, floodplain and lacustrine fines, basaltic extrusive and intrusive			
2	Pronounced Onlap; Diverging in east, west toward marginal ridge still divergent with high a hummocky amplitudes	Absent	Absent	Absent	Absent	Barremian age,	Sandstone with silty claystone , siltstone Fluvio-deltaic to paralic environment	Continental to paralic, syn-rift fill, Continental to paralic deposition, volcanics and possible carbonates against and marginal ridge Likely arenaceous, siltstones, mudstones, massive volcanics (extrusive and intrusive) at and on marginal ridge Volcanics and possible carbonates on marginal ridge			

Unit/ Surface	Main characteristics	Seismic facies Inner shelf	Seismic facies outer shelf/upper slope	Seismic facies Slope	Seismic facies lower slope/ basin floor	Tentative correlation with well 2513-8 (ages, SBs, MFS)	Lithology in well 2513-8	Interpretation of unit/surface	Lithology prediction Inner Shelf	Lithology prediction Outer Shelf/upper slope	Lithology prediction Lower slope/basin floor
3	Prograding and then Aggrading Interval, Onlap on basement	Hummocky becoming to sub-continuous to the west, slight divergent	Hummocky with sub-continuous patches, pronounced divergent	Hummocky with sub-continuous patches, slight divergent	Slight Hummocky to subcontinuos	Aptian age Albianage and Early Cenomian **Top of 3** - (98.0 Ma SB forms upper limit on the interval And 98.25Ma MFS onlapping on the inner shelf	(Aptian age)- Sandstone (Fluvio-Deltaic) (Albian age)- Siltstone and Argillaceous Sandstone (marine, marginal delta front ? deltaic) Siltstone with Limestone and trace Marl (Marine, marginal delta front to inner neritic)	Transgressive system tract in lower third of Sequence,Boundary,Transgressive system tract with a strong aggradation pattern (strong thermal subsidence, rapid sea level rise with good sediment supply-aggradation	Fluvio deltaic throughout(hummocky pattern)	Mudstone (prograding pattern) s in the lower section grading into sandstones in the upper section, Visible mid Slope to lower slope instability	Mudstone dominated, mounted features at base of slope?

Unit/ Surface	Main characteristics	Seismic facies Inner shelf	Seismic facies outer shelf/upper slope	Seismic facies Slope	Seismic facies lower slope/ basin floor	Tentative correlation with well 2513-8 (ages, SBs, MFS)	Lithology in well 2513-8	Interpretation of unit/surface	Lithology prediction Inner Shelf	Lithology prediction Outer Shelf/upper slope	Lithology prediction Lower slope/basin floor
4	Onlap surfaces			Hummocky	Hummocky		plain influence	LST			Basin floor fan, turbidites
5	Prograding then Aggrading, Top lap surfaces	Hummocky	Hummocky to sub-continuous	Hummocky	Hummocky	Early to Middle Cenomanian Turonian U/C, Turonian age? Forming top of the sequence	Siltstone with Limestone and trace Marl (Marine, marginal delta front to inner neritic),Siltstone with minor Limestone (marine, inner neritic with lower delta plain influence	HST	Fluvio deltaic sandstones and mudstones throughout for the prograding,	Deltaic with slope instability at delta front	
6	Prograding then Aggrading, Downlap and Top Surfaces	Hummocky to sub-continuous	Complex Sigmoid Oblique	Hummocky to sub-continuous Hummocky	Hummocky (due to slumping)			HST	Sandstones throughout	Deltaic shallow marine sands	Slumped poorly developed outer slope

Unit/ Surface	Main characteristics	Seismic facies Inner shelf	Seismic facies outer shelf/upper slope	Seismic facies Slope	Seismic facies lower slope/ basin floor	Tentative correlation with well 2513-8 (ages, SBs, MFS)	Lithology in well 2513-8	Interpretation of unit/surface	Lithology prediction Inner Shelf	Lithology prediction Outer Shelf/upper slope	Lithology prediction Lower slope/basin floor
7	Prograding then Aggrading, top is erosional truncation	Slight Hummocky (Fluvial) to sub-continuous due to slope instability	Regular/ Subparallel-continuous	Slightly divergent, sub continuous	Hummocky(due to slumping)	Santonian U/C, Santonian Age (inner shelf on top of 7)	Argillaceous, Sandstone and Siltstone (Marginal marine, delta front to delta plain)	HST	Fluvio deltaic	Shallow marine deltaic sandstones	Instable Delta front sandstone
8	Aggrading , Top Lap Surfaces	Oblique Tangential	Oblique Tangential	Divergent	Hummocky to sub-continuous	Intra-Campanian SB (on top of 8)	Silty Sandstone with Limestone and Argillaceous Limestone Marine, Inner neritic to marginal	HST	Delta top to mouth bar silty Sandstones and mudstones	Mudstones with sandstones	
9	Lower boundary (Santonian U/C)			channelized mounted hummocky	sub-continuous to hummocky			LST			Mudstones with channelized turbidites sands

Unit/ Surface	Main characteristics	Seismic facies Inner shelf	Seismic facies outer shelf/upper slope	Seismic facies Slope	Seismic facies lower slope/ basin floor	Tentative correlation with well 2513-8 (ages, SBs, MFS)	Lithology in well 2513-8	Interpretation of unit/surface	Lithology prediction Inner Shelf	Lithology prediction Outer Shelf/upper slope	Lithology prediction Lower slope/basin floor
10	Prograding Erosional Truncation, Downlap Surface	Absent	sub-continuous	sub-continuous	sub-continuous	No well control (But likely maastrichan/top cretaceous		HST		Shallow marine Sandstone	Sandstones, down dip mass flow deposits (debris/turbidite channels?)
11	Aggradation, then Prograding, (some Retrograding pattern), Downlap Surfaces	Sub-continuous to Hummocky	Sub-continuous	Sub-continuous	Parallel Subcontinuos			HST	Shallow marine sandstones (sandstones from high sediment input)	Shallow marine sandstones	Shallow marine sandstones
12	Aggradation, then Prograding, then Degrading, Onlap Surfaces	Hummocky	Hummocky	Sub-continuous	Sub-continuous to Hummocky			HST	Fluvio deltaic- fluvio channel sand,floodplain,mudstones	Fluvio deltaic to delta front	Delta front sandstones and mudstones

Unit/ Surface	Main characteristics	Seismic facies Inner shelf	Seismic facies outer shelf/upper slope	Seismic facies Slope	Seismic facies lower slope/ basin floor	Tentative correlation with well 2513-8 (ages, SBs, MFS)	Lithology in well 2513-8	Interpretation of unit/surface	Lithology prediction Inner Shelf	Lithology prediction Outer Shelf/upper slope	Lithology prediction Lower slope/basin floor
13 14 15	Aggradation, then Prograding, then Degrading, Onlap and erosional Surface at outer shelve/slope position	sub-continuous	sub-continuous	Sub-continuous to slight hummocky (due to slumping)	Mounted hummocky slumped complexes			Late HST continuing	Shallow marine sandstones	Shallow marine sandstones	Mixture of Sandstones and mudstones
16	Absent	Absent	hummocky	Hummocky to slightly Clinoforms	Hummocky to sub-continuous			LST (sequence boundary on top		Muddy Deposits	Debrites b (all muddy)
17	Aggrading then Prograding, Onlap Surfaces	Sub-Continuous to slight hummocky	Sub continuous to continuous	Continuous to Hummocky and mounted	Continuous parallel			Transgressive to HST	A bit of fluvial influence , shallow marine sandstones	Mudstones, fine sandstones	Muddy slope deposits and basin deposits, contourite sandstones
18	Aggrading, Onlap surface on slope	Sub-Continuous to Continuous	Continuous	Continuous	Hummocky			Transgressive		Muddy Deposits	Muddy slope deposits and basin deposit,contourite influence
19	Aggrading; shows erosion features possibly contourite currents		Continuous	Continuous						Fine grained sandstone	contourite sandstone

Appendix 2: Non-Interpreted seismic dip line GPN13-212-032 that was used for the study.

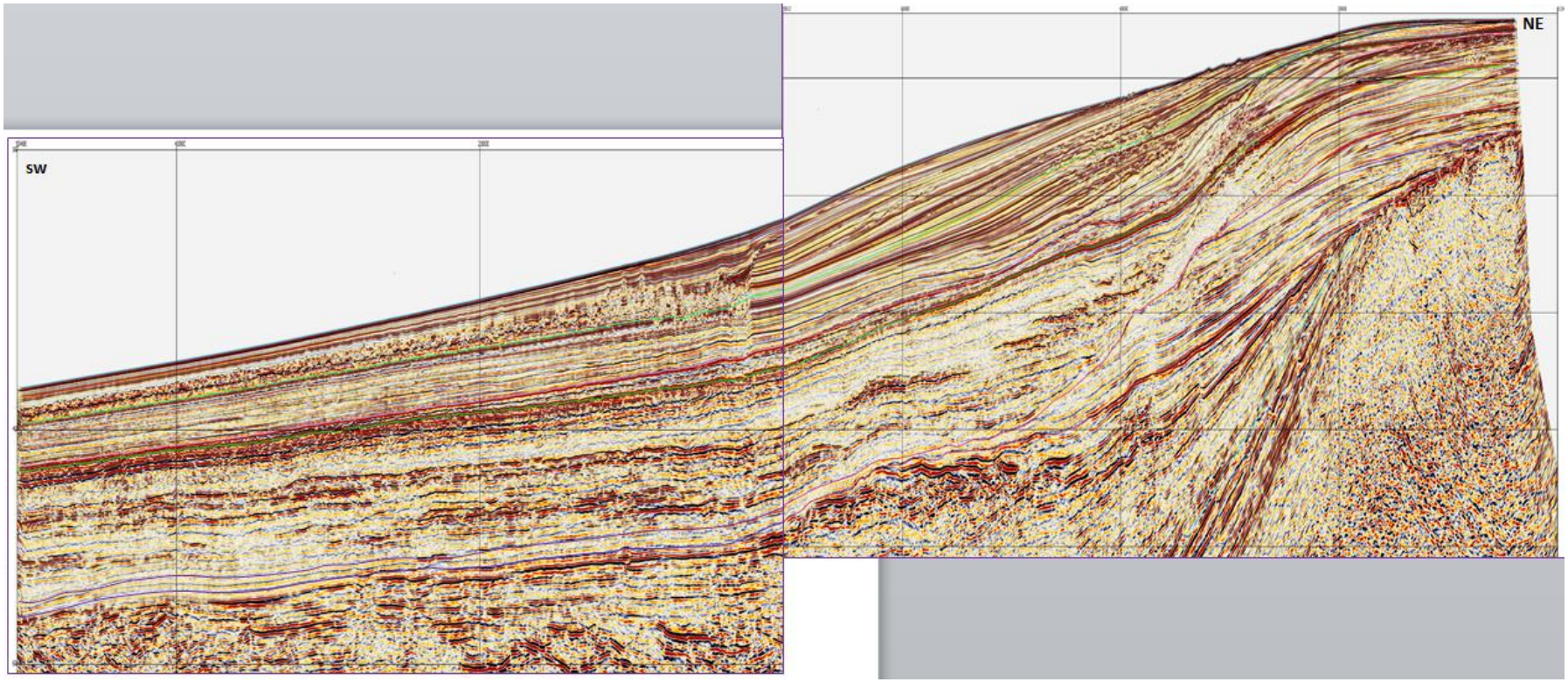

Appendix 3: Interpreted dip line GPN13-212-032 inluding numbered Seismic Intervals (SI 1-19) and main horizons.

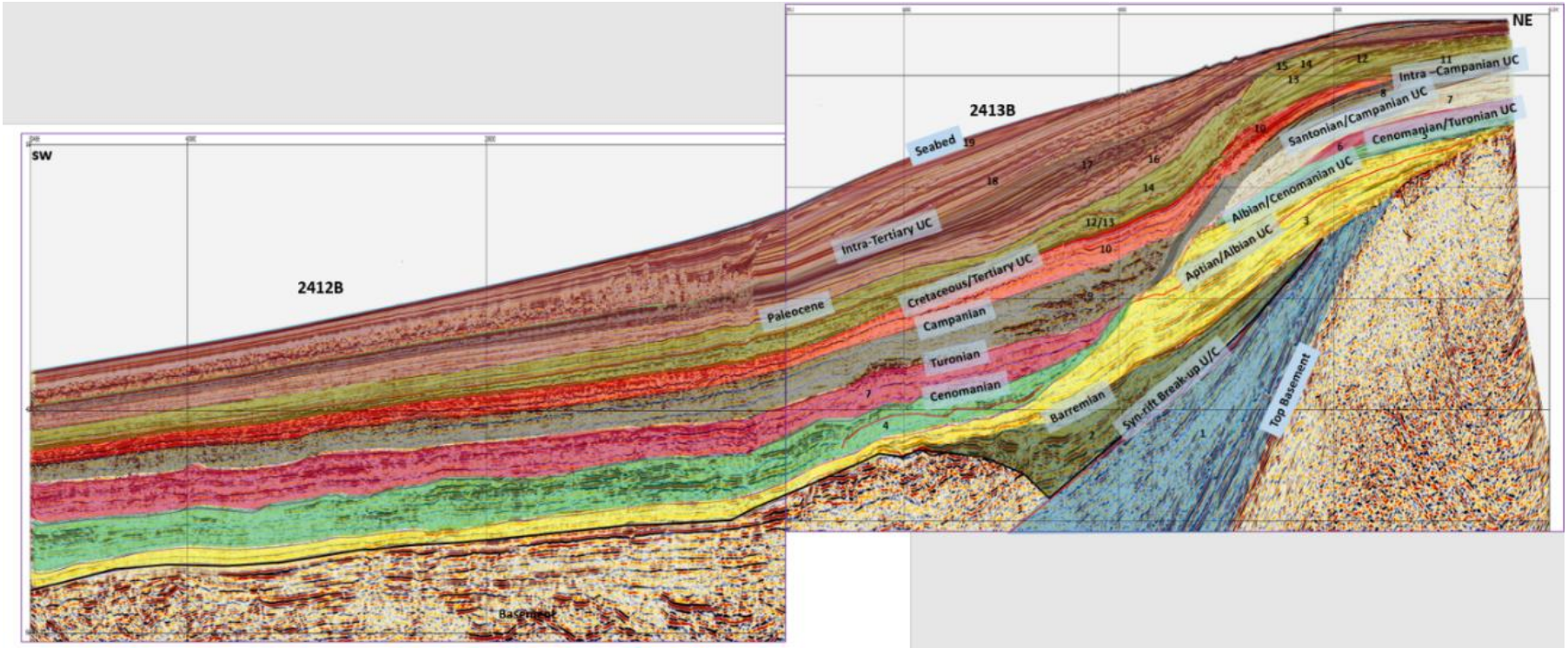

Appendix 4: Tables with input data for the three wells (well 2513/8-1, Pseudo well 1 and Pseudo well 2) modelled in PetroMod.

Input table for modelled Pseudo well 2.

Main input for Pseudo_well_2

Present day input: Depth Thickness Show paleo balance Model from picks... Top names Layer names

Age [Ma]	Name top/well pick	Depth [m]	Thickness [m]	Event type	Name layer/event	Paleodeposition/ erosion [m]	Lithology	PSE	Kinetic	TOC [%]	HI [mgHC/gTOC]
0.00	Sea Bed	967									
			1086	Deposition	Sea Bed		Clay-dominated lithotype	Overburden Rock			
54.00	Tertiary	2053									
			129	Deposition	Tertiary		Sandstone (clay rich)	Seal Rock			
55.00	Paleocene U/C	2182									
			0	Erosion	Paleocene U/C	-50					
60.00	Paleocene	2182									
			366	Deposition	Paleocene	50	Sandstone (clay rich)	Seal Rock			
70.00	Top Cretaceous	2548									
			526	Deposition	Top Cretaceous		Sandstone (clay rich)	Seal Rock			
82.60	Campanian	3073									
			273	Deposition	Campanian		Sandstone (clay poor)	Reservoir Rock			
90.00	Turonian	3346									
			326	Deposition	Turonian		Siltstone (organic rich, 2-3% TOC)	Source Rock			
98.70	Cenomanian	3672									
			504	Deposition	Cenomanian		Sandstone (clay rich)	Seal Rock			
121.00	Top Albian/Early Cenomanian U/C	4176									
			0	Erosion	Top Albian/Early Cenomanian U/C	-300					
121.50	Aptian	4176									
			300	Deposition	Aptian	300	Argill. silic. mudstone	Source Rock	Burnham(1989)_TII	5.00	400.00
125.00	Barremian	4476									
			560	Deposition	Barremian		Sandstone (wacke)	Source Rock	Burnham(1989)_TII	5.00	400.00
131.00	Top Synrift	5036									

Input table for modelled well 2513/8/1.

Main input for 2513_8_1

Present day input: Depth Thickness Show paleo balance Model from picks... Top names Layer names

Age [Ma]	Name top/well pick	Depth [m]	Thickness [m]	Event type	Name layer/event	Paleodeposition/ erosion [m]	Lithology	PSE	Kinetic	TOC [%]	HI [mgHC/gTOC]
0.00	Sea Bed	270									
			348	Deposition	Sea Bed		Clay-dominated lithotype	Overburden Rock			
56.00	Paleocene	618									
			0	Erosion	Paleocene UC	-600					
66.00	Base Tertiary	618									
			462	Deposition	Base Tertiary	600	Clay-rich carb. mudstone	Seal Rock			
82.00	Intra-Campanian U/C	1080									
			0	Erosion	Intra-Campanian U/C	-312					
82.60	Campanian	1080									
			241	Deposition	Campanian	312	Sandstone (clay poor)	Reservoir Rock			
85.00	Santonian-Early Campanian U/C	1321									
			0	Erosion	Santonian-Early Campanian U/C	-195					
85.70	Upper Santonian	1321									
			32	Deposition	Upper Santonian	195	Sandstone (arkose, typical)	Reservoir Rock			
86.00	Lower Santonian	1353									
			116	Deposition	Lower Santonian		Sandstone (clay rich)	Seal Rock			
88.80	Coniacian	1470									
			12	Deposition	Coniacian		Siltstone (organic lean)	none			
92.40	Turonian	1482									
			80	Deposition	Turonian		Siltstone (organic rich, 2-3% TOC)	Source Rock	Burnham(1989)_TII	3.00	117.00
98.70	Middle-Early Cenomanian	1562									
			39	Deposition	Middle-Early Cenomanian		Siltstone (organic lean)	Underburden Rock			
112.20	Albian	1601									
			293	Deposition	Albian		Sandstone (clay rich)	Underburden Rock			
121.00	Aptian	1894									
			386	Deposition	Aptian		Sandstone (typical)	Underburden Rock			
128.00	Barremian	2280									
			270	Deposition	Barremian		Conglomerate (typical)	Underburden Rock			
131.00	Top Synrift	2550									

Input table for modelled Pseudo well 1.

Main input for pseudo_well_1

Present day input: Depth Thickness Show paleo balance Model from picks... Top names Layer names

Age [Ma]	Name top/well pick	Depth [m]	Thickness [m]	Event type	Name layer/event	Paleodeposition/ erosion [m]	Lithology	PSE	Kinetic	TOC [%]	HI [mgHC/gTOC]
0.00	Sea Bed	367									
			116	Deposition	Sea Bed		Clay-dominated lithotype	Overburden Rock			
55.00	Paleocene U/C	483									
			0	Erosion	Paleocene U/C	-600					
56.00	Top Paleocene	483									
			275	Deposition	Top Paleocene	600	Sandstone (clay rich)	Seal Rock			
66.00	Top Cretaceous / Base Tertiary	758									
			170	Deposition	Top Cretaceous / Base Tertiary		Sandstone (clay rich)	Seal Rock			
77.88	Intra-Campanian U/C	928									
			0	Erosion	Intra-Campanian U/C	-312					
82.60	Campanian	928									
			346	Deposition	Campanian	312	Sandstone (clay poor)	Reservoir Rock			
85.00	Santonian-Early Campanian U/C	1274									
			0	Erosion	Santonian-Early Campanian U/C	-195					
86.00	Santonian	1274									
			26	Deposition	Santonian	195	Sandstone (arkose, typical)	Reservoir Rock			
92.40	Turonian	1300									
			86	Deposition	Turonian		Siltstone (organic rich, typical)	Source Rock			
98.70	Cenomanian	1386									
			60	Deposition	Cenomanian		Sandstone (clay poor)	Reservoir Rock			
108.00	Top Albian/Early Cenomanian U/C	1446									
			0	Hiatus	Top Albian/Early Cenomanian U/C						
113.00	Aptian/Albian	1446									
			208	Deposition	Aptian/Albian		Sandstone (clay rich)	Source Rock			
120.00	Top Basement	1654									

McKenzie boundary conditions for heat flow.